Mathematical Modelling of Helicopter Slung-Load Systems

R.A. Stuckey

Air Operations Division
Aeronautical and Maritime Research Laboratory

ABSTRACT

The primary goal of this work is to use mathematical modelling to assist in defining the operational limits of the Australian Army CH-47D Chinook when carrying mixed density slung loads. This report presents the first phase in the program: the development of a simple helicopter slung-load model for simulation and analysis of the system dynamics.

General system equations of motion are obtained from the Newton-Euler equations in terms of generalized coordinates and velocities. The system is partitioned into coordinates such that the motion due to cable stretching is separated from that due to rigid-body, coupled dynamics. In the formulation used, the constraint forces appear explicitly and a solution to the resultant generalized accelerations can be determined by modelling the cable as a simple spring. An inelastic solution is also possible by nulling the stretching coordinates to obtain a relation for the suspension forces. The system equations are also extended for the multiple load case.

The model is verified by imposing certain constraints in order to approximate a simple pendulum system and then comparing its behaviour with analytical results. Various configurations of the complete helicopter slung-load system, based on the CH-47B Chinook carrying standard military containers, are then examined in an investigation of the open-loop characteristics. In the investigation, several parameters such as the helicopter-load mass ratio, suspension configuration, and number of loads are varied and the resulting system modes examined. A number of simulations are also presented which demonstrate the characteristic behaviour of such systems.

APPROVED FOR PUBLIC RELEASE

DEPARTMENT OF DEFENCE

DEFENCE SCIENCE & TECHNOLOGY ORGANISATION

DSTO

Mathematical Modelling of Helicopter Slung-Load Systems

EXECUTIVE SUMMARY

In the past, the operations of helicopters carrying externally slung loads has often been limited and, in some cases, seriously hindered by stability and control problems. Several incidences have been reported by the Australian Army alone, in which possible aerodynamic excitation or dynamic instability, resulting in uncontrollable oscillations, has forced premature release of the load. Hence, the main goal of the study is to develop a comprehensive helicopter slung-load model which will provide a better understanding of the system dynamics and various effects involved. Furthermore, there is a requirement for the carriage of multiple loads of varying type, which has not previously been investigated in this manner. This report presents the first phase in the program: the development of a simple helicopter slung-load model for simulation and analysis of the system dynamics. Following this, a full nonlinear flight dynamic model is to be developed, incorporating additional detail, such as the automatic flight control system, rotor wake effects, load aerodynamics, and sling elasticity.

The simulation model used for this first phase of work is based on the helicopter slung load system first introduced at NASA Ames Research Center. In this formulation, the general system equations of motion are obtained from the Newton-Euler equations in terms of generalized coordinates and velocities. Using the explicit constraint method, the system is then partitioned into coordinates such that the motion due to cable stretching is separated from that due to rigid-body, coupled dynamics. As a consequence, the constraint forces appear explicitly and a solution to the resultant generalized accelerations is determined by assuming a simple spring model for the cable. It is also possible to obtain a solution to the inelastic approximation by nulling the stretching coordinates, yielding an explicit relation for the suspension forces. The result is computationally more efficient than the conventional formulation and is readily integrated with the elastic suspension model. Another benefit of the formulation is that it is easily applied to complex multiple body systems, and in the current work, the system equations are extended for the case of multiple loads. All code development has been done in the MATLAB numerical computing environment, which provides a high-performance language amenable to modelling and simulation type work. The main functions used in the simulation and analysis have been included in the report.

The model is verified by imposing certain constraints in order to approximate a simple pendulum system and then comparing its behaviour against both analytical solutions and previously documented numerical results. A complete helicopter slung-load system, based on a CH-47B Chinook carrying a standard military container, is then examined in an investigation of the open loop characteristics. In this simple model, neither the load aerodynamics nor the effect of rotor downwash on the load is taken into account. Several parameters such as the helicopter-load mass ratio, suspension configuration, and number of loads are varied and the resulting system modes examined. In order to extract these modes, a linearised form of the model is first obtained by numerical approximation of the partial derivatives. For the configurations examined, an increase in the load mass was generally found to have a mild destabilising effect, particularly in the lateral axes. A number of

simulations were also run in order to demonstrate the dynamic characteristics of several different configurations. From the response data, the oscillatory modes in longitudinal and lateral axes were identified, including the unstable phugoid and pendulum modes. In all of the simulations examined, the cable tension was found to reach a maximum of approximately 1.5 times the static load.

Author

Roger A Stuckey
Air Operations Division

Roger Stuckey received the degree of Bachelor of Engineering in Aeronautical Engineering from the University of Sydney in 1990. He then stayed on with the Department to begin postgraduate studies and in 1995 received the degree of Doctor of Philosophy in Aeronautical Engineering. His research thesis involved the development of an approach for the identification of parameters that characterise nonlinear behaviour in high-order dynamic systems. The software was successfully used in estimating the unsteady aerodynamics associated with wing-spoilers on the F-111C aircraft. Roger currently holds the position of Research Scientist in the Air Operations Division of AMRL and is working on helicopter modelling tasks. His research interests include aircraft flight dynamics and control, nonlinear system analysis, and parameter identification and simulation in aeronautical systems.

Contents

Appendices

Figures

Tables

Acronyms

AFCS	Automatic Flight Control System
AOSC	Air Operations Simulation Centre
AOD	Air Operations Division
AMRL	Aeronautical and Maritime Research Laboratory
cg	Centre of Gravity
DOF	Degrees of Freedom
DSTO	Defence Science and Technology Organisation
HSLSIM	Helicopter Slung-Load Simulation
KTAS	Knots True Airspeed
SAS	Stability Augmentation System

Nomenclature

Variables

A	square $6n \times 6n$ matrix defining the kinematic relation $v = Au$
$A1, L$	column partitions of A for elastic and inelastic components of the suspension, respectively
$AI1^T, \Lambda^T$	row partitions of A^{-1}
c	number of constraints imposed by the inelastic system
d	number of degrees of freedom (DOF) of the system
D	block-diagonal matrix of the system's rigid-body masses and inertias
fa	vector of the aerodynamic forces and moments on each body
fc	vector of the cable suspension forces and moments on each body
fg	vector of the gravitational forces on each body
f^*	vector of the translational and rotational inertia reaction forces on each body
fo	vector of the sum of all external forces and inertia coupling terms
FAj_N, MAj_j	aerodynamic forces and moments on body Bj ; $j = 1, 2, \ldots, n$
FCj_N, MCj_j	cable suspension forces and moments on body Bj ; $j = 1, 2, \ldots, n$
g	gravitational constant
hj	vector of forces and moments per unit tension on each body due to cable Cj ; $j = 1, 2, \ldots, m$
H	matrix representing a basis of the linear vector space Λ containing fc
I, O	identity and zero matrices
Kj, cj	spring constant and damping coefficients for cable Cj ; $j = 1, 2, \ldots, m$
$l0j, lj$	unloaded and loaded lengths of cable Cj ; $j = 1, 2, \ldots, m$
m	number of cables and links in the suspension
mj, Jj	mass and body-axes inertia matrices for body Bj ; $j = 1, 2, \ldots, n$
n	number of rigid bodies in the system
r, v	vectors of inertial cg position and Euler angle attitudes, and the inertial cg velocities and angular velocities of the n bodies
R, V	position and velocity vectors relative to inertial space; appended numbers indicate specific locations or line segments joining points; the superscript star denotes the cg of the body
s	suspension force parameters
τ_j	vector of cable tensions in cable Cj ; $j = 1, 2, \ldots, m$
$T_{a,b}$	transformation of physical vectors from frame $\mathcal{F}_a$ to $\mathcal{F}_b$; all transformations are defined from Euler angles
u	generalised velocity coordinates for the unconstrained system

$u1$, $\dot{\lambda}$	generalised velocity coordinates defining the inelastic and elastic components of the system motion, respectively
va	body axes configuration velocity
Wi	transformation matrix between angle rates ωi_i, and angular velocities αi for body Bj
X	vector of kinematic accelerations from Euler's equations for each body
α, w	rigid body Euler angle triplet and inertial angular velocity; appended numbers indicate specific body
δ	vector of control inputs for each body
ξij_i	moment per unit tension of cable Cj on body Bj
u, v, w	x, y, and z velocity components in body axes
p, q, r	roll, pitch, and yaw rates in body axes
ϕ_b, θ_b, ψ_b	bank, pitch, and yaw angles for body b
δ_b, δ_a, δ_r, δ_c	pitch (longitudinal stick), roll (lateral stick), yaw (pedal), and collective control inputs
ρ	atmospheric air density
X, Y, Z	aerodynamic forces along each corresponding body axes
$X_u, \ldots, X_\delta$	stability and control derivatives in X formulated with respect to the variables defined above
$Y_u, \ldots, Y_\delta$	stability and control derivatives in Y
$Z_u, \ldots, Z_\delta$	stability and control derivatives in Z
L, M, N	aerodynamic moments about each corresponding body axes
$L_u, \ldots, L_\delta$	stability and control derivatives in L
$M_u, \ldots, M_\delta$	stability and control derivatives in M
$N_u, \ldots, N_\delta$	stability and control derivatives in N
I_{xx}, I_{yy}, I_{zz}	moments of inertia about x, y, and z axes
I_{xz}	product of inertia in $x - z$ plane
$\bar{q}$	dynamic pressure

Operators

$\bullet$, $\times$	dot and cross product operators for physical vectors
$()_a$	physical vector given by its coordinates in the frame $\mathcal{F}_a$
$()^T$	transpose of ()
$()^*$	quantity associated with cg of a rigid body in the system
$S(V_a)$	skew-symmetric matrix representing cross-product operation for vectors, V referred to $\mathcal{F}_a$

DSTO–TR–1257

1 Introduction

The operations of helicopters carrying externally slung loads has often been limited and, in some cases, seriously hindered by stability and control problems. Several incidences have been reported by the Australian Army alone in which aerodynamic excitation or dynamic instability, resulting in uncontrollable oscillations, has forced premature release of the load.

A program was consequently initiated within the Defence Science and Technology Organisation (DSTO) to use computer modelling and simulation to assist in defining the operational limits of the Australian Army CH-47D Chinook when carrying slung loads. The first phase in this program has entailed the development of a simple helicopter slung-load model for simulation and analysis in order to provide a better understanding of the system dynamics and various effects involved. The results from this work are presented here. In the second phase, a more comprehensive helicopter model is to be integrated into the multi-body system. The simulation model will incorporate additional detail, such as the automatic flight control system, load aerodynamics, rotor wake effects, and sling elasticity. Furthermore, there is a requirement to model the dynamics of the helicopter with multiple slung loads of varying mass and aerodynamic properties, which has not previously been investigated in this manner.

In this report, Section 2 presents a broad overview of prior research into helicopter slung-load systems. The three areas of analytical studies, experimental testing and, flight simulation are covered.

Section 3 introduces the equations of motion for a generalised helicopter slung-load model. Both inelastic and elastic formulations are included. The overall simulation procedure is then explained in general terms. The full set of equations which constitute the simulation model are listed in Appendix A.

In Section 4, the results obtained from the analysis of a simple pendulum-type model are presented. These include a comparison of the characteristic system modes and longitudinal and lateral simulations of two different configurations.

In Section 5, the dynamics of the helicopter slung-load model are discussed. The modes of the linearised system are displayed over a range of mass and sling configurations and the characteristic behaviour of a Super Stallion CH-53D cargo helicopter with MILVAN container load are compared against previous results.

Finally, some concluding remarks are drawn and proposals for further research made.

2   Background

There has been a small but significant amount of work done in investigating the behaviour and control of helicopter slung-load systems. This work can be roughly divided into three veins: analytical studies, experimental testing, and flight simulation and automatic control. In the early years, most of this effort was concentrated in analytical studies, including various control designs. Experimental testing in flight and wind tunnel was mainly limited to the establishment of operational limits based on gross aerodynamic instabilities. With the advancement of digital computing, however, came the ability to perform dynamic, piloted simulations in real time and develop more complex models. This increase in the complexity of the system led to a requirement for better aerodynamic models — for both helicopter and load — and the emphasis in experimental work shifted accordingly. These days, there is still some analytical work being conducted, particularly in the design of automatic control systems, but much of the research is now undertaken using simulation.

2.1   Analytical Studies

Some of the earliest studies in helicopter slung-load behaviour was carried out by Lucassen and Sterk [1] in 1965 to provide a better understanding of the dynamics and indicate means to avoid undesirable effects, since they were known to cause a reduction in the helicopter's operational capabilities. In this work, the equations of motion were restricted to the vertical plane with three degrees of freedom (DOF), and load aerodynamics was not included. Later, Dukes [2] used a similar approximation to examine the modes of the system in the frequency domain and explore various feedback and open-loop control systems for damping the pendulous helicopter-load motion. Cliff and Bailey [3] also used a simplified model of a helicopter with a singly tethered load, which neglected all aerodynamics other than drag. In their formulation, the nonlinear equations of motion were linearised about a steady level flight condition, and then the resulting perturbation equations were separated into longitudinal and lateral-directional sets. Although the authors were able to make some inferences regarding the stability effects of various parameters, such as mass ratio and tether length, they suggested that more complete dynamical models needed investigation. An attempt to increase the fidelity of the aerodynamic load model was made by Feaster [4] and Feaster *et al* [5] using an experimentally determined yaw-damping coefficient in a linearised small perturbation stability analysis, which considered both single-cable and two-cable tandem suspension systems. The results agreed well with the previous model and full-scale tests and also demonstrated that the two-cable tandem suspension system offered a satisfactory means of transporting the standard cargo container examined. Around the same time, Prabhakar and Sheldon [6] and Prabhakar [7] undertook a theoretical study of a Westland Sea King helicopter carrying a standard cargo container on a two point longitudinal suspension. Again, the aerodynamic stability derivatives used in the model were determined through experiment and it was found that the pitch and yaw rate derivatives were strongly destabilising.

Over the following several years, Nagabhushan [8, 9] and Nagabhushan and Cliff [10] produced several reports on the dynamics, stability, and control of helicopters carrying

externally suspended loads. Several mathematical models of varying order were developed to describe the dynamics of such systems. However, unlike much of the previous analytical work, which was based on the Newton-Euler equations, the nonlinear formulation was derived from Lagrange's equations for general dynamical systems. In these reports, the low-speed stability characteristics of a conventional helicopter with an external sling load on a single-point suspension were investigated. Typically, towing cable length, towed body-to-vehicle mass ratio, and load factor in a turn were found to affect the stability of the aircraft and its sling load.

In 1986, Ronen [11] and Ronen *et al* [12] developed a new model for a helicopter carrying a sling load on a single point suspension in order to improve on the existing dynamic models and investigate the open loop characteristics of the system. For the first time, the model took into account the effects of rotor downwash on the load and the unsteady aerodynamics of bluff-body type loads. The nonlinear equations of motion were derived and then separated into two sets: the nonlinear trim equations and the linearised equations for small perturbation about the equilibrium. More recently, Curtiss [13] derived a full set of equations for the twin lift system, linearised about a hover trim condition.

2.2   Experimental Testing

Although there has been a substantial amount of experimental work in determining the aerodynamic behaviour of various slung loads using wind-tunnels, little has been done through full scale flight-testing. In 1968, Gabel and Wilson [14] presented the results of an extensive program of simulation, wind-tunnel, and flight tests, which were conducted to assist in solving the problems of sling load vertical bounce, sling-leg web flapping, and aerodynamic yaw instability. Some years later, Hone [15] utilised the data from actual flight tests on a Sikorsky CH-54 heavy-lift helicopter to investigate the validity of a model developed by Briczinski and Karas [16]. The aim of this work was to explore phenomena associated with the carriage of externally suspended loads on helicopters, and to establish more reliable strength requirement data for the load slings and their interfaces.

Other work in experimental testing includes those presented by Kesler *et al* [17], Feaster [4], Feaster *et al* [5], and Matheson [18].

2.3   Flight Simulation and Control

One of the first investigations into automatic control for helicopters with slung loads was conducted by Wolkovitch and Johnston [19] in 1965. The single-cable dynamic model was developed in a straightforward application of the Lagrange equations. Abzug [20] later expanded on this model to consider the case of two tandem cables. However, his formulation was based on the Newton-Euler equations of motion for small perturbations, separated into longitudinal and lateral sets. Aerodynamic forces on the cables and the load were neglected, as were the rotor dynamic modes.

In recognition of suspension-related problems encountered with the carriage of external cargo by helicopters, the US Army in 1970 initiated a program aimed at the establishment of design criteria for sling members and hard-points. This program, as well as many

subsequent investigations, were undertaken by the Eustace Directorate, US Army Air Mobility Research and Development Laboratory (USAAMRDL). Part of the first phase in the contract, reported by Briczinski and Karas [16], involved the computerised simulation of a helicopter and external load in real time with a pilot in the loop. Load aerodynamics were incorporated into the model, as well as rotor-downwash effects in hover. Soon after this program, Liu [21] conducted an extensive study to select the best technical approaches for stabilising a wide spectrum of externally slung helicopter loads at forward speeds. The simulation model used extended that of Abzug [20] to include load aerodynamics. Several stabilisation systems were evaluated using a moving-base simulator and of those, an electronic system providing rate and acceleration inputs to the helicopter's stability augmentation system (SAS) was favoured. The design and assessment of automatic control systems continued with Asseo and Whitbeck [22] in their paper on the control requirements for sling-load stabilisation. Linearised equations of motion of the helicopter, winch, cable, and load complex were developed for a variable suspension geometry and were then used in conjunction with modern control theory to design several control systems for each type of suspension. The next year, Gera and Farmer [23] examined the feasibility of stabilising external loads by means of controllable fins attached to the cargo. In their simple linear model representing the yawing and the pendulous oscillations of the slung-load system, it was assumed that the helicopter motion was unaffected by the load.

Following the first program of work sponsored by the Eustace Directorate, a further study to define important flight control system design and handling qualities criteria for moving loads slung beneath tandem-rotor helicopters was conducted by Kesler et al [17]. It included theoretical analyses, acquisition, and evaluation of both wind tunnel and flight test data, analysis of various problems, and the actual flight simulation of a Model-347 advanced tandem-rotor helicopter with an external load. Another program under the same sponsorship, investigated by Alansky et al [24], looked into the quantitative limitations of the CH-47 helicopter performing terrain flying with external loads. The simulation used in this investigation comprised a fully coupled total force and moment model and an alternative method of load-control named the Active Arm External Load Stabilisation System (AAELSS).

Some time later, a generalised real time, piloted, visual simulation of a single rotor helicopter, suspension system, and external load was developed by Shaughnessy et al [25], and subsequently validated for the full flight envelope of a CH-54 helicopter and cargo container. The mathematical model described used modified nonlinear classical rotor theory for both the main rotor and tail rotor, nonlinear fuselage aerodynamics, an elastic suspension system, nonlinear load aerodynamics, and a load-ground contact model.

In 1980, Sampath [26] completed his PhD dissertation on the dynamics of a tandem-rotor helicopter slung-load system, which involved modelling and simulation as well as experimental wind-tunnel tasks. In his formulation, Lagrange's equations were used to write the equations of motion and were divided into two sets: one for the towing vehicle and the other for the slung load. The cables of the sling were modelled as massless linear springs with viscous damping and no aerodynamic properties. The aerodynamic models for the helicopter and load were both implemented using tabulated static data. Some years later, a full nonlinear simulation model of the CH-47B helicopter, developed by the Boeing Vertol Company, was adapted for use in the NASA Ames Research Center (ARC) simulation facility by Weber et al [27]. The mathematical model developed was based

on a total force approach in six rigid-body DOF along with the option for an externally suspended load in three DOF. The aerodynamic models were also quite comprehensive, including steady-state rotor flapping and load aerodynamic effects.

More recently, research into the automatic control of load dynamics has continued with Raz *et al* [28] in an investigation of an active aerodynamic Load Stabilisation System (LSS) for a helicopter sling-load system. The general theoretical model used was based on previous work [11] for configurations with a single suspension point.

Some of the most recent work in the simulation of helicopter slung-load systems has been conducted by Cicolani and Kanning [29, 30] and Cicolani *et al* [31] at the NASA ARC. In this work, the general simulation equations were derived for the motion of slung-load systems consisting of several rigid bodies connected by straight-line cables or links, assumed to be either elastic or inelastic. A formulation for the general system was obtained from the Newton-Euler rigid-body equations with the introduction of generalised velocity coordinates. The same approach for simulating helicopter slung-load dynamics has been adopted in the current work at AMRL. In addition, the equations of motion have been extended to the case of multiple loads with disparate mass and aerodynamic characteristics and sling configurations.

2.4   Surveys and Overviews

In his book on the dynamics of helicopter flight, Saunders [32] devoted one section to piloting problems associated with the carriage of external loads. The normal trim state and origins of load oscillation were first examined using a simple helicopter-load mass model. Various problems, including uncontrollable load oscillations, aerodynamic excitation, active control, and poor visibility were then discussed in a broad context.

In 1976, Matheson [18] compiled a review of the developments and data concerning the operation of helicopters with slung loads. The report focused on the problems of aerodynamic instability, vertical bounce, and sling-leg flapping. Methods for reducing these instabilities and procedures for extending the operating limits of a helicopter with different types of slung loads were also discussed.

Around the same time, Shaughnessy and Pardue [33] conducted a survey of the helicopter sling load accident/incident records provided by various US organisations for the period from 1968 to 1974. From the data, the highest percentage of accidents occurred during hover, and it was therefore concluded that hovering was the most critical sling load flight operation. Furthermore, the accidents and incidents caused by swinging loads during cruise were generally much less severe than the hover mishaps.

3   System Representation

3.1   Description of System

Helicopter slung-load systems fall into a class of multibody dynamic systems consisting of two or more rigid bodies connected by massless links. The links can be considered either elastic or inelastic, although the rigid-body assumption excludes any helicopter or load elastic modes. Typically, the system is characterised by the configuration geometry, mass, inertia, and aerodynamic behaviour of both helicopter and load, as well as the elastic properties of the links.

In general terms, the system of interest consists of a single helicopter supporting one or more loads by means of some suspension. Several examples of the various configurations under consideration are illustrated in Figure 1. The model is comprised of n rigid bodies, $B1,B2,...,Bn$, with m straight-line links supporting a single force in the direction of the link. For cables, this is strictly a tensile force — cable collapse is not considered. If the links are modelled as inelastic, c ($\leq m$) holonomic constraints[1] are imposed on the motion of the bodies and the system has $d = 6n - c$ DOF. If the links are modelled as elastic, there are $6n$ DOF.

In the model used, a number of simplifying assumptions were made. These included the exclusion of cable aerodynamics and rotor-downwash effects. Furthermore, load aerodynamics have been neglected for this initial stage of the work. Despite these limitations, the system defined above has proven adequate for simulation studies [31] in which the low-frequency behaviour is of primary interest.

3.2   Generalized Equations of Motion

The simulation model used for this first stage of work was based on the helicopter slung-load system introduced by Cicolani and Kanning [29]. In this formulation, the general system equations of motion are obtained from the Newton-Euler equations in terms of generalised coordinates and velocities. Following the explicit constraint method, which utilises d'Alembert's principle, the system is partitioned into coordinates such that the motion due to cable stretching is separated from that due to rigid-body, coupled dynamics. As a consequence, the constraint forces appear explicitly and a solution to the resultant generalised accelerations is determined by assuming a simple spring model for the cable.

It is also possible to obtain a solution to the inelastic approximation by nulling the stretching coordinates to obtain an explicit relation for the suspension forces. The result is computationally more efficient than conventional procedures and is readily integrated with the formulation for elastic suspension. Another benefit of the formulation is that it is easily applied to complex, multiple body systems, as in the current work. To date, all code development has been done in the MATLAB numerical computing environment,

---

[1]Holonomic constraints represent excess coordinates which are independent and can be eliminated through equations of constraint.

which provides a high-performance language, amenable to modelling and simulation type work.
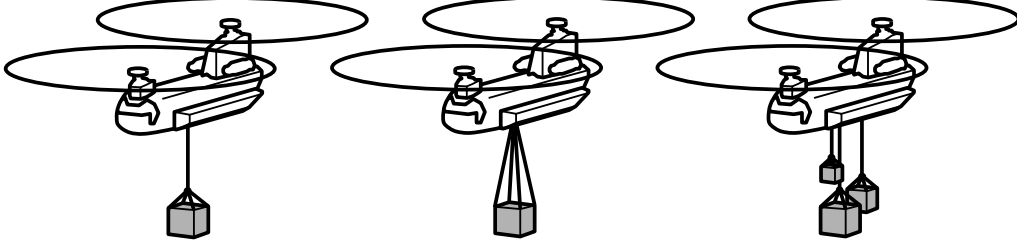
Figure 1: Single Point Slung-Load Configurations

The Newton-Euler equations of motion for a system of n rigid bodies can be expressed in six DOF as

$$\begin{array}{rcl} mi\,g_N + \ FAi_N + \ FCi_N - \ mi\,\dot{V}i_N^* & = & 0 \\ MAi_i + \ MCi_i - \ Ji\,\dot{\omega}i_i - \ S(\omega i_i)\,Ji\,\omega i_i & = & 0 \end{array} \quad ; \quad i = 1, 2, \ldots n \qquad (1)$$

In this expression, the first set of equations represents the balance of translational forces, where the subscript N denotes the inertial axes. The second set represents the sum of moments about each body's cg, where the subscript i denotes the corresponding body axes. Both equations are comprised of several terms including the forces and moments due to gravity, aerodynamics, and inertia. The first term, $mi\,g_N$, is the gravity force acting through each cg, FAi_N and MAi_i are the aerodynamic forces and moments respectively, and FCi_N and MCi_i the cable forces and moments respectively. The terms $mi\,\dot{V}i_N^*$ and $Ji\,\dot{\omega}i_i$ constitute the inertial reaction of each body, and $S(\omega i_i)\,Ji\,\omega i_i$ is the moment induced by the Coriolis effect.

It is convenient to write these equations as a single expression in matrix form. Denoting the configuration position vector as r and the configuration velocity as v for the system,

$$r = \begin{bmatrix} R1_N^* \\ \vdots \\ Rn_N^* \\ \alpha 1 \\ \vdots \\ \alpha n \end{bmatrix} \qquad v = \begin{bmatrix} V1_N^* \\ \vdots \\ Vn_N^* \\ \omega 1_1 \\ \vdots \\ \omega n_n \end{bmatrix} \qquad (2)$$

where the rigid-body cg positions $Ri_N^* = \begin{bmatrix} x_i & y_i & z_i \end{bmatrix}^T$ and Euler angles $\alpha i = \begin{bmatrix} \phi_i & \theta_i & \varphi_i \end{bmatrix}^T$. The corresponding velocities $Vi_N^* = \dot{R}i_N^* = \begin{bmatrix} \dot{x}_i & \dot{y}_i & \dot{z}_i \end{bmatrix}^T$ and the angular rates $\omega i_i = \begin{bmatrix} p_i & q_i & r_i \end{bmatrix}^T$ are related to the Euler angle rates via the transformation

$$\omega i_i = Wi_i\,\dot{\alpha}i \qquad (3)$$

where

$$Wi_i = \begin{bmatrix} 1 & 0 & -\sin\theta_i \\ 0 & \cos\phi_i & \sin\phi_i\cos\theta_i \\ 0 & -\sin\phi_i & \cos\phi_i\cos\theta_i \end{bmatrix} \qquad (4)$$

Using fg, fa, fc, and f^*, for the combined force-moment vectors due to gravity, aerodynamics, cable suspension, and inertia plus Coriolis effects, the equations of motion can be written

$$fg + fa + fc + f^* = 0 \tag{5}$$

where

$$fg = \begin{bmatrix} m1\,g_N \\ \vdots \\ mn\,g_N \\ 0 \\ \vdots \\ 0 \end{bmatrix} \qquad fa = \begin{bmatrix} FA1_N \\ \vdots \\ FAn_N \\ MA1_1 \\ \vdots \\ MAn_n \end{bmatrix} \qquad fc = \begin{bmatrix} FC1_N \\ \vdots \\ FCn_N \\ MC1_1 \\ \vdots \\ MCn_n \end{bmatrix} \tag{6}$$

and

$$f^* = -D\dot{v} - X \tag{7}$$

where

$$D = \begin{bmatrix} m1 & & & & & \\ & \ddots & & & 0 & \\ & & mn & & & \\ & & & J1 & & \\ & 0 & & & \ddots & \\ & & & & & Jn \end{bmatrix} \qquad X = \begin{bmatrix} 0 \\ \vdots \\ 0 \\ S(\omega1_1)\,J1\,\omega1_1 \\ \vdots \\ S(\omega n_n)\,Jn\,\omega n_n \end{bmatrix} \tag{8}$$

Here, D is a block-diagonal matrix comprising masses and inertias along the main diagonal, $\dot{v}$ is the configuration acceleration and the matrix X contains the Coriolis terms due to the use of rotational coordinates in body-axes

In order to derive a set of simulation equations for the system, a solution to the equations of motion described above must be found; that is, an expression for the configuration acceleration in terms of the system states and applied forces. For the helicopter slung-load system under consideration, it is useful to first formulate a set of generalized coordinates and velocities which describe the motion of the inelastic system and the effect of cable stretching as two distinct subsets. An inelastic system with n bodies and c constraints will have $d = 6n - c$ DOF. The cable constraints on the helicopter slung-load system can be considered holonomic. In addition, for the following system, the constraints will be posed as time invariant. The special cases of cable winching and attachment-point movement are not considered.

The system can be partitioned according to the $6n$ generalized position coordinates as follows:

$$q = \begin{bmatrix} q1 \\ \lambda \end{bmatrix} \tag{9}$$

where $q1$ is the list of d position coordinates for a system with inelastic suspension and λ are the c coordinates which describe the variation in cable length due to stretching. The configuration velocity can be expressed as a linear function of the generalized velocity coordinates

$$v = Au \tag{10}$$

where

$$u = \begin{bmatrix} u1 \\ \dot{\lambda} \end{bmatrix} \qquad A = \begin{bmatrix} A1 \\ L \end{bmatrix} \tag{11}$$

Differentiating Equation (10) and substituting $\dot{v}$ into Equation (7) yields

$$f^* = -D\dot{A}u - DA\dot{u} - X \tag{12}$$

Now, replacing f^* in Equation (5), the following simplified version of the equations of motion can be written:

$$fo + fc - DA\dot{u} = 0 \tag{13}$$

where the vector fo is the sum of all external forces and inertial coupling terms, i.e.

$$fo = fg + fa - D\dot{A}u - X \tag{14}$$

Since the system has been specified in terms of its generalized coordinates, A is a square $6n \times 6n$ nonsingular matrix and a solution for the generalized acceleration coordinates exists. From Equation (13), the acceleration equation is

$$\dot{u} = A^{-1}D^{-1}[fo + fc] \tag{15}$$

It should be noted here that the inverse matrix A^{-1} simply represents the relation $u(v)$ that can be derived analytically from the kinematics. Therefore, it is unnecessary to perform a costly numerical inversion to obtain $\dot{u}$. In partitioned form, the acceleration equation is

$$\begin{bmatrix} \dot{u}1 \\ \ddot{\lambda} \end{bmatrix} = \begin{bmatrix} AI1^T \\ \Lambda^T \end{bmatrix} D^{-1}[fo + fc] \tag{16}$$

where $AI1^T$ and Λ^T are the $6n - c$ and c rows of A^{-1} which define the relations $\dot{u}1$ and $\ddot{\lambda}$ respectively. From the first set of equations representing the inelastic component, the solution for $\dot{u}1$ is

$$\dot{u}1 = AI1^T D^{-1}[fo + fc] \tag{17}$$

The second set of equations represents the elastic component

$$\ddot{\lambda} = \Lambda^T D^{-1}[fo + fc] \tag{18}$$

An alternate formulation for the accelerations $\dot{u}1$ can be obtained by first differentiating the expanded form of the configuration velocity from Equation (10) as follows:

$$v = A1u1 + L\dot{\lambda} \tag{19}$$

and then substituting into Equation (7) to give

$$f^* = -D\dot{A}1u1 - DA1\dot{u}1 - D(L\ddot{\lambda} + \dot{L}\dot{\lambda}) - X \tag{20}$$

If fo is redefined:

$$fo = fg + fa - D\dot{A}1u1 - X \tag{21}$$

9

then replacing f^* in Equation (5) and solving for $\dot{u}1$ produces

$$\dot{u}1 = [A1^T D A1]^{-1} A1^T [fo - D(L\ddot{\lambda} + \dot{L}\dot{\lambda}) + fc] \tag{22}$$

The last step required in determining a solution for the generalized accelerations is to calculate the constraint force fc. For a system with c constraints, the constraint force can be expressed as

$$fc = Hs \tag{23}$$

where the columns of the matrix H are configuration vectors and rank $H = c$. The elements of the vector s are arbitrary scalars to be determined. The exact form of this equation and its solution depend on whether the cables are considered elastic or not.

Elastic System

For a general elastic system with M cable-body attachments, the suspension forces on each body can be given as the sum of forces and moments applied at each attachment point on that body, i.e.

$$fc = \sum_{j=1}^{M} hj\, \tau_j \tag{24}$$

In this formulation, the configuration vector hj defines the force and cg moment due to a unit load at the jth cable attachment, and τ_j is the cable tension. Referring to Figure 2, $\mathbf{kcj}$ and $(\mathbf{Ri^*j} \times \mathbf{kcj})$ denote the constraint force and moment per unit tension respectively, on body $Bi(j)$ due to the jth cable attachment. The vector $\mathbf{kcj}$ is the cable direction outward from the body, and $\mathbf{Ri^*j} = (\mathbf{Rj} - \mathbf{Ri^*})$ is the moment-arm of the attachment point about the cg.
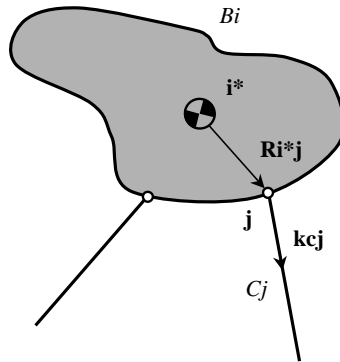

Figure 2: Suspension Forces on a Rigid Body

The tension in each cable is given by a simple spring model as

$$\tau_j = \max\{0, Kj(\ell j - \ell oj\} + cj\dot{\ell}j\} \quad ; \quad j = 1, 2, \ldots, M \tag{25}$$

where ℓoj and ℓj are the unloaded and instantaneous cable lengths, and Kj and Cj are the cable spring and damping constants.

Inelastic System

It can be shown that the columns of H and Λ both form bases of the same linear vector space and therefore Λ can be used to define the constraint force, i.e.

$$fc = \Lambda s \tag{26}$$

where the vector s will have units of force if the coordinates λ are lengths. To find a solution for the inelastic system, the constraint acceleration is set to zero, i.e. $\ddot{\lambda} = 0$. Substituting into Equation (18) gives

$$0 = \Lambda^T D^{-1}[fo + \Lambda s] \tag{27}$$

the solution to which is

$$s = -[\Lambda^T D^{-1}\Lambda]^{-1}\Lambda^T D^{-1}fo \tag{28}$$

3.3 Simulation of Helicopter Slung Load System

Prior to executing the simulation, several components must be customised to the helicopter slung-load configuration of interest.

The first step in setting up the simulation equations involves determining the constraints of the inelastic system and then defining the generalised velocity coordinates ($u1$, $\dot{\lambda}$). Using these coordinates in kinematic relations for the system, it is then possible to obtain expressions for the system matrices A, A^{-1}, and $\dot{A}$. The selection of appropriate coordinates is case specific; however, it is possible to choose them so that they consist largely of natural vectors. In most applications, including that discussed in this report, u is comprised of the cg velocity of a reference body (typically the helicopter), the cable velocities, and the angular velocities of all bodies including both helicopter and loads.

Next, an appropriate representation for the suspension cables must be chosen. For inelastic cables, fc is calculated from any basis of the constraint force space Λ and the corresponding constraint force parameters s as in Equation (28).

For the last step, the aerodynamic and inertial properties of both the helicopter and loads need to be implemented in the model. For most rigid bodies, the aerodynamic forces and moments are a function of the configuration velocities and displacements v and r, and the control inputs δ. Typically, the helicopter aerodynamic model neglects position-dependent and acceleration-dependent effects such as interbody-ground interference and unsteady aerodynamics. However, these are often secondary in nature and the resulting model is adequate for simulation under most conditions. Aerodynamic models for loads, which are generally unsteady and of much higher order, are less well understood or replicated.

Once the system has been configured, the dynamic simulation can proceed. First, the initial state (u, r) and the trim state (u_0, r_0) must be set. Then the integration loop is started and the following steps are executed in sequence, according to the flow-diagram of Figure 3:
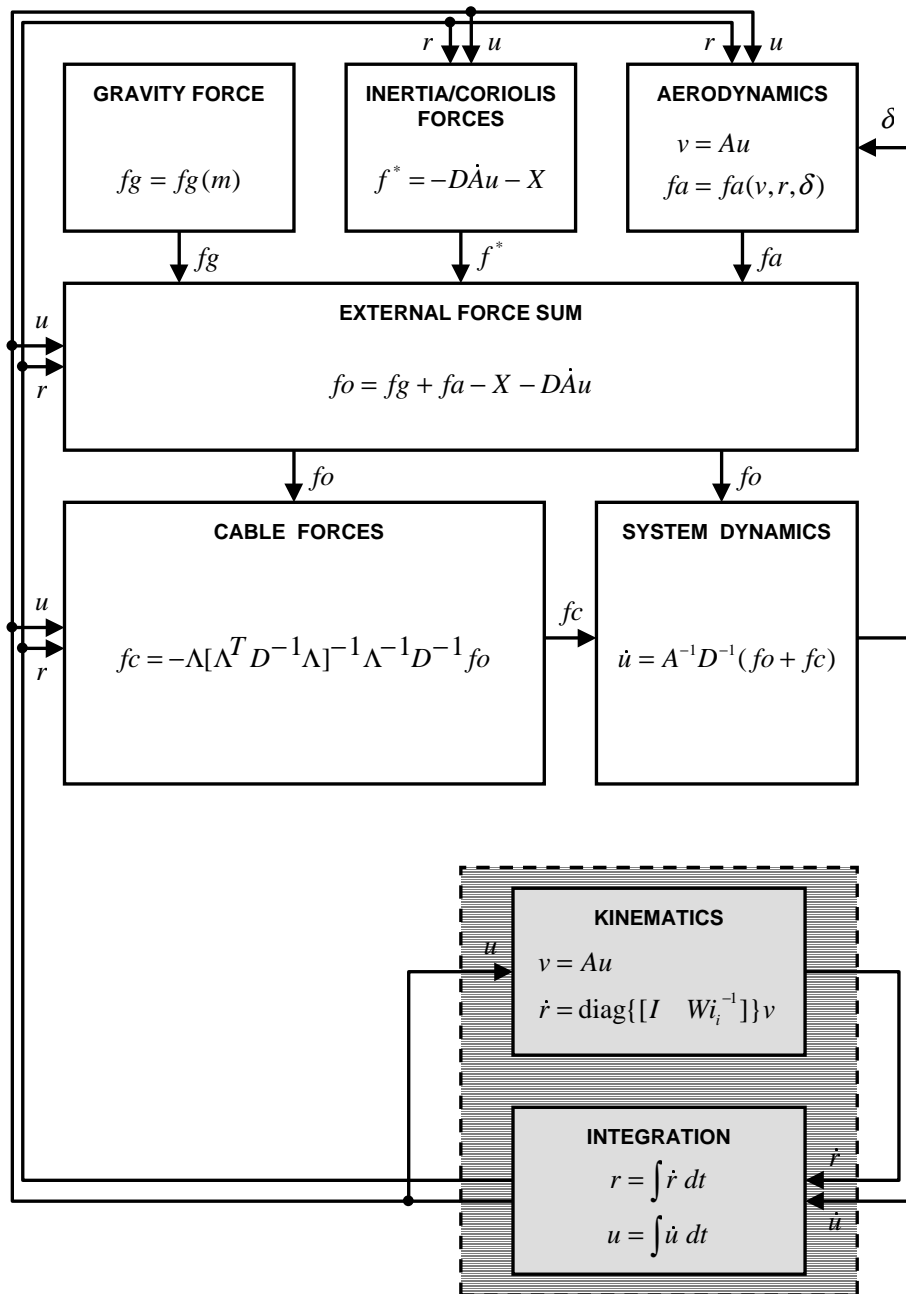
Figure 3: Simulation Flow Diagram

1. Determine the aerodynamic force fa, inertia, and Coriolis forces f^*, and gravity force fg, all in inertial axes. Assuming the aerodynamic model is written in body axes, an angular transformation will be required for fa. The configuration velocity v can be calculated from the generalised velocity u using the kinematic matrix A.

2. Sum the external forces fa, f^*, and fg to yield the configuration force fo.

3. Using the configuration force along with matrices derived from the current state (u, r) and the configuration geometry, solve the cable force fc for either elastic or inelastic suspension models.

4. Compute the generalised accelerations $\dot{u}$ from the inverse kinematic matrix A^{-1}, and the inverse mass matrix D^{-1}.

5. Compute the velocity $\dot{r}$ from the configuration velocity and inverse transformation matrix W^{-1}.

6. Apply an integration step to predict the new state (u, r) and repeat the sequence.

At this early stage, all code development has been done in the MATLAB [34] numerical computing environment, which provides a high-performance language amenable to modelling and simulation work. It is important to stress that this *pilot* simulation was not intended to run in real time, but rather produce the appropriate output for subsequent replay and analysis. At a later stage, the code will be ported to a platform-specific compiled language suitable for piloted, real time simulation.

The Helicopter Slung-Load Simulation (HSLSIM) program, consists of several modules. These including the main script, integration function, differential equation solution, aerodynamic model, and various output and replay functions. The simulation is run through the main script, which generates the control inputs, configures the helicopter-load system properties (geometric and inertial), sets the initial system state, and then executes the integration function. The integration function ODE45 is problem independent and based on an algorithm which combines 4th and 5th order Runge-Kutta formulas for ordinary differential equations. It requires a function tailored to the problem at hand, which provides a point solution to the differential equation. For the helicopter slung-load simulation, this function represents the core of the code and implements much of the above flow diagram. The aerodynamic models for both helicopter and loads are called from within this function. They can be as simple or as complex as desired, but must output total force and moment variables. Hence, if small-perturbation aerodynamic models are to be used, they must be augmented with the corresponding trim forces and moments. The cable elastic model can also be implemented as a separate function, although this was not done, since the spring-damper model is fairly standard and easily included in the solution function. Following summation of the external forces and solution of the internal (cable) forces, the solution function computes the generalised accelerations and velocities $(\dot{u}, \dot{r})$ at the current state. This point solution is passed to the integration function and the simulation loop continues.

It is also possible to calculate a linear model by numerical approximation of the Jacobians $\bigtriangledown_u \dot{u}$ and $\bigtriangledown_\delta \dot{u}$ from the nonlinear system.

This model will have the form

$$\dot{u} = [\bigtriangledown_u \dot{u}]u + [\bigtriangledown_\delta \dot{u}]\delta \tag{29}$$

and can be used for an alternative linear simulation about the trim state. Another use is in various linear system analyses, such as the determination of the natural modes, which will be discussed in the following section.

4 Simple Pendulum System Dynamics

The first phase of the analysis involved an investigation of the dynamics of pendulum-type systems. For this purpose, the full helicopter slung-load simulation model developed in Section 3 was constrained so as to approximate a two-body pendulum system. Furthermore, the aerodynamic effects of both helicopter and load were excluded from the model.

4.1 System Properties

The simulation was validated for both free and constrained models using the system given in Reference [11] for a CH-53D helicopter with a single slung load. The CH-53D is a twin-turbine, main and tail rotor transport helicopter with mass and inertia properties as outlined below.

Mass (lb)	Moments of Inertia (slug.ft^2)			
m_h	I_{xx}	I_{yy}	I_{zz}	I_{xz}
35000	36100	191500	179200	14800

The slung load chosen was a standard military container, known as a MILVAN, which is a common helicopter cargo used in many commercial and military operations. The dimensions of a MILVAN container are $20 \times 20 \times 8$ ft and the mass typically varies from 4000 lb (empty) to 20000 lb (full). In the Reference cited above, examples with masses outside this range were also checked to demonstrate very low density and very heavy loads. The moments of inertia for the container load were approximated with linear functions of its mass by

$$I_{xx} = 0.33 * m_l \qquad I_{yy} = I_{zz} = 1.20 * m_l \tag{30}$$

where the moments of inertia are in slug.ft^2 and the mass is in lb.

4.2 Analysis of System Modes

In order to validate the simulation developed, comparisons were made against those previously reported in a numerical example given in Reference [11]. In addition, analytical results were calculated for the modes of similar pendulum systems. The governing equations for these systems are detailed in Appendix B, along with several simplifying approximations and solutions to each in terms of their natural frequencies.

For the example cited, the mass ratio is $m_l/m_h = 0.05$. Using Equation (30), this yields the following load properties,

Mass (lb)	Moments of Inertia (slug.ft^2)			
m_l	I_{xx}	I_{yy}	I_{zz}	I_{xz}
1750	577.5	2100	2100	0

The sling configuration used consisted of a single pendant suspension and bridle, as illustrated in Figure 4. The total sling length L between helicopter attachment point and the load cg is 25 ft, and the pendant-to-sling length ratio ℓ/L is 0.6.
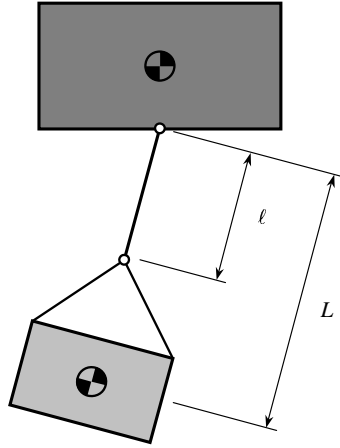
Figure 4: Two-body Pendulum Simulation System

For the system examined, there are two oscillatory modes in both longitudinal and lateral axes. Essentially, the low frequency mode is associated with the pendulous motion of the load along the total sling length. The higher frequency mode is associated with the coupled pitching (or rolling) motion of the load and bridle and the pendant suspension. Values for the natural frequencies obtained from the analytical formulation and the simulation are listed in Table 1. The first column of analytical results was calculated from Equation (B16). The second and third columns pertain to the models generated by the simulation code HSLSIM developed in the current study. Of these, one was constrained so as to approximate the pendulum system used in the analytical derivation, which for the longitudinal case included constraints in translation along both y and z axes, and constraint in rotation about the y axis. The other model was free to move in all axes, providing a closer approximation to the real system. The fourth column lists the frequencies obtained in the previous analysis using the simulation code EOMPROG.

Table 1: Pendulum Mode Frequencies (rad/s) for CH-47B-MILVAN System in Hover

MODE	ANALYTICAL (EQ. (B16))	HSLSIM CONSTRAINED	HSLSIM FREE	EOMPROG (REF. [11])
Longitudinal (mode I)	1.12	1.12	1.15	1.14
Longitudinal (mode II)	3.86	3.86	3.86	3.84
Lateral-roll (mode I)	1.15	1.16	1.25	1.24
Lateral-roll (mode II)	7.17	7.17	7.18	7.14

Agreement between the analytical results and the constrained model is very good. However, there are some small discrepancies between those first two sets and the last two sets — the unconstrained models. This can be explained by an additional coupling effect in the unconstrained models, as the sling force at the attachment point produces a moment about the helicopter cg. The effect is more prominent in the lateral case, since the helicopter moment of inertia is relatively low in that axis. Differences between the unconstrained model generated in HSLSIM and EOMPROG are understandable, as they were generated by two quite different approaches. The simulation code HSLSIM incorporates a full nonlinear representation of the helicopter slung-load system, which was

linearised numerically about the trim state to obtain a Jacobian matrix for model analysis (*see the following section*). Using this Jacobian matrix approach would therefore incur errors from the numerical approximation. EOMPROG, on the other hand, is based on an explicitly linear small-perturbation formulation and, consequently, errors would arise from such simplification as the small angle assumptions and the exclusion of higher order terms.

It is also interesting to see how the analytical solution compares with the unconstrained simulation model HSLSIM for a range of configurations. Figures 5 and 6 show the variation in natural frequency for the longitudinal pendulum modes with load-to-helicopter mass ratio m_l/m_h and pendant-to-sling length ratio ℓ/L, respectively. Clearly, there is quite a large difference in the higher frequency mode over the range of ℓ/L with a smaller deviation in the lower frequency mode. The analytical approximation is most accurate at a length ratio of 0.6, but outside this differs dramatically. At a length ratio of 0.1, the error is close to 50% of the frequency predicted by HSLSIM. At a length ratio of 0.9, the error is approximately 120%. There is less difference in the modes over the range of m_l/m_h. For the configurations examined, the largest error of 20% occurred in the lower frequency mode at a mass ratio of 1.0. This error improved as the mass ratio was decreased, reaching a level of 5% at a ratio of 0.1. Both of these discrepancies are due to the simplification of the analytical model, which prohibits any pitching motion about the helicopter cg. Therefore, as a result of this test, one can conclude that the analytical approximation given in Appendix B is only appropriate for low load-to-helicopter mass ratios and moderate pendant-to-sling length ratios (0.6 for the system examined).

4.3   Longitudinal and Lateral Simulations

Following linear analysis of the modes, several simulations were run so as to gain a better picture of the inherent dynamic behaviour of the slung-load system. Simulations of both longitudinal and lateral subsystems were conducted. From the longitudinal simulations, two cases have been selected for inclusion here to illustrate the effect of heavy loads on the helicopter response. From the lateral simulations, two cases are included, which demonstrate the instability in yaw for a multiple-load system.

For the longitudinal simulations, the helicopter-load configuration was the same as that used in the linear analysis, i.e. a CH-53D helicopter and MILVAN load attached by a single pendant suspension. It was also constrained in the lateral-directional axes, as before. The slung load was initially offset from its static equilibrium position at hover, with the sling cable set at -30° in pitch and the load at -15°. It was then allowed free response over the 10 s duration. The time history response plots for two different load configurations, with mass ratios of 0.05 and 1.0, are presented in Figures 7 and 8, respectively. In the first set of plots, it can be seen that the load, with a small mass compared to the helicopter, has very little effect on the helicopter motion, as expected. Both low and high pendulum natural frequencies (0.18 and 0.61 Hz) of the load can be readily identified in the traces of forward velocity and pitch rate, respectively. The normal acceleration and cable force oscillate at approximately twice the high pendulum natural frequency and are highly correlated, with peaks at the pitch rate extremes (0.36 Hz). For the cable force, these peaks have magnitudes which are roughly 1.5 times the static load. The longitudinal
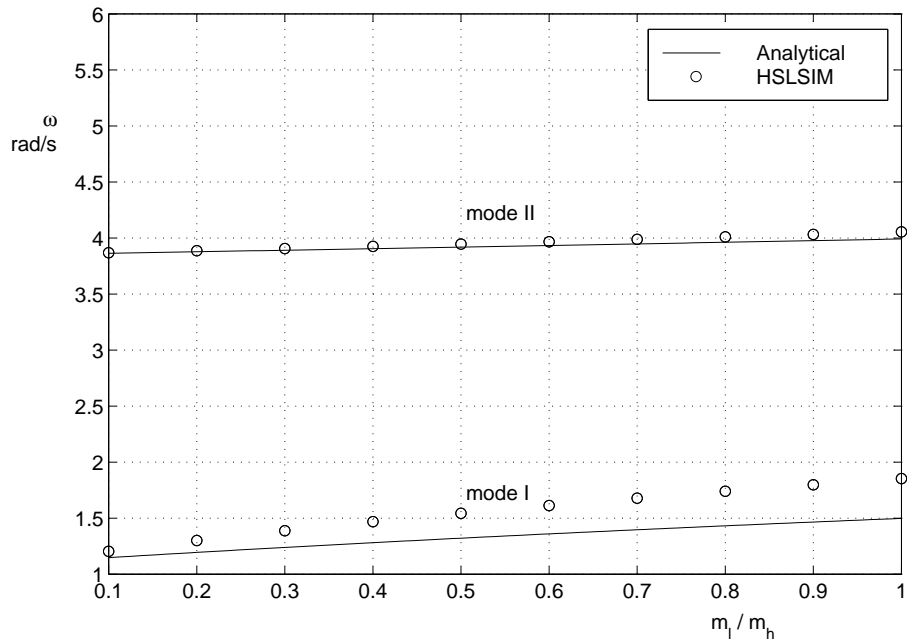
Figure 5: CH-53D-MILVAN System Longitudinal Pendulum Modes – Variation in Frequency with Load-to-Helicopter Mass Ratio
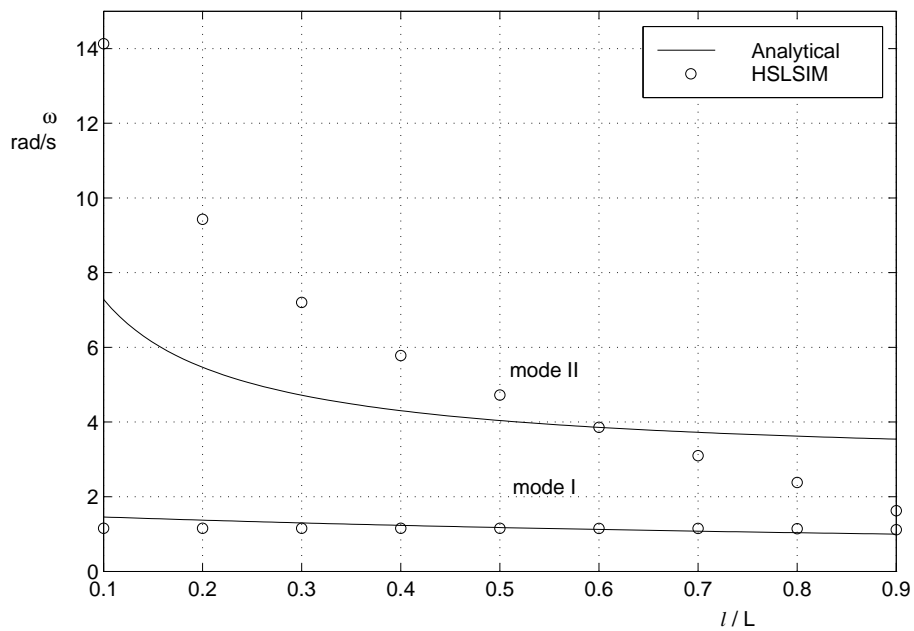
Figure 6: CH-53D-MILVAN System Longitudinal Pendulum Modes – Variation in Frequency with Pendant-to-Sling Length Ratio

acceleration is also highly correlated with the cable angle. In the second set of plots, it is clear that the load, now with mass equal to the helicopter, has had a significant effect on the helicopter motion. The pendulum natural frequencies are also less well defined (0.30 and 0.64 Hz). Unlike the first simulation, in this case the helicopter reaches velocities of similar magnitude, as the load and the accelerations in forward and normal directions are out of phase by 180°. Once again, the cable force oscillates at approximately twice the high pendulum natural frequency, with peaks near the pitch rate maxima (0.33 Hz).

For the lateral simulations, a CH-47B helicopter and two box containers attached by multiple (bridle) cables were used. The helicopter was constrained in the longitudinal and lateral axes, which restricted it to a yawing/side motion. The forward-attached slung load was initially offset by a bank angle of -30° so as to be displaced to the starboard side of the helicopter, and the aft-attached slung load was offset by an angle of 30°, resulting in a displacement to the port side. Once again the system was allowed free response over 10 s. The time history response plots are presented in Figures 9 and 10, for configurations with total mass ratios of 0.05 and 1.0. From these plots, the symmetric nature of one of the pendulum modes can be seen. Specifically, the velocity component v, bank angle ϕ, pitch angle θ, and acceleration component $\dot{v}$ for each load is 'mirrored' by the other. Slight deviations have come about because of the different attachment point locations with respect to the helicopter cg. It is also important to note that there is a very low frequency response in yaw for both helicopter and load, which manifests itself through the yaw rate r and azimuth angle ψ. Although these two traces seem to be diverging, they are actually just at the start of a long period (< 0.01 Hz) oscillation. This oscillation has an amplitude of approximately 160° in the helicopter azimuth angle. The effect of the loads swinging in this manner therefore has a significant influence on the yaw of the helicopter.
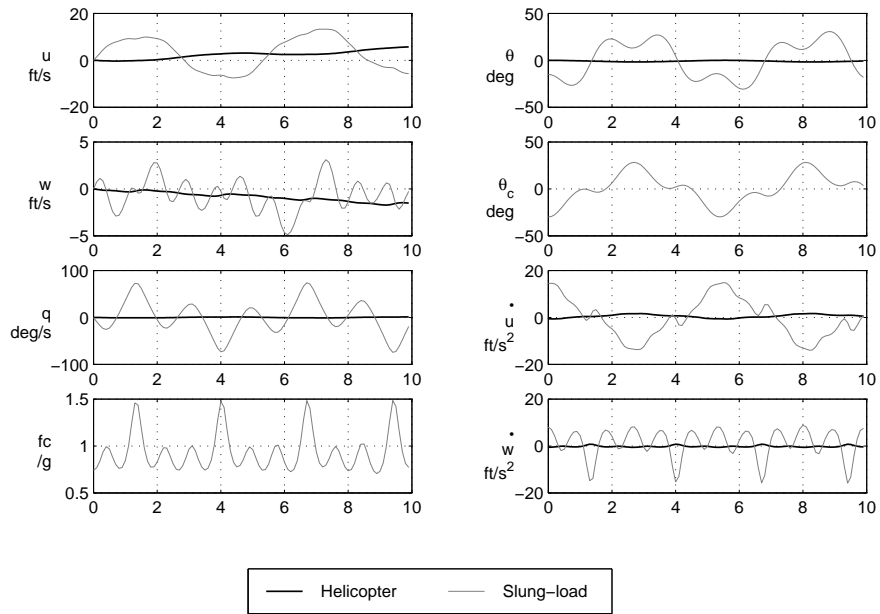
Figure 7: CH-53D-MILVAN System Time History Response — Mass Ratio 0.05
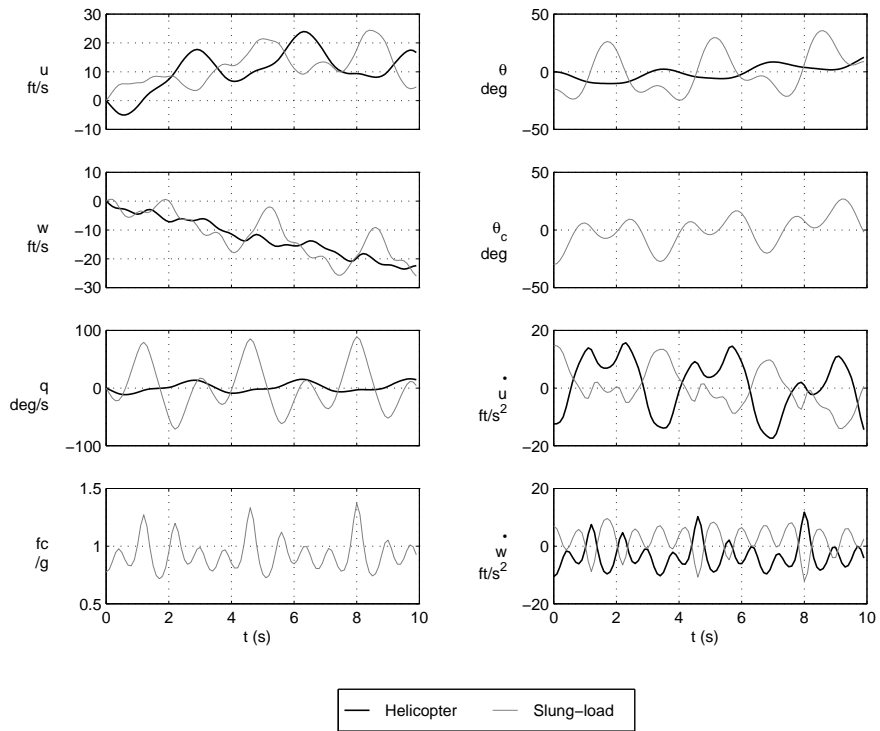
Figure 8: CH-53D-MILVAN System Time History Response — Mass Ratio 1.00
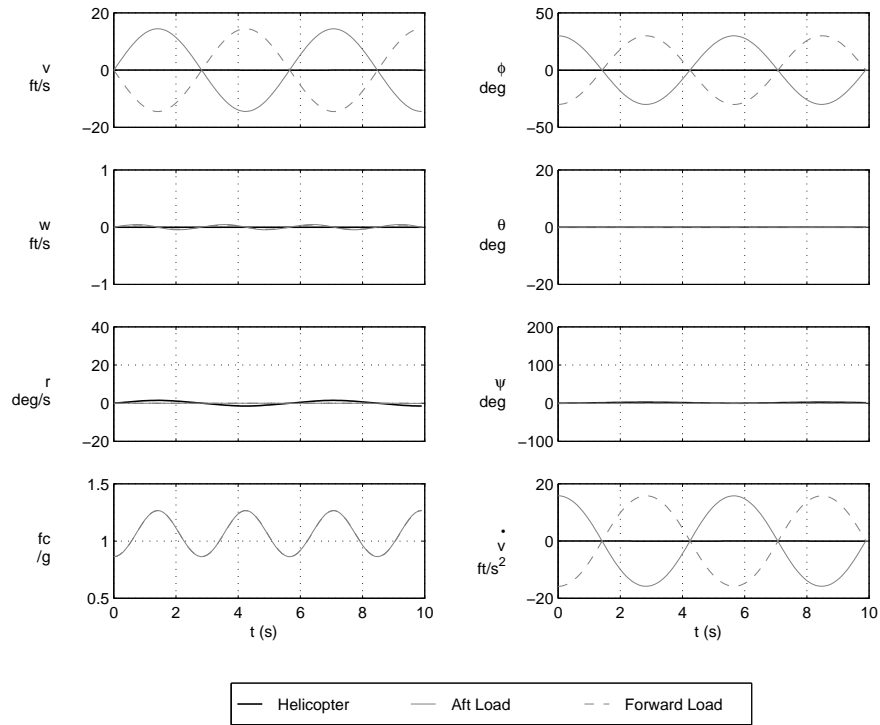
Figure 9: *CH-47B with Dual Load System Time History Response — Individual Mass Ratio 0.025*
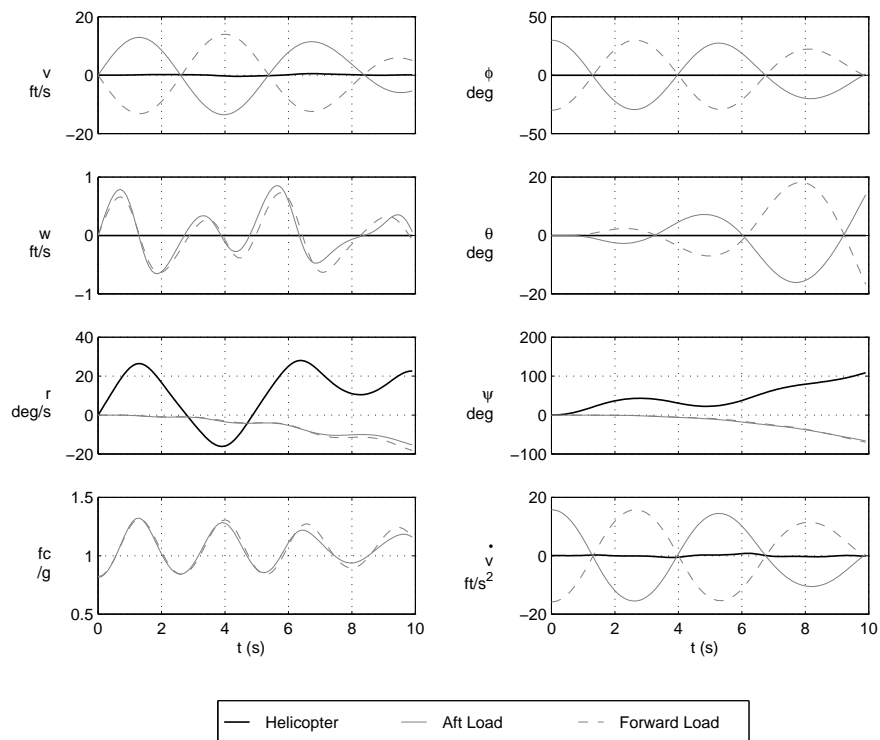
Figure 10: *CH-47B with Dual Load System Time History Response — Individual Mass Ratio 0.50*

5 Helicopter Slung-Load Dynamics

The second phase of the analysis examined the dynamics of the full helicopter slung-load simulation model. Both the CH-53D and the CH-47B helicopters with various slung-load configurations were considered. These models were free in all axes and incorporated basic helicopter aerodynamics.

The CH-53D helicopter model was essentially the same as used in the previous section, but with the inclusion of aerodynamic effects. Furthermore, the same MILVAN slung load was used in all of the single-load configurations examined. The main focus of the analysis, however, was various configurations of the CH-47B helicopter with slung loads. The CH-47B is a twin-turbine, tandem rotor transport helicopter with multiple sling attachment points. It has the following mass and inertia properties:

Mass (lb)	Moments of Inertia (slug.ft^2)			
m_h	I_{xx}	I_{yy}	I_{zz}	I_{xz}
33000	34000	202500	191000	14900

5.1 Unloaded Helicopter Dynamic Modes

The aerodynamic model used for both helicopters was based on simple linear state-space formulation with six degrees of freedom and four control inputs. For the CH-53D, the stability and control derivatives, as well as the corresponding trim conditions, were obtained from Reference [35]. Several small modifications were also made as applied in Reference [11] in order to perform a valid comparison. For the CH-47B, the derivatives and trim conditions were obtained from Reference [27]. Since the aim of this analysis was simply to determine the modes of oscillation for the helicopter slung-load system, the Automatic Flight Control System (AFCS) was not implemented.

In the above references, the stability and control derivatives for both helicopter models were tabulated for a range in trim airspeed. For the CH-53D, the derivatives were given for speeds of 0, 10, 20, 40, 60, 80, 100, 120, and 140 KTAS. Furthermore, to illustrate the change in behaviour of the unloaded helicopter, the eigenvalues were calculated at each of these airspeeds and drawn on the complex plane in the form of a root locus plot.

Validation of the helicopter model developed in the current work was performed by calculating the same eigenvalues at each airspeed and then comparing against those reported in Reference [11]. Figure 11 presents the eigenvalues for the CH-53D obtained from both analyses.

Although there are some small differences, the eigenvalues are generally quite close. As in the previous section, those differences can be explained by the different linearisation approaches. There was also some inherent error in transcribing the published results to another graph by hand. The behaviour of the CH-53D is fully analysed in Reference [11] and will not be discussed here. Instead, the behaviour of the CH-47B over a range of airspeeds will be examined. In Reference [27], the stability and control derivatives were given for speeds of 0.1, 20, 40, 60, 80, 100, 120, and 130 KTAS. Again, the eigenvalues
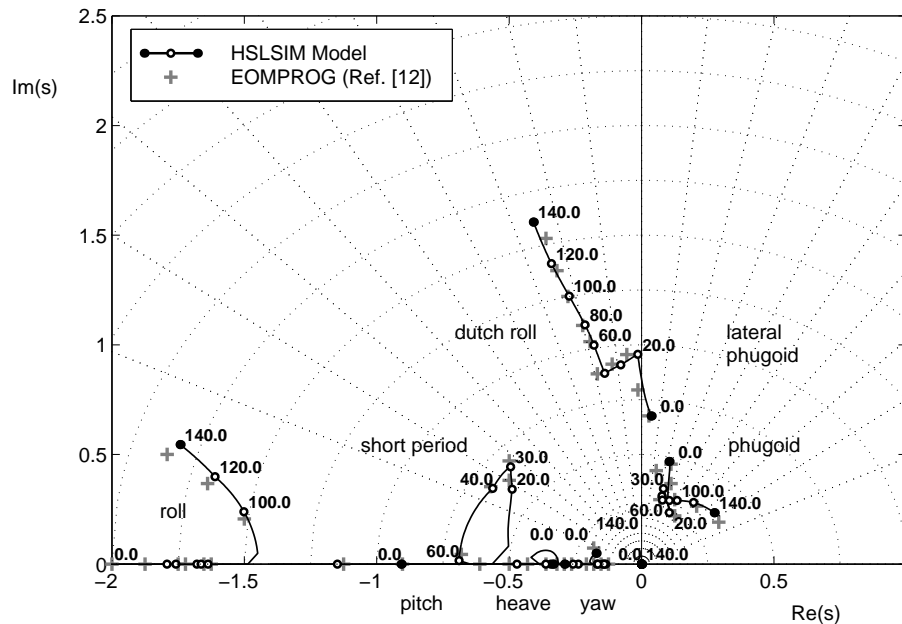
Figure 11: CH-53D System Eigenvalues — Variation with Trim Airspeed (in KTAS)

were calculated at each of these airspeeds and drawn on the complex plane, as shown in Figure 12.

The gridlines in each of these graphs represent lines of constant frequency and constant damping factor. The curved lines define lines of constant frequency, which increase in value from zero as they radiate out from the origin. The straight lines define lines of constant damping factor. They decrease in a clockwise direction from a value of 1.0 (along the negative real axis) to a value of -1.0 (along the posisive real axis). The positive imaginary axis represents zero damping. Any modes on the positive right-hand side of the real axis thus have a negative damping factor and are therefore unstable. Eigenvalues with non-zero imaginary components represent oscillatory modes with a certain frequency and damping factor, while those that lie along the real axis represent pure damping modes.

The CH-47B, like most conventional helicopters, has essentially three longitudinal modes and three lateral modes. However, it should be noted that these modes change markedly with airspeed and tend to be highly coupled. The modes consist of:

- A low-frequency, marginally unstable *phugoid* mode in hover, which decreases slightly in damping as the airspeed increases to 20 KTAS. The frequency then decreases and becomes stable at around 40 KTAS. Between 40 and 60 KTAS, the frequency increases before decreasing again through to 130 KTAS. There is a distinct kink in the root locus at 60 KTAS, mainly due to rapid changes in the influential stability derivatives in this airspeed regime. Above 80 KTAS, the mode takes on a significant lateral component, or side-motion. At 130 KTAS, the mode comprises all three translational u, v, and w velocity components equally.

- A higher frequency, marginally unstable *lateral phugoid* mode, which also decreases slightly in damping as the airspeed increases to 20 KTAS. From 20 to 130 KTAS,
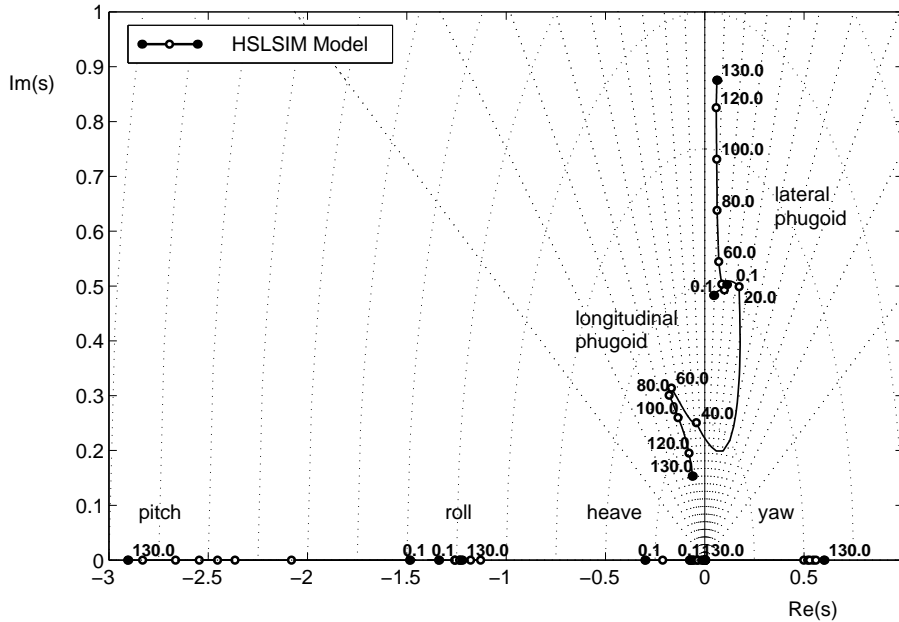
Figure 12: CH-47B System Eigenvalues — Variation with Trim Airspeed (in KTAS)

the frequency increases uniformly and the damping remains relatively constant. In hover, the lateral phugoid mode resembles the low-frequency 'swinging' motion of the longitudinal phugoid mode. As the airspeed increases, however, the mode looks much more like a dutch-roll mode, typical of fixed-wing aircraft.

- A stable, pure damping mode in pitch, or *pitch subsidence*, which initially decreases and then increases in damping with an increase in airspeed. This mode actually has a larger roll-rate component at hover, then as the airspeed increases the pitch-rate component becomes more dominant, reaching a peak at 40 KTAS before decreasing. Above 60 KTAS, the mode has a large w velocity component.

- Another stable, pure damping mode in roll, or *roll subsidence*, which initially increases and then decreases in damping with an increase in airspeed. Complimentary to the previous mode, this mode has a larger pitch-rate component at hover, and as the airspeed increases, the roll-rate component becomes more dominant. There is little change in the mode shape thereafter.

- A stable, pure damping *heave subsidence* mode, which generally decreases in damping with an increase in airspeed. The u and v velocity components increase and the w velocity component decreases from hover to approximately 30 KTAS. At this point, the u and v velocity components both decrease to near-zero values. The w velocity decreases by only a small amount before remaining relatively constant through to 130 KTAS.

- An initially stable pure damping mode in *yaw*, which decreases in damping with an increase in airspeed, becoming statically unstable at approximately 32 KTAS. The damping continues to decrease rapidly until an airspeed of 40 KTAS, when it settles to a constant value. The v velocity component varies throughout the speed range,

while the u any w components both increase greatly at the crossover airspeed. The pitch rate component also increases at 32 KTAS, becoming the dominant part of the motion. The yaw rate component, however, actually decreases from its value at hover and remains small by comparison.

The eigenvalues representing each of these modes at airspeeds of 0.1 KTAS (hover) and 130 KTAS are tabulated below. The corresponding natural frequency and damping factor are also listed for each mode.

Table 2: Natural Frequency and Damping for CH-47B at 0.1 KTAS

Mode	Eigenvalue	Natural Frequency (rad/s)	Damping Factor
Longitudinal phugoid	$0.1099 \pm 0.5026i$	0.5145	-0.2137
Pitch subsidence	-1.4853	1.4853	1.0000
Heave subsidence	-0.3003	0.3003	1.0000
Lateral phugoid	$0.0453 \pm 0.4829i$	0.4850	-0.0934
Roll subsidence	-1.3396	1.3396	1.0000
Yaw mode	-0.0766	0.0766	1.0000

Table 3: Natural Frequency and Damping for CH-47B at 130.0 KTAS

Mode	Eigenvalue	Natural Frequency (rad/s)	Damping Factor
Longitudinal phugoid	$-0.0619 \pm 0.1534i$	0.1654	0.3744
Pitch subsidence	-2.9048	2.9048	1.0000
Heave subsidence	-0.0144	0.0144	1.0000
Lateral phugoid	$0.0610 \pm 0.8754i$	0.8775	-0.0695
Roll subsidence	-1.2224	1.2224	1.0000
Yaw mode	0.6008	0.6008	1.0000

5.2   Analysis of Helicopter Slung-Load System Modes

As with the unloaded helicopter model, the results obtained for the combined helicopter and load were compared with those documented in Reference [11]. The eigenvalues for a range of configurations of the CH-53D in hover with a MILVAN load were examined. In particular, the load-to-helicopter mass ratio m_l/m_h was varied between 0.1 and 0.6. The load was slung using multiple cables (sling legs) and a single helicopter attachment point, and the distance between the attachment point and load cg was 25 ft. Figures 13 and 14 illustrate the root loci for this system in both longitudinal and lateral axes.

The additional eigenvalues in these diagrams represent the modes associated with the pendulous motion of the load and will be discussed later in this section. Note also that the heave subsidence and yawing modes were not included in the previous results and are therefore not shown here. Nonetheless, all of the remaining modes agree quite well,

Figure 13: CH-53D with Single Slung Load Longitudinal Eigenvalues at Hover — Variation with Load-to-Helicopter Mass Ratio
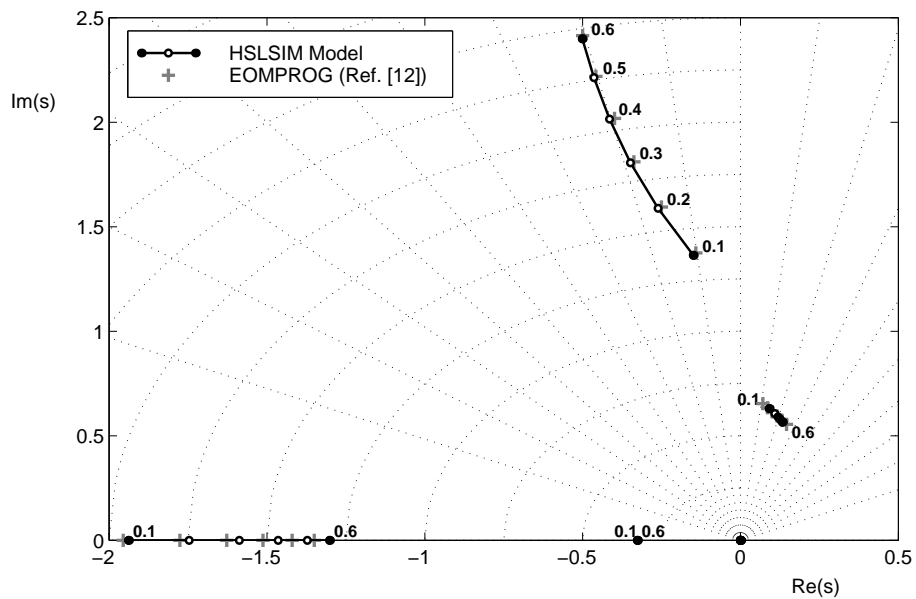
Figure 14: CH-53D with Single Slung Load Lateral Eigenvalues at Hover — Variation with Load-to-Helicopter Mass Ratio

particularly in the lateral axes. Small discrepancies have come about due to the same reasons discussed above.

A similar numerical analysis was conducted with the CH-47B in hover and a single MILVAN load attached with the same sling configuration as the CH-53D, shown in Figure 15.
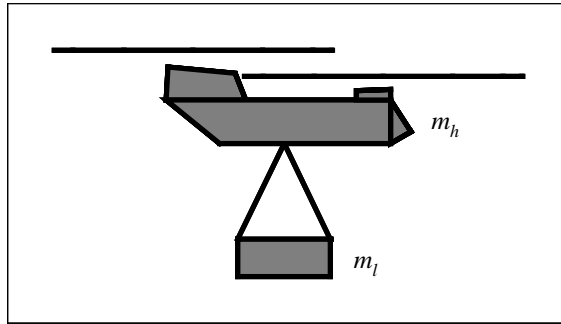
Figure 15: Multiple Cable Sling Configuration

The load-to-helicopter mass ratio in this case was varied from 0.1 to 1.0. Figures 16 and 17 illustrate the change in system behaviour with mass ratio.

The helicopter slung-load system comprises the same typical helicopter modes introduced previously, as well as an additional pendulum mode in each axis. These pendulum modes can be attributed to the simple swinging motion of the load beneath the helicopter. For low load weights, the modes are largely decoupled from the helicopter motion and approach that of a similar pendulum system, with frequencies as given in Appendix B, Equation (B23). As the load weight is increased, it has more influence on the motion of the helicopter. The frequencies approach that of a double-pendulum system, as in Equation (B21), in the appendix[2]. Furthermore, the damping for both lateral and longitudinal pendulum modes generally increases, producing a stabilising effect.

In contrast, the effect of increasing the load mass on the other modes is destabilising. The damping of the pitch, heave, and roll modes generally decreases; the yaw mode changes very little. The effect on the unstable phugoid modes is perhaps more critical. From the diagrams, the longitudinal phugoid mode mainly changes in frequency — only decreasing by a small amount. The lateral phugoid mode, however, undergoes a significant decrease in damping as the load weight increases. Since this mode is already unstable, this would result in a more rapid divergence from trim. In summary, the net effect of increasing the load weight would therefore be a marginal stabilisation of the pendulum modes and a more significant destabilisation of the phugoid modes.

Another numerical experiment with the CH-47B in hover and a single MILVAN load attached with a range of sling configurations was also conducted. In this test, the load and bridle arrangement was attached by a single pendant cable to the helicopter, as shown in Figure 18.

The ratio of the pendant length to total sling length, ℓ/L, was varied from 0.1 to 0.9.

---

[2]A more accurate estimate which incorporates the helicopter's moment of inertia can be obtained by using Equation (B15).
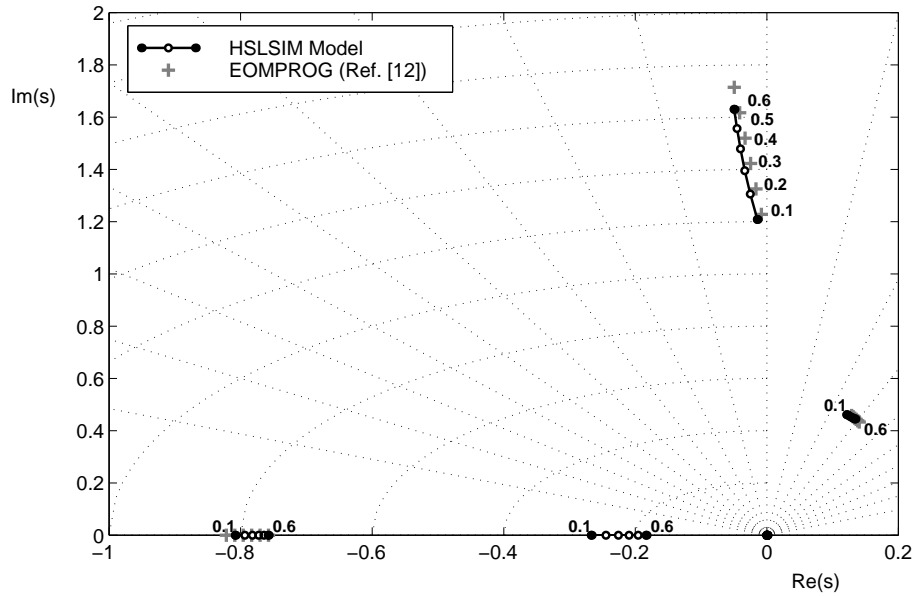
Figure 16: CH-47B with Single Slung Load Longitudinal Eigenvalues at 0.1 KTAS — Variation with Load-to-Helicopter Mass Ratio
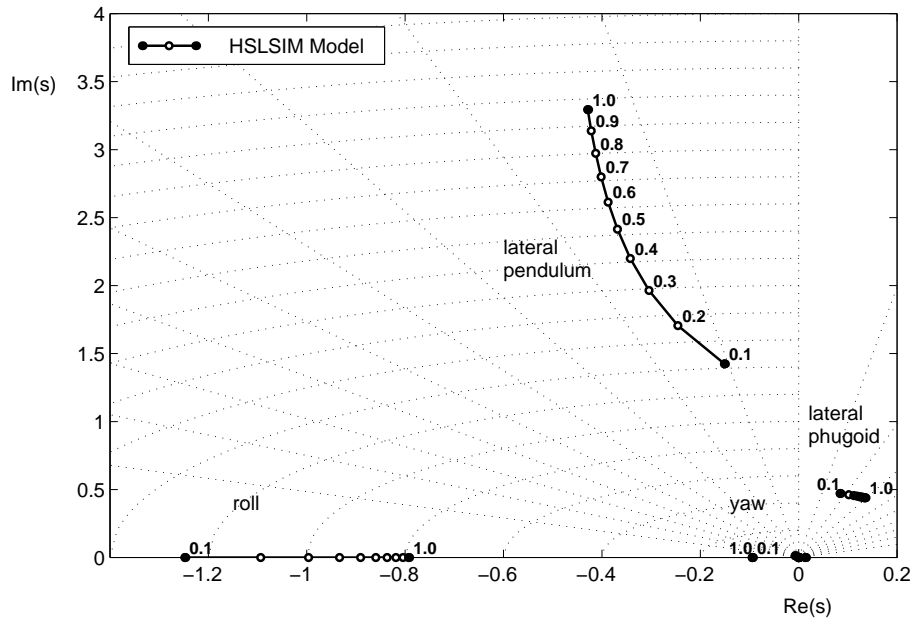
Figure 17: CH-47B with Single Slung Load Lateral Eigenvalues at 0.1 KTAS — Variation with Load-to-Helicopter Mass Ratio
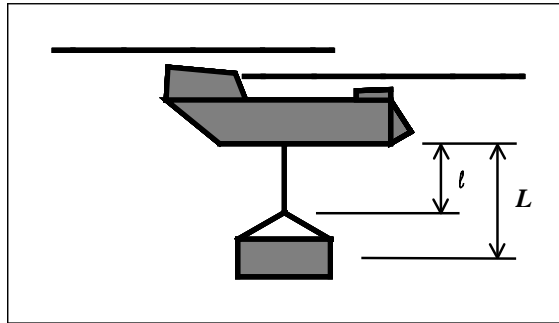
Figure 18: Single Cable Sling Configuration

The total sling length (the distance between the helicopter attachment point and load cg) remained constant at 25 ft and the mass ratio was 0.05. Root locii for the longitudinal and lateral modes are illustrated in Figures 19 and 20, respectively.

In this configuration, there are two pendulum modes in each axis, which reflect the extra two degrees of freedom in load pitch and load roll. The first low-frequency mode can be associated with the gross swinging motion of the load-bridle subsystem beneath the helicopter. The second high-frequency mode can be associated with the pitching or rolling motion of the load about its cg. Since the mass ratio in this case is quite low, the natural frequencies of oscillation can be estimated quite accurately using Equation (B15) in Appendix B.

As the length ratio increases, this second pendulum mode increases in frequency quite dramatically. For this particular load, the frequency of the lateral mode is approximately double that of the longitudinal mode due to the smaller moment of inertia about the roll axis. All other modes, including the low frequency pendulum modes, do not change by any significant amount with an increase in the length ratio.

The last component in the analysis of the system modes was concerned with multiple-load configurations. To this end, the dynamic characteristics of the CH-47B with multiple, individually slung loads was examined. It could be reasonably assumed that the addition of extra loads would simply add more pendulum modes to the system. However, it is interesting to see the placement of those modes, as well as any effect on the other modes. Figure 21 illustrates the variation in the system modes for zero, one, two, and three individually attached loads. The parameter n denotes the number of bodies, including the helicopter, in the system.

For this analysis, simple box-type loads were used. As with the MILVAN, the moments of inertia for each load were approximated with linear functions of their mass by

$$I_{xx} = I_{yy} = I_{zz} = 0.33 * m_l \tag{31}$$

The weight of each load was the same, and for each configuration, the total load-to-helicopter mass ratio was kept constant at 1.0. The loads were each slung using multiple cables (sling legs) attached to individual helicopter hook points, and the distance between each attachment point and the corresponding load cg was 25 ft.
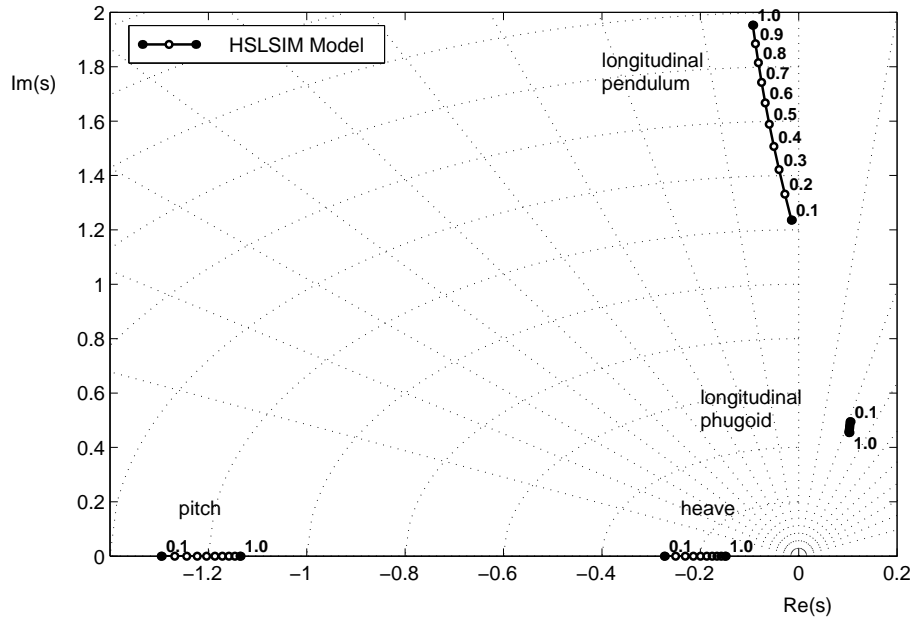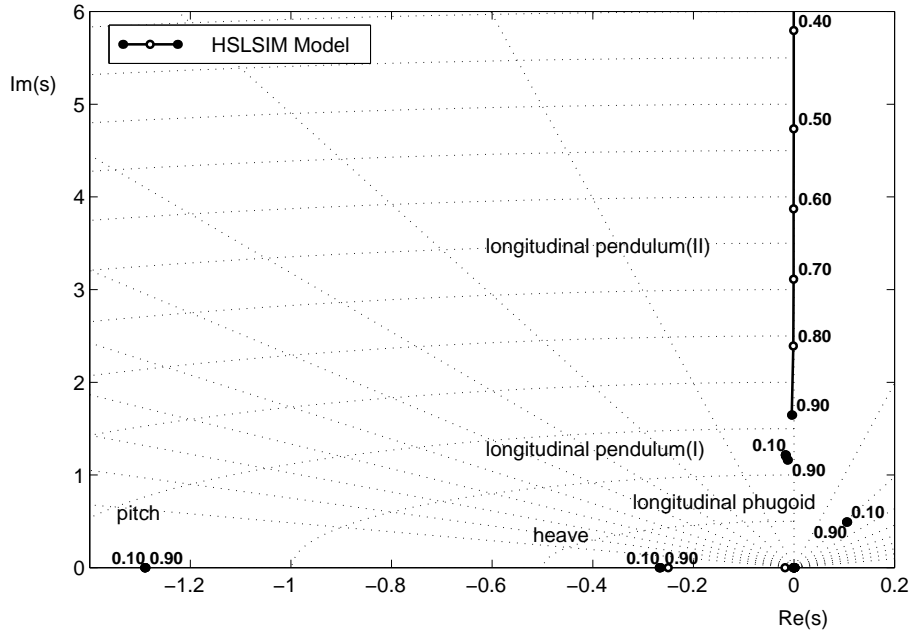
Figure 19: CH-47B with Single Slung Load Longitudinal Eigenvalues at 0.1 KTAS — Variation with Pendant-to-Sling Length Ratio
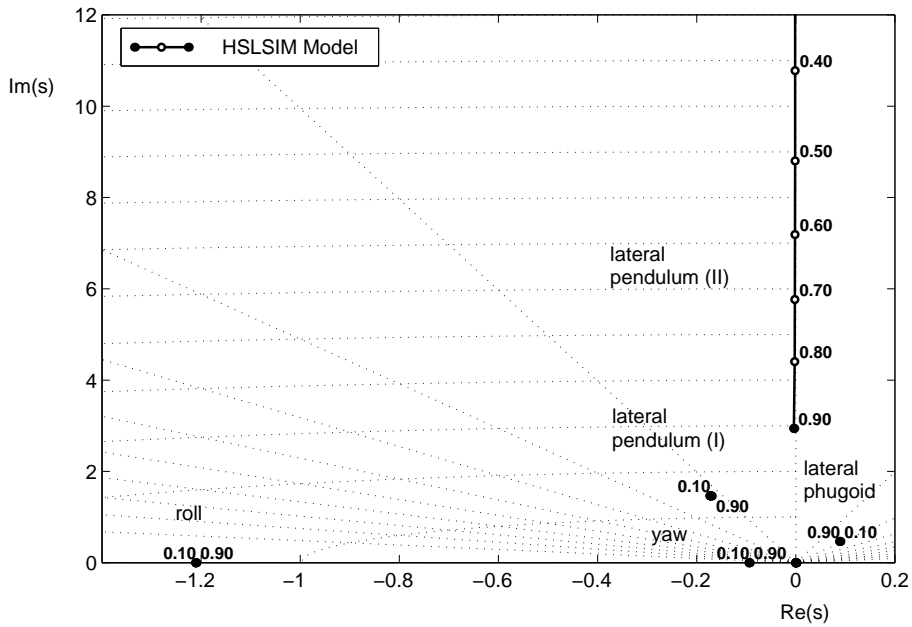
Figure 20: CH-47B with Single Slung Load Lateral Eigenvalues at 0.1 KTAS — Variation with Pendant-to-Sling Length Ratio
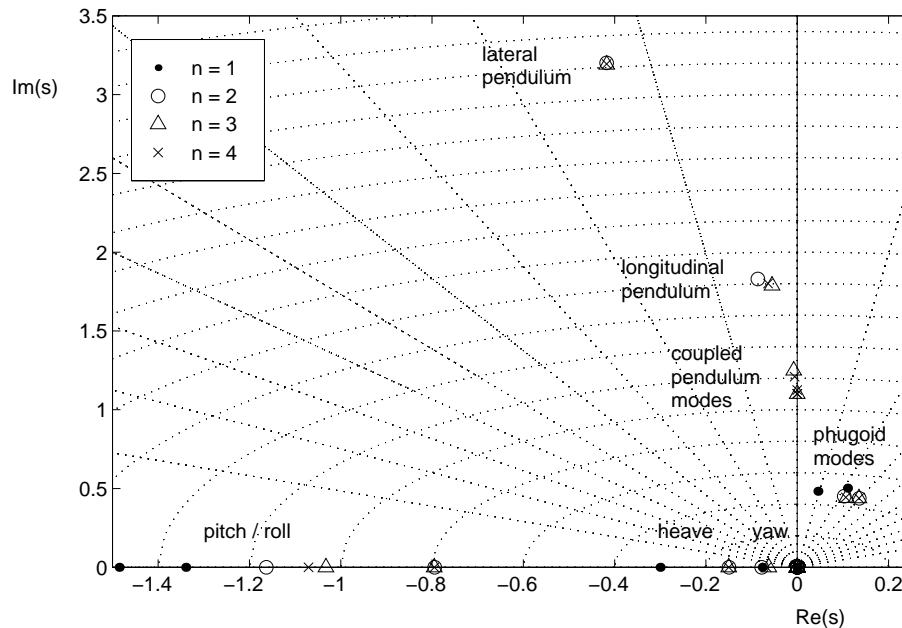
Figure 21: CH-47B with Multiple Slung Loads Eigenvalues at 0.1 KTAS — Variation with Number of Loads

For the unloaded helicopter, the modes consist of two oscillatory modes (longitudinal and lateral phugoid) and four damping modes (including pitch, roll, heave, and yaw subsidence). Recall from the previous section that the pitch and roll modes are actually swapped around in hover. The single-load (centre hook) configuration has two additional modes (one longitudinal and one lateral pendulum mode), both of which are stable. However, the addition of one or more loads, or a number of loads further destabilises the lateral phugoid mode. It also significantly decreases the damping in pitch, roll, and heave modes and, to a much lesser extent, the yaw mode. The dual-load (forward and aft hooks) configuration has those, plus two more oscillatory modes, which are all highly coupled. The first two pendulum modes, which have approximately the same locations as in the single-load case, describe longitudinal and lateral motions in which the loads swing in phase. The next two pendulum modes are very lightly damped and describe motions in which the loads swing out of phase. They have little effect on the helicopter motion. The triple-load (all hooks) configuration also has the typical single-load style modes, plus four additional pendulum modes. They describe two longitudinal and two lateral motions in which the loads swing in various combinations.

5.3   Flight Simulation

Further to the modal analysis, a number of simulations were run in order to demonstrate the typical behaviour of helicopter slung-load systems. The first of these demonstrates the longitudinal response of a simple single-load configuration. In this case, a MILVAN load was slung with a single pendant cable to a CH-47B helicopter, as in the configuration shown previously (Figure 18). The ratio of the pendant length to total sling length was set to 0.6, and the total sling length to 25 ft. The load-to-helicopter mass ratio

was 0.05.

Figure 22 shows time-histories of the body-axis velocities, pitch rate and angle, cable angle and tension, and control inputs. Figure 23 illustrates the motion of the helicopter and slung load through the duration of the simulation.

In the time-history plots, u and w are the velocities in x and z directions of the body axes respectively, q is the pitch rate, θ is the pitch angle, and θ_c is the cable angle displaced from the vertical position. The cable tension force, nondimensionalised by the load weight, is denoted by fc. The longitudinal cyclic and collective control inputs are represented by δ_b and δ_c, respectively.

For this 10 second simulation, the helicopter and slung load were given an initial forward velocity of 80 ft/s and the load was displaced from its static equilibrium position by 30°. The control inputs were generated so as to maintain a nose-level attitude in the helicopter. Both primary and secondary pendulum modes can be readily identified in the response of the load, most notably in the cable angle. In general, the system behaved as expected, with the load having little effect on the behaviour of the helicopter. It is also worth noting that the peaks in the cable tension correspond to the extremes of the pitch rates and have a maximum value of up to 1.5 times their static load.

The second simulation demonstrates the combined longitudinal and lateral response of the same single-load configuration. However, for this case, the mass ratio was increased to 1.0. The duration was 20 seconds, although only the first 10 seconds of the simulation are shown in Figure 24. Variables shown are the body-axis velocities and accelerations, the angular displacements and rates, and the cable angles and tension. The flight path of the helicopter and slung load are depicted in Figure 25.

In these plots, v is the velocity in the y direction of the body axes, p and r are the roll and yaw rates, ϕ is the bank angle, and ϕ_c is the cable angle displaced from the vertical position. The variables $\dot{u}$, $\dot{v}$, and $\dot{u}$ represent the accelerations in body axes.

Unlike the previous simulation, the initial state was hover. The load was displaced from its static equilibrium position by 30° in pitch and 15° in bank. In order to observe the influence of the load on the helicopter, the controls were held fixed (at zero) for the entire 20 second simulation. Both primary and secondary longitudinal pendulum modes are visible in the cable pitch angle, and both lateral modes are also visible in the cable bank angle. These also induce a yawing motion, seen in the yaw rate, due to lateral-directional coupling, and although it may seem so, this motion is not oscillatory. The rolling modes are generally of higher frequency than the pitching modes, given their lower moment of inertia. However, due to the more unstable lateral phugoid mode of the helicopter, the rolling motion of the load has a greater consequence on the resultant motion of the system. This is what causes the rapid divergence in the velocity v. Again, the cable tension reached a peak of nearly 1.5 times the static load.

The last simulation that has been included in this report demonstrates the full response of a multiple-load configuration. Three box-shaped containers with an equal mass ratio of 0.33 were attached to the three hook points under the CH-47B. They were each slung using four cables (Figure 15), and the length from the helicopter attachment points to each load cg was set to 15, 20, and 25 ft.
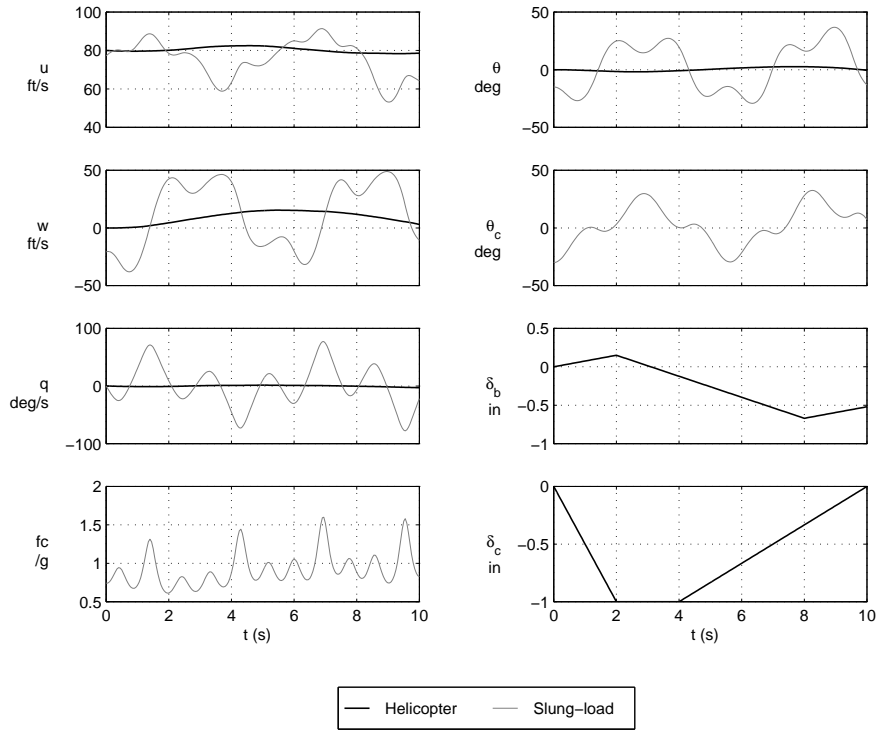
Figure 22: *Longitudinal Dynamic Response Simulation of CH-47B with Single Slung Load — Time Histories* ($m_l/m_h = 0.05$)
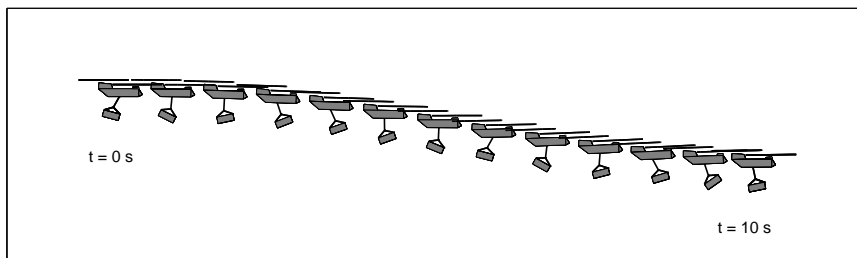
Figure 23: *Longitudinal Dynamic Response Simulation of CH-47B with Single Slung Load — Simulation Frames* ($m_l/m_h = 0.05$)
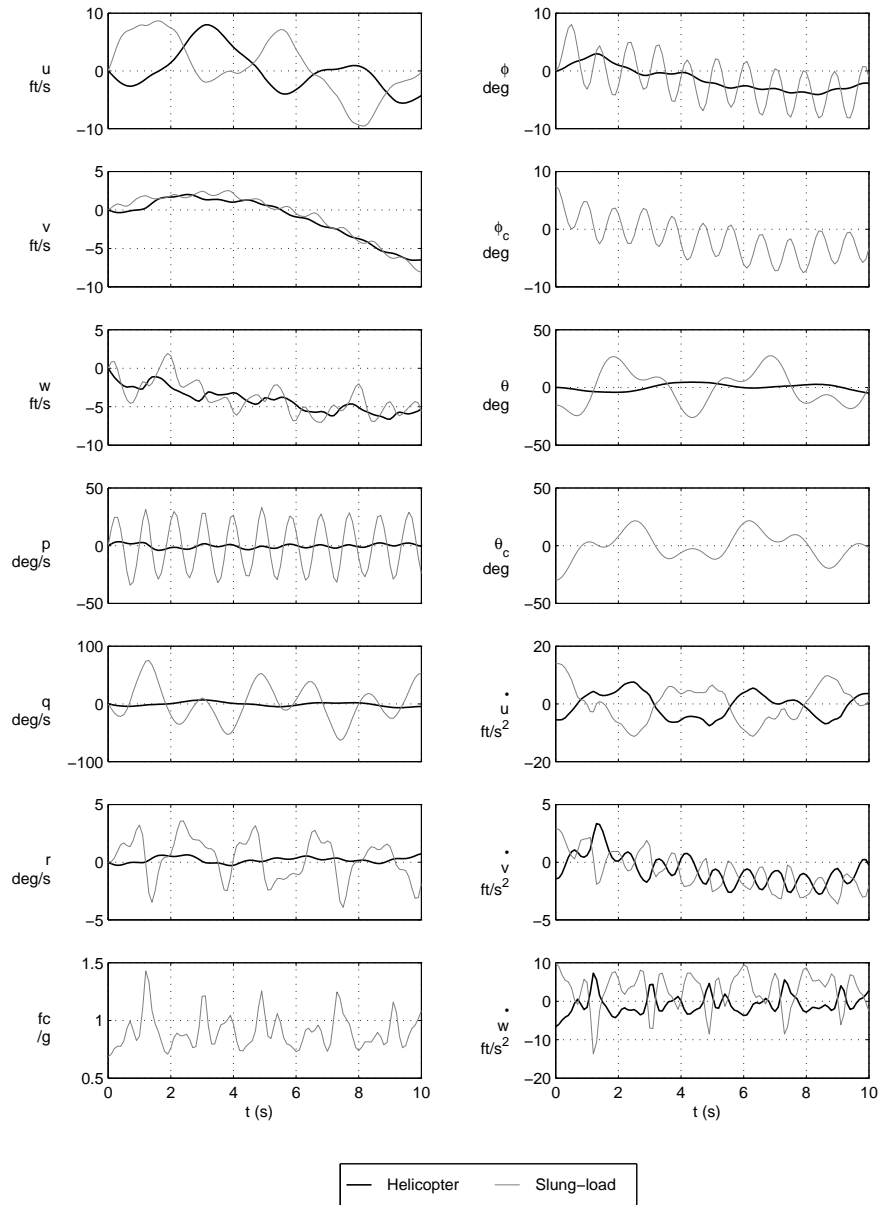
Figure 24: *Coupled Dynamic Response Simulation of CH-47B with Single Slung Load — Time Histories ($m_l/m_h = 1.0$)*
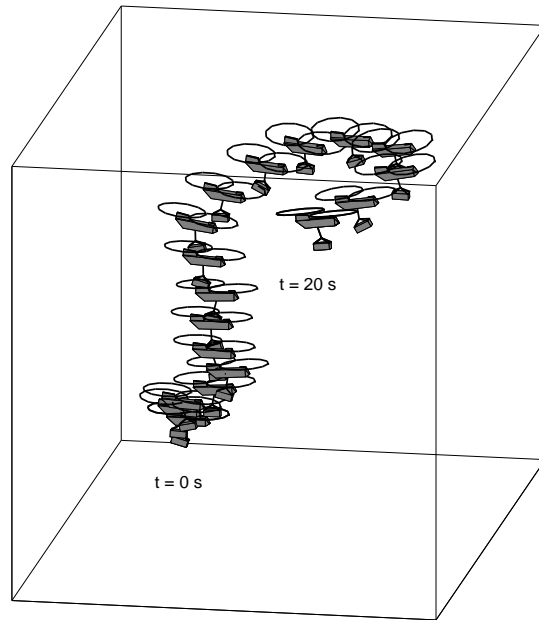
Figure 25: Coupled Dynamic Response Simulation of CH-47B with Single Slung Load — Simulation Frames ($m_l/m_h = 1.0$)
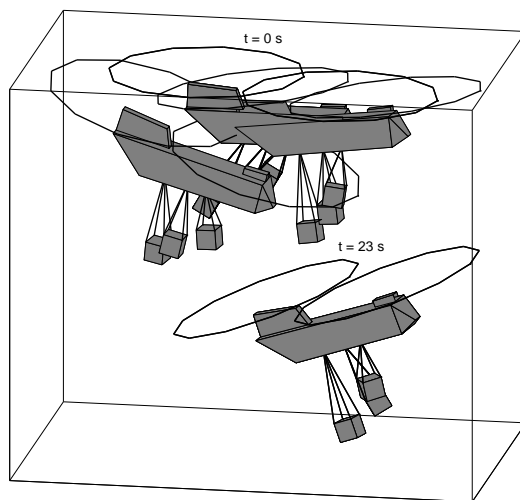
Figure 26: Coupled Dynamic Response Simulation of CH-47B with Three Slung Loads — Simulation Frames ($m_l/m_h = 0.33$)

Figures 26 and 27 contain the simulation time histories and helicopter slung-load flight path respectively. Again, only the first 10 seconds of the time histories are shown.

As before, the initial state for the helicopter was hover. All of the loads were displaced from their equilibrium positions in both pitch and bank by arbitrary angles from $0°$ to $30°$. The controls were also held fixed for the duration of the simulation, which was just over 20 seconds. From the first set of plots, the fundamental frequency for each of the slung loads is visible. The slight difference in their frequency, due to the different sling lengths, is perhaps best seen in the pitch rate and angle. There is also a significant coupling effect, which induces a yawing motion. Unstable longitudinal and lateral modes again cause divergence in the velocities u and v.
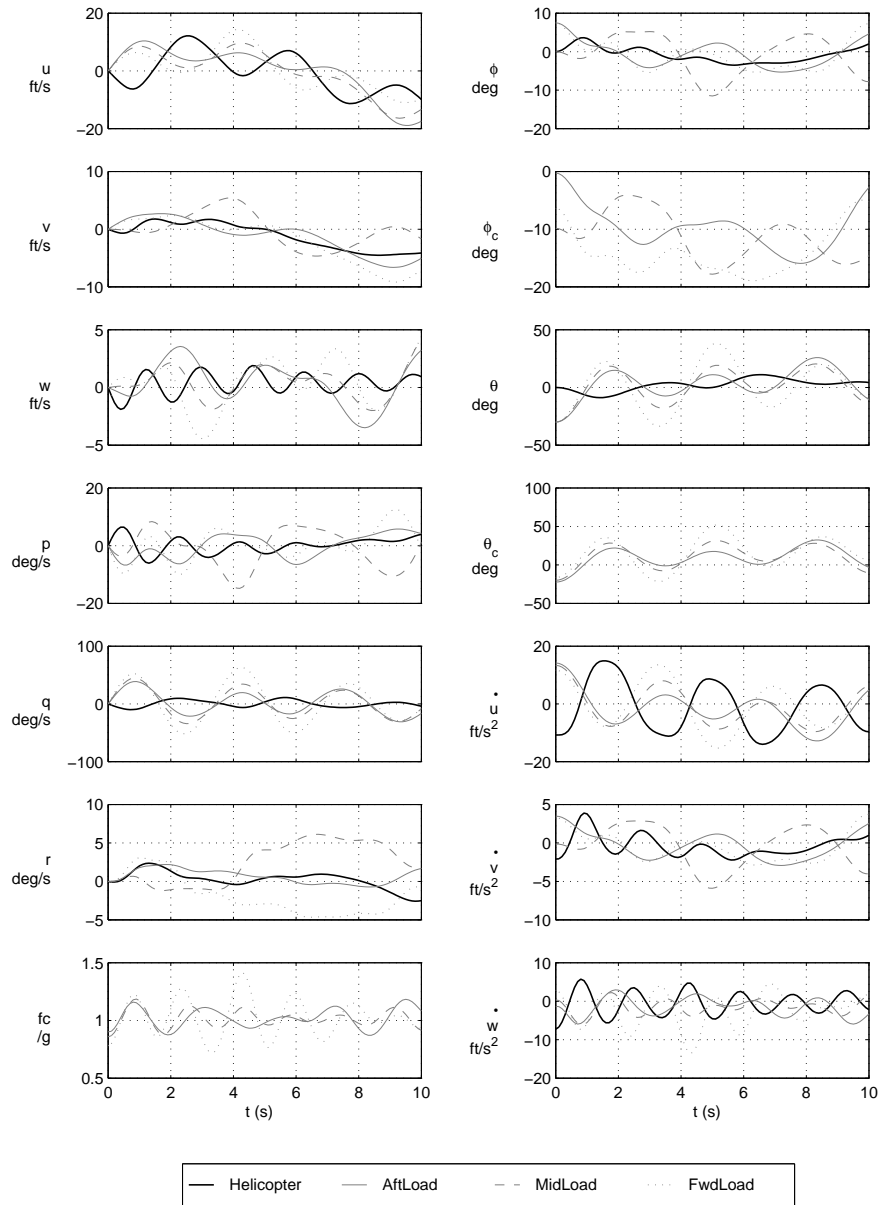
Figure 27: Coupled Dynamic Response Simulation of CH-47B with Three Slung Loads — Time Histories ($m_l/m_h = 0.33$)

6 Concluding Remarks

A simulation model was produced using the equations of motion for general slung-load systems developed by Cicolani and Kanning [29]. The formulation used is based on the Newton-Euler equations written in terms of generalised coordinates and can be readily adapted to systems with either elastic or inelastic suspension. All code development, including the simulation routine, linear analysis, and graphical replay tools, was done in MATLAB. Further to the model described, the simulation has also been extended to incorporate multiple-load systems.

Following comparison of the behaviour of a simple pendulum-type system against both analytical solutions and previously published results, the open-loop characteristics of a full helicopter slung-load system was examined. The results presented include the modal analysis of a single-load system and the simulation of a multiple-load system. It was found that the frequency of the longitudinal and lateral pendulum modes generally increases with the load-to-helicopter mass ratio. More importantly, the lateral phugoid mode becomes significantly unstable as the mass ratio is increased. For the simulation demonstrated, the dominant natural frequencies were identified.

References

1. Lucassen, L. & Sterk, F. (1965) Dynamic stability analysis of a hovering helicopter with a sling load, *Journal of the American Helicopter Society* **10**, 6–12.

2. Dukes, T. (1972) *The Princeton Pennsylvania Army Avionics Research Program. Elements of Helicopter Hovering and Near Hover Operations with a Sling Load Final Report, 1 Sep. 1966 - 30 Dec. 1971*, Technical Note AD-750618, Princeton Univ., NJ.

3. Cliff, E. & Bailey, D. (1975) Dynamic stability of a translating vehicle with a simple sling load, *AIAA Journal of Aircraft* **12**, 773–777.

4. Feaster, L. (1975) *Dynamics of a Slung Load*, PhD thesis, Massachusetts Univ., MA.

5. Feaster, L., Poli, C. & Kirchhoff, R. (1977) Dynamics of a slung load, *AIAA Journal of Aircraft* **14**, 115–121.

6. Prabhakar, A. & Sheldon, D. (1976) *Dynamic Stability of a Helicopter Carrying an Underslung Load*, Technical Note RCMS TN-AM-78, Dept. of Mechanical Engineering, Royal Military College of Science.

7. Prabhakar, A. (1978) Stability of a helicopter carrying an underslung load, *Vertica* **2**(2), 121–143.

8. Nagabhushan, B. (1977) *Systematic Investigation of Models of Helicopter with a Slung Load*, PhD thesis, Virginia Polytechnic Inst. and State Univ., VA.

9. Nagabhushan, B. (1985) Low-speed stability characteristics of a helicopter with a sling load, *Vertica* **9**(4), 345–361.

10. Nagabhushan, B. & Cliff, E. (1982) Maneuver stability of a vehicle with a towed body, *in AIAA Atmospheric Flight Mechanics Conference*, number AIAA-82-1347, American Institute of Aeronautics and Astronautics.

11. Ronen, T. (1986) *Dynamics of a Helicopter with a Sling Load*, PhD thesis, Stanford Univ., CA.

12. Ronen, T., Bryson, A. J. & Hindson, W. (1986) Dynamics of a helicopter with a sling load, *in AIAA Atmospheric Flight Mechanics Conference*, number AIAA-86-2288, American Institute of Aeronautics and Astronautics.

13. Curtiss, H.C., J. (1988) *Studies of the Dynamics of the Twin-Lift System. Interim Report, Jul. 1983 - Sep. 1987*, Contractor Report NASA-CR-183273, Dept. of Mechanical and Aerospace Engineering, Princeton Univ., NJ.

14. Gabel, R. & Wilson, G. (1968) Test approaches to external sling load instabilities, *in 24th Annual National Forum*, number AHS-230, American Helicopter Society.

15. Hone, H. (1975) *Flight Load Investigation of Helicopter External Loads*, Technical Report USAAMRDL-TR-74-104, U.S. Army Air Mobility Research and Development Laboratory.

16. Briczinski, S. & Karas, G. (1971) *Criteria for Externally Suspended Helicopter Loads*, Technical Report USAAMRDL-TR-71-61, U.S. Army Air Mobility Research and Development Laboratory.

17. Kesler, D., Murakoshi, A. & Sinacori, J. (1974) *Flight Simulation of the Model 347 Advanced Tandem-Rotor Helicopter. Final Report, Jul. 1972 - Oct. 1973*, Technical Report NOR-73-190, Aircraft Div., Northrop Corp., CA.

18. Matheson, N. (1976) *Stability of Helicopter Slung Loads*, Aerodynamics Note ARL/AERO-NOTE-364, Aeronautical & Maritime Research Labs., VIC., Australia.

19. Wolkovitch, J. & Johnston, D. (1965) *Automatic Control Considerations for Helicopter and VTOL Aircraft With and Without Sling Loads*, Technical Report 138-1, Sytems Technology Inc.

20. Abzug, M. (1970) Dynamics and control of helicopters with two cable sling loads, *in AIAA 2nd Aircraft Design and Operations Meeting*, number AIAA-70-929, American Institute of Aeronautics and Astronautics.

21. Liu, D. (1973) *In-Flight Stabilization of Externally Slung Helicopter Loads Final Report, 25 Jun. 1970 - 17 Jan. 1972*, Technical Report NORT-72-39, Electronics Div., Northrop Corp., CA.

22. Asseo, S. & Whitbeck, R. (1973) Control requirements for sling-load stabilization in heavy lift helicopters, *Journal of the American Helicopter Society* **18**, 23–31.

23. Gera, J. & Farmer, S.W., J. (1974) *A Method of Automatically Stabilizing Helicopter Sling Loads*, Technical Note NASA-TN-D-7593, NASA Langley Research Center.

24. Alansky, I., Davis, J. & Garnett, T.S., J. (1977) *Limitations of the CH-47 Helicopter in Performing Terrain Flying with External Loads*, Technical Report USAAMRDL-TR-77-21, Boeing Vertol Co., PA.

25. Shaughnessy, J., Deaux, T. & Yenni, K. (1979) *Development and Validation of a Piloted Simulation of a Helicopter and External Sling Load*, Technical Paper NASA-TP-1285, NASA Langley Research Center.

26. Sampath, P. (1980) *Dynamics of a Helicopter-Slung Load System*, PhD thesis, Maryland Univ., MA.

27. Weber, J., Liu, T. & Chung, W. (1984) *A Mathematical Simulation Model of the CH-47B Helicopter, Volumes 1 & 2*, Technical Memorandum NASA-TM-84351-VOL-1/2, NASA Ames Research Center.

28. Raz, R., Rosen, A. & Ronen, T. (1989) Active aerodynamic stabilization of a helicopter/sling-load system, *AIAA Journal of Aircraft* **26**, 822–828.

29. Cicolani, L. & Kanning, G. (1986) *General Equilibrium Characteristics of a Dual-Lift Helicopter System*, Technical Paper NASA-TP-2615, NASA Ames Research Center.

30. Cicolani, L. & Kanning, G. (1992) *Equations of Motion of Slung-load Systems, Including Multilift Systems*, Technical Paper NASA-TP-3280, NASA Ames Research Center.

31. Cicolani, L., Kanning, G. & Synnestvedt, R. (1995) Simulation of the dynamics of helicopter slung load systems, *Journal of the American Helicopter Society* **40**(4), 44–61.

32. Saunders, G. (1975) *Dynamics of Helicopter Flight*, Wiley-Interscience, New York.

33. Shaughnessy, J. & Pardue, M. (1977) *Helicopter Sling Load Accident/Incident Survey: 1968 - 1974*, Technical Memorandum NASA-TM-X-74007, NASA Langley Research Center.

34. The MathWorks, Inc. (1997) *MATLAB, The Language of Technical Computing: Using Matlab Version 5*, The Mathworks, 24 Prime Park Way, Natick, MA.

35. Heffley, R., Jewell, W., Lehman, J. & Van Winkle, R. (1979) *A Compilation and Analysis of Helicopter Handling Qualities Data. Volume One: Data Compilation*, Contractor Report NASA-CR-3144, Systems Technology Inc., Mountain View, CA.

36. Blevins, R. (1979) *Formulas for Natural Frequency and Mode Shape*, Krieger Publishing Co., Florida.

Appendix A: Governing System Equations

The general helicopter slung-load system under consideration is illustrated in Figure A1. As explained in Section 3, the system consists of a single helicopter supporting one or more loads by means of some suspension. The model is comprised of n rigid bodies, $B1,B2,...,Bn$, with m links supporting a single force. If the loads all have either multiple or single cable suspensions, then $m = n - 1$. Furthermore, if the suspensions are all of single-cable type, as in the example shown, there are m cables, $C2,...,Cn$.
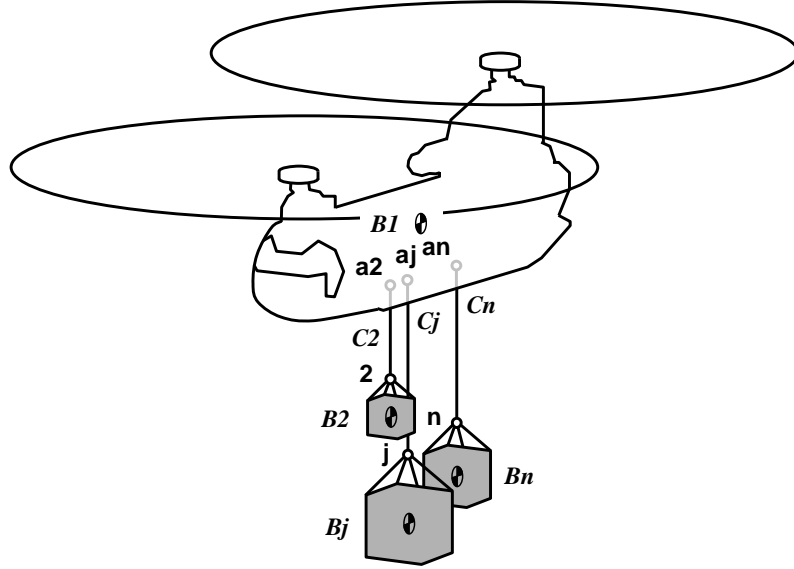
Figure A1: General Helicopter Slung-load System

General Transformation Matrices

For scalar representation of the vector cross products, the general form of the skew-symmetric matrix $S(V_a)$ is defined as

$$
\begin{aligned}
S(V_a) &= \begin{bmatrix} (\mathbf{V} \times \mathbf{ia})_a & (\mathbf{V} \times \mathbf{ja})_a & (\mathbf{V} \times \mathbf{ka})_a \end{bmatrix} \\
&= \begin{bmatrix} 0 & -v_{az} & v_{ay} \\ v_{az} & 0 & -v_{ax} \\ -v_{ay} & v_{ax} & 0 \end{bmatrix}
\end{aligned}
$$

where the columns of $S(V_a)$ represent cross products of $\mathbf{V}$ with the axes of the frame $\mathcal{F}_a$, each referred to $\mathcal{F}_a$.

Using this formulation, the cross products representing Coriolis velocities and accelerations can be written as

$$
\begin{aligned}
(\omega \times \mathbf{R})_a &= S(\omega_a)\, R_a = -S(R_a)\, \omega_a \\
(\omega \times \mathbf{V})_a &= S(\omega_a)\, V_a = -S(V_a)\, \omega_a
\end{aligned}
$$

and the centrifugal accelerations as

$$(\omega \times \omega \times \mathbf{R})_a = S^2(\omega_a) R_a = -S(\omega_a) S(R_a) \omega_a$$

Defining the Euler-angle transformation

$$T_{b,N} = \begin{bmatrix} \cos\psi_b\cos\theta_b & \sin\psi_b\cos\theta_b & -\sin\theta_b \\ \sin\phi_b\cos\psi_b\sin\theta_b - \cos\phi_b\sin\psi_b & \sin\phi_b\sin\psi_b\sin\theta_b + \cos\phi_b\cos\psi_b & \sin\phi_b\cos\theta_b \\ \cos\phi_b\cos\psi_b\sin\theta_b + \sin\phi_b\sin\psi_b & \cos\phi_b\sin\psi_b\sin\theta_b - \sin\phi_b\cos\psi_b & \cos\phi_b\cos\theta_b \end{bmatrix}$$

and the inverse

$$T_{N,b} = T_{b,N}^T$$

the angular velocities can be expressed in terms of the Euler-angle rates via the transformation

$$wb_b = Wb_b \dot{\alpha}b$$

where

$$Wb_b = \begin{bmatrix} 1 & 0 & -\sin\theta_b \\ 0 & \cos\phi_b & \sin\phi_b\cos\theta_b \\ 0 & -\sin\phi_b & \cos\phi_b\cos\theta_b \end{bmatrix}$$

with inverse

$$Wb_b^{-1} = \begin{bmatrix} 1 & \sin\phi_b\tan\theta_b & \cos\phi_b\tan\theta_b \\ 0 & \cos\phi_b & -\sin\phi_b \\ 0 & \sin\phi_b/\cos\theta_b & \cos\phi_b/\cos\theta_b \end{bmatrix}$$

Cable-Axes (Single-Cable Suspension)

Cable-direction vector:

$$kcj_N = \frac{1}{l_{j0}} \left(Rj_N^* + T_{N,j} Rj^* j_j - R1_N^* - T_{N,1} R1^* aj_1 \right)$$

Cable angles:

$$kcj_N = T_{N,cj} kcj_{cj} = \begin{bmatrix} \cos\theta_{cj} & \sin\phi_{cj}\sin\theta_{cj} & \cos\phi_{cj}\sin\theta_{cj} \\ 0 & \cos\phi_{cj} & -\sin\phi_{cj} \\ -\sin\theta_{cj} & \sin\phi_{cj}\cos\theta_{cj} & \cos\phi_{cj}\cos\theta_{cj} \end{bmatrix} \begin{bmatrix} 0 \\ 0 \\ 1 \end{bmatrix}$$

$$= \begin{bmatrix} \cos\phi_{cj}\sin\theta_{cj} \\ -\sin\phi_{cj} \\ \cos\phi_{cj}\cos\theta_{cj} \end{bmatrix}$$

The cable angles are obtained from the cable direction vector

$$\begin{aligned} \phi_{cj} &= \sin^{-1}(-kcj_N(2)) \\ \theta_{cj} &= \sin^{-1}(kcj_N(1) / \cos\phi_{cj}) \end{aligned}$$

43

Velocity of each cable:

$$
\begin{aligned}
Vajj_{cj} &= \dot{l}j \, kcj_{cj} + lj \, kc\dot{j}_{cj} \\
&= \begin{bmatrix} lj\cos\phi_{cj} & 0 & 0 \\ 0 & -lj & 0 \\ 0 & 0 & 1 \end{bmatrix} \begin{bmatrix} \dot{\theta}_{cj} \\ \dot{\phi}_{cj} \\ \dot{l}j \end{bmatrix}
\end{aligned}
$$

where

$$
\begin{aligned}
kc\dot{j}_{cj} = \omega cj_{cj} \times kcj_{cj} &= \begin{bmatrix} \dot{\phi}_{cj} \\ \cos\phi_{cj} \\ -\dot{\theta}_{cj}\sin\phi_{cj} \end{bmatrix} \times \begin{bmatrix} 0 \\ 0 \\ 1 \end{bmatrix} \\
&= \begin{bmatrix} \dot{\theta}_{cj}\cos\phi_{cj} \\ -\dot{\phi}_{cj} \\ 0 \end{bmatrix}
\end{aligned}
$$

so that the cable angle rates can be derived as

$$
\begin{aligned}
\dot{\phi}_{cj} &= -Vajj_{cj}(2)/l_j \\
\dot{\theta}_{cj} &= Vajj_{cj}(1)/l_j\cos\phi_{cj}
\end{aligned}
$$

Simulation Equations for an Arbitrary Number of Loads

Cable lengths:

$$
l_j(r) = |R1_N^* + T_{N,1}R1^*aj_1 - Rj_N^* - T_{N,j}Rj^*j_j|
$$

The cg position of each load:

$$
Rj_N^* = R1_N^* + T_{N,1}R1^*aj_1 + Rajj_N - T_{N,j}Rj^*j_j
$$

and their velocity:

$$
\begin{aligned}
Vj_N^* &= V1_N^* + \dot{T}_{N,1}R1^*aj_1 + Vajj_N - \dot{T}_{N,j}Rj^*j_j \\
&= V1_N^* - T_{N,1}S(R1^*aj_1)w1_1 + Vajj_N + T_{N,j}S(Rj^*j_j)wj_j
\end{aligned}
$$

where

$$
Vajj_N = T_{N,cj}Vajj_{cj}
$$

Hence,

$$
Vj_N^* = V1_N^* + T_{N,cj}Vajj_{cj} + A_{j,n+1}w1_1 + A_{j,n+j}wj_j
$$

and inversely

$$
Vajj_{cj} = -T_{cj,N}V1_N^* + T_{cj,N}Vj_N^* + B_{j,n+1}w1_1 + B_{j,n+j}wj_j
$$

with the elements

$$
\begin{aligned}
A_{j,n+1} &= -T_{N,1}S(R1^*aj_1) \\
A_{j,n+j} &= T_{N,j}S(Rj^*j_j)
\end{aligned}
$$

$$B_{j,n+1} = -T_{cj,N} A_{j,n+1}$$
$$B_{j,n+j} = -T_{cj,N} A_{j,n+j}$$

Configuration kinematics:

$$v = Au$$

$$
\begin{bmatrix}
V1_N^* \\
V2_N^* \\
\vdots \\
Vn_N^* \\
- \\
w1_1 \\
w2_2 \\
\vdots \\
wn_n
\end{bmatrix}
=
\left[
\begin{array}{cccc|cccc}
I & 0 & \cdots & 0 & 0 & 0 & \cdots & 0 \\
I & T_{N,c2} & & 0 & A_{2,n+1} & A_{2,n+2} & & 0 \\
\vdots & & \ddots & & \vdots & & \ddots & \\
I & 0 & & T_{N,cn} & A_{n,n+1} & 0 & & A_{n,2n} \\
- & - & - & - & - & - & - & - \\
 & & & & & & & \\
 & & 0 & & & I & & \\
 & & & & & & & \\
 & & & & & & &
\end{array}
\right]
\begin{bmatrix}
V1_N^* \\
Va22_{c2} \\
\vdots \\
Vann_{cn} \\
- \\
w1_1 \\
w2_2 \\
\vdots \\
wn_n
\end{bmatrix}
$$

$$u = A^{-1}v$$

$$
\begin{bmatrix}
V1_N^* \\
Va22_{c2} \\
\vdots \\
Vann_{cn} \\
- \\
w1_1 \\
w2_2 \\
\vdots \\
wn_n
\end{bmatrix}
=
\left[
\begin{array}{cccc|cccc}
I & 0 & \cdots & 0 & 0 & 0 & \cdots & 0 \\
-T_{c2,N} & T_{c2,N} & \cdots & 0 & B_{2,n+1} & B_{2,n+2} & \cdots & 0 \\
\vdots & \vdots & \ddots & & \vdots & \vdots & \ddots & \\
-T_{cn,N} & 0 & & T_{cn,N} & B_{n,n+1} & 0 & & B_{n,2n} \\
- & - & - & - & - & - & - & - \\
 & & & & & & & \\
 & & 0 & & & I & & \\
 & & & & & & & \\
 & & & & & & &
\end{array}
\right]
\begin{bmatrix}
V1_N^* \\
V2_N^* \\
\vdots \\
Vn_N^* \\
- \\
w1_1 \\
w2_2 \\
\vdots \\
wn_n
\end{bmatrix}
$$

Acceleration vector:

$$\dot{v} = \dot{A}u + A\dot{u}$$

Applied forces and inertia coupling:

$$fo = fg + fa - X - D\dot{A}u$$

$$
\begin{bmatrix} F01_N \\ F02_N \\ \vdots \\ F0n_N \\ - \\ M01_1 \\ M02_2 \\ \vdots \\ M0n_n \end{bmatrix} = \begin{bmatrix} m_1 g_N \\ m_2 g_N \\ \vdots \\ m_n g_N \\ - \\ 0 \\ 0 \\ \vdots \\ 0 \end{bmatrix} + \begin{bmatrix} FA1_N \\ FA2_N \\ \vdots \\ FAn_N \\ - \\ MA1_1 \\ MA2_2 \\ \vdots \\ MAn_n \end{bmatrix} - \begin{bmatrix} 0 \\ 0 \\ \vdots \\ 0 \\ - \\ S(\omega 1_1)J1\omega 1_1 \\ S(\omega 2_2)J2\omega 2_2 \\ \vdots \\ S(\omega n_n)Jn\omega n_n \end{bmatrix} - \begin{bmatrix} 0 \\ m2\dot{A}_2 u \\ \vdots \\ mn\dot{A}_n u \\ - \\ 0 \\ 0 \\ \vdots \\ 0 \end{bmatrix}
$$

where

$$
\dot{A} = \left[\begin{array}{cccc|cccc} 0 & 0 & \cdots & 0 & 0 & 0 & \cdots & 0 \\ 0 & \dot{A}_{2,2} & \cdots & 0 & \dot{A}_{2,n+1} & \dot{A}_{2,n+2} & \cdots & 0 \\ \vdots & \vdots & \ddots & & \vdots & \vdots & \ddots & \\ 0 & 0 & & \dot{A}_{n,n} & \dot{A}_{n,n+1} & 0 & & \dot{A}_{n,2n} \\ \hline - & - & - & - & + & - & - & - & - \\ & & & & & & & \\ & 0 & & & & 0 & & \\ & & & & & & & \\ & & & & & & & \end{array} \right]
$$

where the elements

$$
\begin{aligned}
\dot{A}_{j,j} &= T_{N,cj}S(wcj_{cj}) \\
\dot{A}_{j,n+1} &= -T_{N,1}S(w1_1)S(R1^* aj_1) \\
\dot{A}_{j,n+j} &= T_{N,j}S(wj_j)S(Rj^* j_j)
\end{aligned}
$$

Suspension forces:

$$
fc = H\tau
$$

$$
\begin{bmatrix} FC1_N \\ FC2_N \\ \vdots \\ FCn_N \\ - \\ MC1_1 \\ MC2_2 \\ \vdots \\ MCn_n \end{bmatrix} = \begin{bmatrix} kc2_N & \cdots & kcn_N \\ -kc2_N & & 0 \\ & \ddots & \\ 0 & & -kcn_N \\ - & - & - \\ \xi 12_1 & \cdots & \xi 1n_1 \\ -\xi 22_2 & & 0 \\ & \ddots & \\ 0 & & -\xi nn_n \end{bmatrix} \begin{bmatrix} \tau 2 \\ \vdots \\ \tau n \end{bmatrix}
$$

where

$$
\begin{aligned}
\xi 1j_1 &= (R1^* aj \times kcj)_1 &&= S(R1^* aj)_1 T_{1,N}\, kcj_N \\
\xi jj_j &= (Rj^* j \times kcj)_j &&= S(Rj^* j)_j T_{j,N}\, kcj_N
\end{aligned}
$$

yielding

$$
\tau = \begin{cases} (\max\{0, K_j(lj - loj)\},\ j = 2, \ldots, n)^T & \text{(elastic cables)} \\ -[H^T D^{-1} H]^{-1} H^T D^{-1} fo & \text{(inelastic cables)} \end{cases}
$$

Total specific force:

$$sf = D^{-1}(fo + fc)$$

$$
\begin{bmatrix}
SF1_N \\
SF2_N \\
\vdots \\
SFn_N \\
- \\
SM1_1 \\
SM2_2 \\
\vdots \\
SMn_n
\end{bmatrix}
=
\begin{bmatrix}
(F01_N + FC1_N)/m1 \\
(F02_N + FC2_N)/m2 \\
\vdots \\
(F0n_N + FCn_N)/mn \\
- \\
J1^{-1}(M01_1 + MC1_1) \\
J2^{-1}(M02_2 + MC2_2) \\
\vdots \\
Jn^{-1}(M0n_n + MCn_n)
\end{bmatrix}
$$

Configuration acceleration:

$$\dot{u} = A^{-1}sf$$

Configuration position vector:

$$r = \int \dot{r}(r,v)\, dt$$

$$
r =
\begin{bmatrix}
R1_N^* \\
R2_N^* \\
\vdots \\
Rn_N^* \\
- \\
\alpha 1 \\
\alpha 2 \\
\vdots \\
\alpha n
\end{bmatrix}
=
\int
\begin{bmatrix}
V1_N^* \\
V2_N^* \\
\vdots \\
Vn_N^* \\
- \\
W1_1^{-1}w1_1 \\
W2_2^{-1}w2_2 \\
\vdots \\
Wn_n^{-1}wn_n
\end{bmatrix}
dt
$$

Appendix B: Analytical Results for Pendulum-Type Systems

There are a number of publications, including Reference [36], which list the natural frequencies and mode shapes for various pendulum-type systems. However, for the purpose of this work, the equations of motion were derived and the resulting natural frequencies found for a set of systems that can be used to approximate a helicopter and slung load. The generalised system is analysed first and then several approximations for both single and multiple cable configurations are examined.

Generalised Two-Body system

The generalized two-body system examined in this appendix consists of a sliding mass which is pinned at its centre of gravity and a swinging mass attached below it, as illustrated in Figure B1. The supporting body of mass m_s and inertia J_s is free to pitch and transverse along the x-axis, while the suspended body or load of mass m_l and inertia J_l is constrained just to swing about its attachment point.
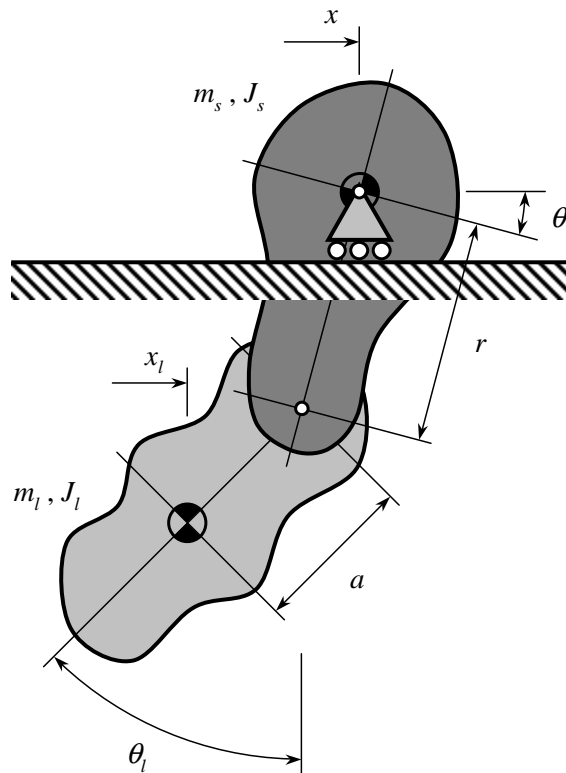
Figure B1: Generalized Two-body Pendulum-type System

In order to solve for the natural frequencies of the system, the equations of motion must first be stipulated. For simplicity, any perturbations about the equilibrium position

are assumed to be *small*. As a result, the trigonometric components of a small angle θ can be reduced to $\sin\theta \approx \theta$ and $\cos\theta \approx 1$.

The sum of moments about the cgs of the support and load are respectively

$$
\begin{aligned}
J_s\ddot{\theta} &= Qr \\
J_l\ddot{\theta}_l &= -Pa(\theta_l - \theta) + Qa
\end{aligned}
\tag{B1}
$$

and the balance of horizontal forces for each body are

$$
\begin{aligned}
m_s\ddot{x} &= P\theta + Q \\
m_l\ddot{x}_l &= -P\theta - Q
\end{aligned}
\tag{B2}
$$

The normal component P of the interaction force can be approximated by the mass-force of the load, whereas the tangential component Q is given by the sum of moments about the supporting body (Eq. (B1)), i.e.

$$
\begin{aligned}
P &\approx m_l g \\
Q &= \frac{J_s}{r}\ddot{\theta}
\end{aligned}
\tag{B3}
$$

Substituting these into Equation (B1) produces the first equation of motion, which can be rewritten as

$$
J_l\ddot{\theta}_l = -m_l ga(\theta_l - \theta) + \frac{J_s a}{r}\ddot{\theta}
\tag{B4}
$$

$$
\frac{J_s a}{r}\ddot{\theta} + m_l ga\theta - J_l\ddot{\theta}_l - m_l ga\theta_l = 0
\tag{B5}
$$

The second equation of motion is derived by subtracting Equations (B2) to give

$$
\ddot{x}_l - \ddot{x} = -\frac{1}{m_l}(P\theta + Q) - \frac{1}{m_s}(P\theta + Q)
\tag{B6}
$$

and applying the geometric relationship

$$
x_l - x = r\theta + a\theta_l
\tag{B7}
$$

This produces the second equation of motion, written as

$$
r\ddot{\theta} + a\ddot{\theta}_l = -\frac{1}{m_l}(m_l g\theta + \frac{J_s}{r}\ddot{\theta}) - \frac{1}{m_s}(m_l g\theta + \frac{J_s}{r}\ddot{\theta})
\tag{B8}
$$

$$
(r + \frac{J_s}{m_l r}k_m)\ddot{\theta} + gk_m\theta + a\ddot{\theta}_l = 0
\tag{B9}
$$

where

$$
k_m = (1 + \frac{m_l}{m_s})
\tag{B10}
$$

In matrix format, Equations (B5) and (B9) can be expressed as

$$
\begin{bmatrix} \frac{J_s a}{r} & -J_l \\ r + \frac{J_s}{m_l r}k_m & a \end{bmatrix}
\begin{bmatrix} \ddot{\theta} \\ \ddot{\theta}_l \end{bmatrix}
+
\begin{bmatrix} m_l ga & -m_l ga \\ gk_m & 0 \end{bmatrix}
\begin{bmatrix} \theta \\ \theta_l \end{bmatrix}
=
\begin{bmatrix} 0 \\ 0 \end{bmatrix}
\tag{B11}
$$

Assuming that the free vibrations are harmonic in time with frequency ω, the equations of motion will have a non-trivial solution if the following determinant is equal to zero:

$$\begin{vmatrix} -\frac{J_s a}{r}\omega^2 + m_l ga & J_l\omega^2 - m_l ga \\ -(r + \frac{J_s}{m_l r}k_m)\omega^2 + gk_m & -a\omega^2 \end{vmatrix} = 0 \tag{B12}$$

This results in the characteristic equation

$$A\omega^4 + B\omega^2 + C = 0 \tag{B13}$$

where

$$\begin{aligned} A &= \frac{J_s a^2}{r} + J_l(r + \frac{J_s}{m_l r}k_m) \tag{B14} \\ B &= -m_l ga^2 - J_l gk_m - m_l ga(r + \frac{J_s}{m_l r}k_m) \\ C &= m_l g^2 ak_m \end{aligned}$$

Finding the roots of Equation (B13) provides a solution for the natural frequencies, i.e.

$$\omega^2 = \frac{-B \pm [B^2 - 4AC]^{1/2}}{2A} \tag{B15}$$

This general system can be used to approximate a helicopter slung-load configuration, where the helicopter is free to pitch about its cg and the load is attached using a multi-cable sling. It is also possible to further simplify the system to represent other configurations as demonstrated in the following sections.

Single-cable System

In order to simulate a single-cable slung-load configuration, shown in Figure B2, the pitching freedom of the supporting body must be translated into that of the single-cable attachment. This may be achieved by setting the inertia of the supporting body to zero while holding the mass constant. If this mass is finite, a sliding-body system results, in which the supporting body is free to transverse along the horizontal. If the mass is infinite, the system simplifies to a fixed-body approximation.

Sliding Body

Setting $J_s = 0$ for the single-cable system, and denoting the lengths $\ell = r$ and $L = \ell + a$, the characteristic equation becomes

$$J_l\ell\omega^4 - (m_l gaL + J_l gk_m)\omega^2 + m_l g^2 ak_m = 0 \tag{B16}$$

with roots

$$\omega^2 = \frac{(m_l gaL + J_l gk_m) \pm [(m_l gaL + J_l gk_m)^2 - 4J_l\ell m_l g^2 ak_m]^{1/2}}{2J_l\ell} \tag{B17}$$
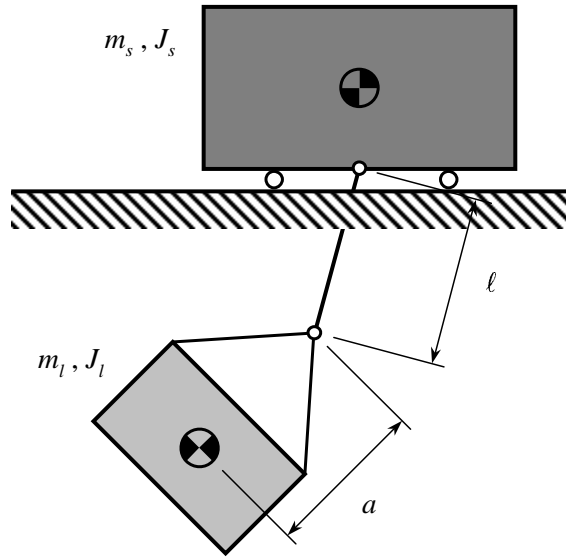
Figure B2: Single-cable Pendulum System

Fixed Body

Again, setting $J_s = 0$, but now let $m_s \to \infty$, which implies that $k_m \to 1$,

$$J_l \ell \omega^4 - (m_l g a L + J_l g)\omega^2 + m_l g^2 a = 0 \tag{B18}$$

$$\omega^2 = \frac{(m_l g a L + J_l g) \pm [(m_l g a L + J_l g)^2 - 4 J_l \ell m_l g^2 a]^{1/2}}{2 J_l \ell} \tag{B19}$$

which corresponds to the solution for a single cable-suspended body, one type of the "double-pendulum" system.

Multi-cable System

To simulate a multi-cable slung-load system, it is possible to either use Equations (B13) and (B15), or further simplify to constrain rotation of the supporting body, shown in Figure B3. This may be implemented by taking the limit as the inertia approaches infinity. Once again, the corresponding mass can be adjusted to simulate either a sliding or fixed-body system.

Sliding Body

For $J_s \to \infty$, the characteristic equation becomes

$$(\frac{a^2}{r} + \frac{J_l}{m_l r} k_m)\omega^4 - \frac{ga}{r} k_m \omega^2 = 0 \tag{B20}$$

with roots

$$\omega^2 = \left\{ 0, \ \frac{m_l g a k_m}{m_l a^2 + J_l k_m} \right\} \tag{B21}$$
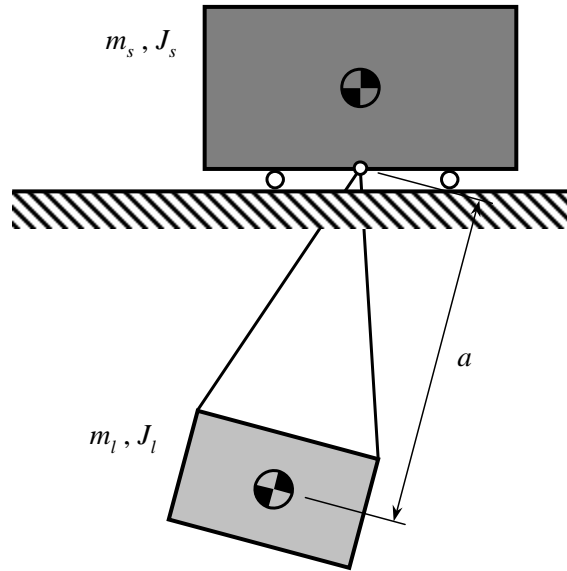
Figure B3: Multi-cable Pendulum System

Fixed Body

As above, $J_s \to \infty$. Also, letting $m_s \to \infty$ results in $k_m \to 1$,

$$(\frac{a^2}{r} + \frac{J_l}{m_l r})\omega^4 - \frac{ga}{r}\omega^2 = 0 \tag{B22}$$

$$\omega^2 = \left\{0, \; \frac{m_l ga}{m_l a^2 + J_l}\right\} \tag{B23}$$

Clearly, this corresponds to the solution for a single pendulum system with mass m_l and inertia J_l.

Appendix C: CH-47D Chinook Helicopter Aerodynamic Model

The aerodynamic model used for the CH-47D was based on a set of linearised stability and control derivatives taken from Reference [27]. The derivatives, as well as associated trim conditions, were computed from a series of simulation runs at various airspeeds using the NASA Ames Research Center simulation model.

In order to make use of this data, the derivatives in the model were interpolated between neighbouring sets with respect to the current airspeed. The resultant aerodynamic forces and moments were then evaluated as a linear function of the state variables. In state-space form, the forces can be written

$$F_A/m_h = Ax + Bu \tag{C1}$$

where F_A is the resultant force, x is the vector of state variables, and A and B are matrices comprising the stability and control derivatives respectively. Expanding Equation (C1)

$$
\begin{bmatrix}
F_{Ax}/m_h \\
F_{Ay}/m_h \\
F_{Az}/m_h \\
M_{Ax}/I_{xx} \\
M_{Ay}/I_{yy} \\
M_{Az}/I_{zz}
\end{bmatrix}
=
\begin{bmatrix}
X_u & X_v & X_w & X_p & X_q & X_r \\
Y_u & Y_v & Y_w & Y_p & Y_q & Y_r \\
Z_u & Z_v & Z_w & Z_p & Z_q & Z_r \\
L_u & L_v & L_w & L_p & L_q & L_r \\
M_u & M_v & M_w & M_p & M_q & M_r \\
N_u & N_v & N_w & N_p & N_q & N_r
\end{bmatrix}
\begin{bmatrix}
u \\
v \\
w \\
p \\
q \\
r
\end{bmatrix}
+
\begin{bmatrix}
X_{\delta b} & X_{\delta a} & X_{\delta r} & X_{\delta c} \\
Y_{\delta b} & Y_{\delta a} & Y_{\delta r} & Y_{\delta c} \\
Z_{\delta b} & Z_{\delta a} & Z_{\delta r} & Z_{\delta c} \\
L_{\delta b} & L_{\delta a} & L_{\delta r} & L_{\delta c} \\
M_{\delta b} & M_{\delta a} & M_{\delta r} & M_{\delta c} \\
N_{\delta b} & N_{\delta a} & N_{\delta r} & N_{\delta c}
\end{bmatrix}
\begin{bmatrix}
\delta_b \\
\delta_a \\
\delta_r \\
\delta_c
\end{bmatrix}
$$

The trim conditions, denoted by subscript "0", and aerodynamic derivatives, in column format, for each of the tabulated airspeeds from 0.1 to 130 KTAS are summarised in the following pages.

Run #33 : Straight & level trim ; 0.1 KTAS ; 97.0 ft ; 33000 lb

	u_0	v_0	w_0	ϕ_0	θ_0	ψ_0	δ_{b_0}	δ_{a_0}	δ_{r_0}	δ_{c_0}
	0.1000	0.0000	0.0000	-0.4453	6.6120	0.0000	-0.0057	0.2262	-0.0032	5.7555

	u	v	w	p	q	r	δ_b	δ_a	δ_r	δ_c
X	-0.0200	-0.0005	0.0301	0.0426	2.7807	-0.1590	0.0570	0.0000	-0.0000	0.9816
Y	-0.0003	-0.1070	0.0022	-2.8362	-0.0073	-0.3305	-0.0005	1.0917	0.0099	0.0657
Z	0.0311	0.0040	-0.2983	-0.1252	-0.2647	-0.0525	0.0499	-0.0001	0.0000	-8.4737
L	-0.0005	-0.0108	0.0004	-1.2795	0.0871	-0.0903	-0.0346	0.4863	-0.1263	-0.0170
M	0.0111	0.0000	0.0006	0.0295	-1.0973	-0.2686	0.3282	0.0000	0.0000	-0.0014
N	0.0007	0.0006	0.0000	-0.0148	-0.1338	-0.0892	0.0541	0.0097	0.1927	-0.0006

Run #37 : Straight & level trim ; 20.0 KTAS ; 97.5 ft ; 33000 lb

	u_0	v_0	w_0	ϕ_0	θ_0	ψ_0	δ_{b_0}	δ_{a_0}	δ_{r_0}	δ_{c_0}
	19.900	0.0000	1.9000	-0.3858	5.4756	0.0000	-1.4901	0.2162	0.2492	5.6003

	u	v	w	p	q	r	δ_b	δ_a	δ_r	δ_c
X	-0.0128	0.0001	0.0268	0.0277	2.8998	-0.1112	0.0422	0.0001	-0.0001	0.7238
Y	0.0021	-0.0460	0.0044	-1.5122	-0.1552	-0.2018	0.0632	1.0867	-0.0077	0.0534
Z	-0.0405	0.0044	-0.2824	-0.1057	-2.7731	0.1764	0.2517	-0.0010	0.0012	-8.4539
L	0.0004	-0.0088	0.0008	-0.8862	0.0239	-0.0647	-0.0105	0.4856	-0.1310	-0.0218
M	0.0156	-0.0009	0.0166	0.0171	-1.6339	-0.2477	0.3355	-0.0000	0.0002	-0.0083
N	0.0009	0.0002	0.0007	-0.0059	-0.1519	-0.0764	0.0525	0.0086	0.1917	0.0021

Run #41 : Straight & level trim ; 40.0 KTAS ; 98.0 ft ; 33000 lb

	u_0	v_0	w_0	ϕ_0	θ_0	ψ_0	δ_{b_0}	δ_{a_0}	δ_{r_0}	δ_{c_0}
	39.900	0.0000	3.0000	-0.2941	4.2599	0.0000	-2.3407	0.2137	0.3750	5.1744

	u	v	w	p	q	r	δ_b	δ_a	δ_r	δ_c
X	-0.0145	0.0007	0.0285	0.0261	2.8099	-0.0915	0.0353	0.0000	0.0000	0.4914
Y	-0.0005	-0.0594	0.0071	-1.7385	-0.2622	-0.2412	0.1073	1.0845	-0.0233	0.0654
Z	-0.1080	0.0016	-0.3498	-0.0939	-3.2915	0.0318	0.6498	-0.0004	0.0002	-7.9678
L	-0.0003	-0.0090	0.0027	-0.9513	-0.0703	-0.0839	0.0163	0.4856	-0.1353	-0.0096
M	0.0007	-0.0015	0.0259	0.0128	-1.7676	-0.2562	0.3744	0.0000	0.0001	0.1235
N	0.0003	0.0003	0.0000	-0.0048	-0.0823	-0.0683	0.0370	0.0076	0.1913	0.0054

Run #57a : Straight & level trim ; 60.0 KTAS ; 98.6 ft ; 33000 lb

	u_0	v_0	w_0	ϕ_0	θ_0	ψ_0	δ_{b_0}	δ_{a_0}	δ_{r_0}	δ_{c_0}
	60.000	0.0000	3.1000	-0.2445	2.9602	0.0000	-1.8241	0.1971	0.2589	4.7454

	u	v	w	p	q	r	δ_b	δ_a	δ_r	δ_c
X	-0.0089	0.0005	0.0343	0.0213	2.6308	-0.0700	0.0475	0.0000	0.0000	0.3276
Y	-0.0014	-0.0723	0.0044	-1.9788	-0.1340	-0.2488	0.0941	1.0852	-0.0444	0.0633
Z	-0.0755	0.0024	-0.5636	-0.0627	0.6404	-0.1804	0.8431	-0.0004	0.0003	-8.1505
L	-0.0008	-0.0093	0.0020	-1.0201	-0.0664	-0.0888	0.0205	0.4867	-0.1417	-0.0018
M	-0.0073	-0.0013	0.0145	0.0199	-1.5813	-0.2736	0.4118	0.0000	0.0001	0.2338
N	0.0003	0.0007	-0.0003	-0.0045	-0.0501	-0.0632	0.0291	0.0063	0.1913	0.0046

Run #57b : Straight & level trim ; 80.0 KTAS ; 98.6 ft ; 33000 lb

	u_0	v_0	w_0	ϕ_0	θ_0	ψ_0	δ_{b_0}	δ_{a_0}	δ_{r_0}	δ_{c_0}
	80.000	0.0000	4.1000	-0.2420	2.9508	0.0000	-1.1228	0.1754	0.1152	4.6284

	u	v	w	p	q	r	δ_b	δ_a	δ_r	δ_c
X	-0.0057	-0.0007	0.0428	0.0206	2.6311	-0.0647	0.0499	0.0000	0.0000	0.4185
Y	-0.0009	-0.0878	0.0024	-2.0591	-0.0412	-0.2442	0.0690	1.0864	-0.0310	0.0473
Z	0.0230	0.0049	-0.6368	-0.0530	-0.4078	-0.1833	0.7232	-0.0006	0.0002	-9.3412
L	-0.0007	-0.0102	0.0018	-1.0358	-0.0584	-0.0864	0.0182	0.4865	-0.1378	-0.0032
M	-0.0081	-0.0008	0.0114	0.0264	-1.6518	-0.2755	0.4302	0.0000	0.0001	0.2260
N	0.0003	0.0013	-0.0006	-0.0118	-0.0279	-0.0622	0.0251	0.0071	0.1915	0.0050

Run #57c : Straight & level trim ; 100.0 KTAS ; 98.7 ft ; 33000 lb

	u_0	v_0	w_0	ϕ_0	θ_0	ψ_0	δ_{b_0}	δ_{a_0}	δ_{r_0}	δ_{c_0}
	100.00	0.0000	4.6000	-0.2679	2.6354	0.0000	-0.6474	0.1746	0.0082	4.7818

	u	v	w	p	q	r	δ_b	δ_a	δ_r	δ_c
X	-0.0126	-0.0014	0.0498	0.0215	2.6825	-0.0649	0.0500	0.0001	0.0000	0.4893
Y	-0.0008	-0.1051	0.0008	-2.0089	0.0256	-0.2401	0.0566	1.0891	-0.0203	0.0572
Z	0.0780	0.0066	-0.6769	-0.0486	-0.5284	-0.1805	0.6178	-0.0008	0.0003	-10.3410
L	-0.0007	-0.0113	0.0013	-1.0130	-0.0210	-0.0829	0.0091	0.4868	-0.1350	-0.0097
M	-0.0068	-0.0004	0.0117	0.0321	-1.7096	-0.2839	0.4471	0.0000	0.0002	0.1998
N	0.0001	0.0018	-0.0007	-0.0178	-0.0608	-0.0606	0.0379	0.0078	0.1921	0.0082

Run #57d : Straight & level trim ; 120.0 KTAS ; 99.0 ft ; 33000 lb

	u_0	v_0	w_0	ϕ_0	θ_0	ψ_0	δ_{b_0}	δ_{a_0}	δ_{r_0}	δ_{c_0}
	120.10	0.0000	4.2000	-0.3341	1.9842	0.0000	-0.3143	0.1934	-0.1074	5.1578

	u	v	w	p	q	r	δ_b	δ_a	δ_r	δ_c
X	-0.0277	-0.0016	0.0523	0.0237	2.7440	-0.0701	0.0528	-0.0000	-0.0001	0.5153
Y	-0.0001	-0.1235	0.0005	-1.8659	0.1258	-0.2030	0.0338	1.0958	-0.0102	0.0643
Z	0.0631	0.0082	-0.7008	-0.0400	-0.4733	-0.2141	0.5106	-0.0009	0.0002	-10.9880
L	-0.0005	-0.0125	0.0011	-0.9612	0.0029	-0.0699	0.0045	0.4884	-0.1328	-0.0128
M	-0.0041	0.0001	0.0121	0.0389	-1.7035	-0.2984	0.4511	0.0000	0.0002	0.1824
N	0.0001	0.0021	-0.0007	-0.0256	-0.0641	-0.0669	0.0412	0.0085	0.1933	0.0135

Run #53 : Straight & level trim ; 130.0 KTAS ; 99.6 ft ; 33000 lb

	u_0	v_0	w_0	ϕ_0	θ_0	ψ_0	δ_{b_0}	δ_{a_0}	δ_{r_0}	δ_{c_0}
	130.20	0.0000	1.7000	-0.3833	0.7495	0.0000	-0.2349	0.2098	-0.1583	5.4493

	u	v	w	p	q	r	δ_b	δ_a	δ_r	δ_c
X	-0.0378	-0.0018	0.0426	0.0248	2.7638	-0.0789	0.0658	0.0000	0.0000	0.3553
Y	0.0003	-0.1351	0.0029	-1.7771	0.1674	-0.1854	0.0272	1.1066	-0.0152	0.0593
Z	0.0132	0.0082	-0.7058	-0.0358	-0.3024	-0.2564	0.4628	-0.0004	0.0001	-11.1430
L	-0.0005	-0.0132	0.0013	-0.9303	0.0149	-0.0707	0.0021	0.4918	-0.1355	-0.0147
M	-0.0022	0.0003	0.0124	0.0420	-1.6772	-0.3087	0.4460	0.0000	0.0001	0.1911
N	-0.0001	0.0023	-0.0007	-0.0293	-0.0689	-0.0565	0.0440	0.0083	0.1952	0.0150

Appendix D: Matlab Source Code

HSL_INIT.M

```
% HSL_INIT : Initialisation script for helicopter slung-load simulation
%
%               HSL_INIT

% For details of the simulation, see reference [1].
%
% 1. Stuckey, R.A
%     "Mathematical Modelling of Helicopter Systems"
%     DSTO-TR-000, Defence Science and Technology Organisation, Sep, 1999

% R.A. Stuckey  17/08/99  (c) 1999, Defence Science and Technology Organisation
% ----------------------------------------------------------------------------

global opt_ HDAT_ LDAT_ CDAT_ % GLOBAL variables (defined below)

% First, define the simulation parameters: number of simulation points, time,
% control inputs, plus a few options such as the simulation axes, angular
% representation, the cable elasticity and nonlinear solution flags.
% Also define the number of bodies in the system (slung-loads + helicopter).

N = 101;                % Number of points for simulation
t = [0:N-1]'*0.1;       % Time vector

TD = [t,zeros(N,4)];    % Matrix of time & control input vectors
                        % TD = [ t db da dr dc ]
                        %
                        % db : longitudinal stick (in)
                        % da : lateral stick (in)
                        % dr : pedal (in)
                        % dc : collective (in)

opt_ = { 'com'          % Simulation axes ['longitudinal'|'lateral'|'combined']
         'eul'          % Angular representation ['euler'|'quaternion']
          0             % Elastic cable model [0|1]
          1     };      % Nonlinear simulation [0|1]

n = 3;                  % Number of bodies


% Next, create/load the data structures for the helicopter and loads. These
% will contain all the relevent aerodynamic, mass, inertial and geometric
% information. Before starting, define some temporary variables (which are not
% required by the main program) for convinience. For each vector here, the
% first element not used but present merely to maintain consistency in the
% numbering.

eta  = [ 0 0.33 0.33 ]; % Vector of mass ratios
lonL = [ 0 0.0 0.6 ];   % Vector of length ratios ('0' for multiple-cable)
L    = [ 0 20.0 25.0 ]; % Vector of total lengths (ft)
K    = [ 0 0.0 0.0 ];   % Vector of cable stiffness ('0' for inelasticity)

% The functions 'hsl_ch47bdat' and 'hsl_boxdat' have been written to simplify
```

```
% the creation of standard helicopter and load data structures. The inputs
% required by the load function are, respectively: the load mass; the load
% inertia matrix; the bridle (sling-leg) length; the sling configuration; and
% the box size (ft). Empty matrices given for any of these will trigger their
% default values. The data structures for both helicopter and loads have
% exactly the same fields.

HDAT_    = hsl_ch47bdat; % GLOBAL struct for the helicopter and load, below

LDAT_    = struct('Name',[], ... % Name of body
                  'V',   [], ... % Velocity vector (kn)
                  'A',   [], ... % Aerodynamic derivative matrix
                  'm',   [], ... % Body mass (slugs)
                  'J',   [], ... % Inertia matrix (slugs.ft^2)
                  'S',   []);    % Geometric model struct

LDAT_(2) = hsl_boxdat(eta(2)*HDAT_.m,[],[],'multiple',[ 3.0 3.0 3.0 ]);
LDAT_(3) = hsl_boxdat(eta(3)*HDAT_.m,[],(lonL(3)-1)*L(3),'single',[ 3.0 3.0 3.0 ]);

% The geometric model struct comprises patches, lines and links for rendering
% an image of the model. The links are also used in the mathematical model for
% solution of the equations of motion. That is, the (possibly elastic) slings
% are assumed to extend from the link(s) on each load to the correspondign link
% or attachment point on the helicopter. These structures look like:
%
% S.Patches.Data       : Patch matrix (ft)
% S.Patches.CoordIndex : Patch coordinates
% S.Lines.Data         : Line matrix (ft)
% S.Links.Data         : Link matrix (ft)

% Create the data structures for the cables supporting each load. These contain
% the respective link attachment indices, cable lengths, cable stretch rates
% and the stiffness and damping constants. The link attachment matrix lists the
% helicopter link indices in the first row and the corresponding load link
% indices in the second row for each cable.

CDAT_    = struct('i'   ,[], ... % Link attachment matrix
                  'l0'  ,[], ... % Cable lengths - unloaded (ft)
                  'l'   ,[], ... % Cable lengths - current (ft)
                  'ldot',[], ... % Cable stretch rates - current (ft/s)
                  'K'   ,[]);    % Cable stiffness & damping matrix

% The first load is supported by multiple (4) cables attached to the first
% (forward-most) link under the helicopter. The individual cable lengths are
% calculated from the bridle lengths and the total length (helicopter
% attachment to load cg). The stiffness matrix is empty, since this simulation
% is inelastic - as defined in opt_, above - and the remaining lengths and
% rates are set to their initial values.

CDAT_(2).i = [ 1 1 1 1 ; 1 2 3 4 ];
CDAT_(2).l0 = sqrt(sum((-LDAT_(2).S.Links.Data+ones(4,1)*[ 0 0 -L(2) ]).^2,2))';
CDAT_(2).K = []; CDAT_(2).l = CDAT_(2).l0; CDAT_(2).ldot = 0*CDAT_(2).l0;

% The second load is supported by a single cable attached to the second (middle)
% helicopter link. The cable length is determined by the cable-to-total sling
% length ratio and the other fields are set as in the first load.

CDAT_(3).i = [ 3 ; 1 ];
```

```
CDAT_(3).l0 = lonL(3)*L(3);
CDAT_(3).K = []; CDAT_(3).l = CDAT_(3).l0; CDAT_(3).ldot = 0*CDAT_(3).l0;


% The next step is to compile the combined system mass/inertia matrix from the
% corresponding helicopter and slung load matrices defined above. To constrain
% the motion of either helicopter or load in any of the [ x y z ] axes, just
% set the appropriate element(s) of the explicitly defined [ 0 0 0 ] vectors
% below to 'inf'. Note that this applies to both rectillinear motion, for the
% mass sub-matrices, and angular motion for the inertial sub-matrices.

D = zeros(n*6);

jj = [1:3];
D(jj,jj) =  HDAT_.m*eye(3) + diag([ 0 0 0 ]); % Helicopter [ x y z ] mass
D(n*3+jj,n*3+jj) = HDAT_.J + diag([ 0 0 0 ]); % Helicopter [ x y z ] inertia

for j = 2:n
   jj = (j-1)*3+[1:3];
   D(jj,jj) =  LDAT_(j).m*eye(3) + diag([ 0 0 0 ]); % Load [ x y z ] mass
   D(n*3+jj,n*3+jj) = LDAT_(j).J + diag([ 0 0 0 ]); % Load [ x y z ] inertia
end


% Set the trim state for the helicopter slung-load system. The vector u0
% contains the generalised velocity coordinates. The vector r0 contains the
% configuration position coordinates. For the single cable case, the matrix
% ac0 contains the cable angles (in cable-axes). These variables are all
% temporary - the only vector required by the main program is the trim state
% of the system x0.

u0 = zeros(n*6,1); % Trim rate vector : Single-cable case
                   % u = [ V1*_N ; Va22_c2 ; ... ; Vann_cn
                   %          w1_1 ;   w2_2  ; ... ;   wn_n  ]
                   %                        : Multiple-cable case
                   % u = [ V1*_N ; Va22*_2 ; ... ; Vann*_n
                   %          w1_1 ;   w2_2 ; ... ; wn_n    ]

r0 = zeros(n*6,1); % Trim position vector
                   % r = [ R1*_N ;   R2*_N ; ... ;   Rn*_N
                   %           a1 ;      a2 ; ... ;      an ]

ac0 = zeros(n,3);  % Trim cable-angle matrix : Single-cable case only
                   % ac = [ [ 0 0 0 ]' ac2 ... acn ]

% From the documentation [*], the sub-vectors are defined:
%                          . . .
% V1*_N   : helicopter [x,y,z] velocity vector in inertial axes
% Vajj_cj : load velocity vectors in cable axes
% w1_1    : helicopter [p,q,r] angular velocity vector in body axes
% wj_j    : load [p,q,r] angular velocity vector in body axes
% Vajj*_j : load velocity vectors in load axes
%
% R1*_N   : helicopter [x,y,z] position vector in inertial axes
% Rj*_N   : load [x,y,z] position vector in inertial axes
% a1      : helicopter [phi,theta,psi] Euler angular position vector
% aj      : load [phi,theta,psi] Euler angular position vector
%
```

```
% acj     : cable/cg-line [phi,theta,psi] angles in cable-axes

% The function 'hsl_load' can be used to calculate the positions of the loads,
% Rj*_N, from the helicopter positions, the helicopter and load attitudes
% (all included in the vector, r0), the cable angles (in the vector, ac0) and
% the cable lengths (supplied globally through CDAT_.l0).

r0 = hsl_load(r0,ac0);

% Finally, the complete state vector can be constructed from the velocity and
% position vectors.

x0 = [u0;r0];


% Set the initial state for the helicopter slung-load system. The operations
% are exactly the same as those for the trim state variables. Setting them to
% different (non-zero) values will create an initial disturbance in the system.

u = zeros(n*6,1);
u(1:3) = [ 0 0 0 ]';

r = zeros(n*6,1);
r(n*3+[1:n*3]) = [   0    0    0 ...
                    -5   10    0 ...
                     0    0    0 ]'*pi/180;
ac = ac0;
ac(:,1:n)     = [   0    0    0
                    0    0    0
                    5  -10    0 ]'*pi/180;

r = hsl_load(r,ac);

x = [u;r];


% Now clear extraneous variables from the workspace and run the main program.
% The required inputs, as specified above, are:
%
% opt_ HDAT_ LDAT_ CDAT_ n t TD D x0 x
%
% The outputs are:
%
% U   : Generalised velocity coordinate matrix
% R   : Configuration position coordinate matrix using Euler angles
% R_q : Configuration position coordinate matrix using quaternions
% X   : Full state variable matrix using Euler angles
% X_q : Full state variable matrix using quaternions

clear eta lonL L K j jj u0 r0 ac0 u r ac

hslsim

% Lastly, Plot the primary state and control variables as time histories.

xn = [1:N]; hslplot
```

HSL_CH47BDAT.M

```
function D = hsl_ch47bdat(mass,inertia,links)

% HSL_CH47BDAT : Aircraft aerodynamic, mass, inertial and geometric data
%
%                DAT = HSL_CH47BDAT((mass)(,inertia)(,links))
%
%                mass    : Helicopter mass (slugs)
%                inertia : Inertia matrix (slug.ft^2)
%                links   : Links data matrix (see HSL_INIT)
%
%                DAT     : Data structure (see HSL_INIT)

% Mass, inertial and aerodynamic data obtained from reference [1].
%
% 1. Weber, J.M. and Liu, T.Y. and Chung, W.
%    "A Mathematical Simulation Model of the CH-47B Helicopter, Volumes 1 & 2"
%    NASA-TM-84351-VOL-1/2, NASA Ames Research Center, Aug, 1984

% R.A. Stuckey  01/06/99  (c) 1999, Defence Science and Technology Organisation
% ----------------------------------------------------------------------------

if nargin<3, links   = []; end
if nargin<2, inertia = []; end
if nargin<1, mass    = []; end

% Set some defaults

if isempty(mass),    mass = 33000/32.174; end
if isempty(inertia)
   inertia = [ 34000 0      14900
               0      202500 0
               14900 0      191000 ];
end

D = struct('Name',[],'V',[],'A',[],'m',[],'J',[],'S',[]);

D.Name = 'CH-47B';

D.V = [ 0.1 20 40 60 80 100 120 130 ]'; % Trim airspeed (KTAS)

% Construct the aerodynamic coefficient matrix

D.A = zeros(8,10*6,2);

% SAS Off
%
% v = 0.1 KTAS
%
A = [
 -1.99980e-002 -2.78070e-004  3.11490e-002 -5.32570e-004  1.10900e-002  7.34520e-004
 -4.59450e-004 -1.07040e-001  4.00190e-003 -1.07710e-002  9.49780e-006  5.81320e-004
  3.00850e-002  2.23380e-003 -2.98310e-001  3.99760e-004  6.38150e-004  4.24930e-005
  4.26000e-002 -2.83620e+000 -1.25200e-001 -1.27950e+000  2.95300e-002 -1.48080e-002
  2.78070e+000 -7.31250e-003 -2.64720e-001  8.71280e-002 -1.09730e+000 -1.33780e-001
 -1.59040e-001 -3.30450e-001 -5.25060e-002 -9.02880e-002 -2.68610e-001 -8.91680e-002
  5.70000e-002 -4.84860e-004  4.98650e-002 -3.46400e-002  3.28160e-001  5.40720e-002
```

```
     1.00060e-005   1.09170e+000 -7.62340e-005   4.86300e-001   7.42500e-006   9.74910e-003
    -4.76460e-007   9.86840e-003   0.00000e+000 -1.26340e-001   0.00000e+000   1.92690e-001
     9.81570e-001   6.56800e-002 -8.47370e+000 -1.70400e-002 -1.43180e-003 -5.52630e-004
    ]'; D.A(1,:,1) = A(:)';

    % v = 20.0 KTAS
    %
    A = [
    -1.28440e-002   2.05350e-003 -4.05230e-002   3.66750e-004   1.55770e-002   9.33590e-004
     1.43630e-004 -4.60310e-002   4.43150e-003 -8.76990e-003 -8.73300e-004   2.30440e-004
     2.67660e-002   4.35330e-003 -2.82440e-001   8.33700e-004   1.66480e-002   7.13630e-004
     2.76530e-002 -1.51220e+000 -1.05700e-001 -8.86220e-001   1.71360e-002 -5.86890e-003
     2.89980e+000 -1.55240e-001 -2.77310e+000   2.38660e-002 -1.63390e+000 -1.51860e-001
    -1.11160e-001 -2.01820e-001   1.76410e-001 -6.46980e-002 -2.47710e-001 -7.64320e-002
     4.21820e-002   6.31740e-002   2.51680e-001 -1.04610e-002   3.35480e-001   5.25400e-002
     9.33870e-005   1.08670e+000 -1.04440e-003   4.85580e-001 -2.16560e-005   8.61240e-003
    -7.28990e-005 -7.71500e-003   1.22740e-003 -1.30970e-001   2.10380e-004   1.91730e-001
     7.23840e-001   5.33870e-002 -8.45390e+000 -2.18100e-002 -8.30050e-003   2.06350e-003
    ]'; D.A(2,:,1) = A(:)';

    % v = 40.0 KTAS
    %
    A = [
    -1.45080e-002 -4.56290e-004 -1.07970e-001 -2.78280e-004   7.31330e-004   2.52740e-004
     7.12390e-004 -5.94030e-002   1.55100e-003 -8.99530e-003 -1.53180e-003   3.20370e-004
     2.85410e-002   7.10780e-003 -3.49780e-001   2.74400e-003   2.58770e-002   2.49070e-005
     2.60640e-002 -1.73850e+000 -9.39210e-002 -9.51320e-001   1.28110e-002 -4.82000e-003
     2.80990e+000 -2.62180e-001 -3.29150e+000 -7.03350e-002 -1.76760e+000 -8.23200e-002
    -9.15160e-002 -2.41250e-001   3.18470e-002 -8.39020e-002 -2.56190e-001 -6.83260e-002
     3.53470e-002   1.07320e-001   6.49750e-001   1.62620e-002   3.74440e-001   3.69750e-002
     3.09700e-005   1.08450e+000 -4.11670e-004   4.85580e-001   7.42500e-006   7.62330e-003
     9.52930e-006 -2.32600e-002   1.90590e-004 -1.35310e-001   1.06420e-004   1.91260e-001
     4.91350e-001   6.53500e-002 -7.96780e+000 -9.56590e-003   1.23530e-001   5.36610e-003
    ]'; D.A(3,:,1) = A(:)';

    % v = 60.0 KTAS
    %
    A = [
    -8.90430e-003 -1.36390e-003 -7.54850e-002 -7.78620e-004 -7.26000e-003   2.75770e-004
     4.56690e-004 -7.23000e-002   2.38840e-003 -9.29200e-003 -1.28440e-003   7.42330e-004
     3.42780e-002   4.36120e-003 -5.63570e-001   2.04470e-003   1.45080e-002 -3.09370e-004
     2.12800e-002 -1.97880e+000 -6.27030e-002 -1.02010e+000   1.99240e-002 -4.54600e-003
     2.63080e+000 -1.34030e-001   6.40370e-001 -6.64380e-002 -1.58130e+000 -5.01390e-002
    -6.99840e-002 -2.48750e-001 -1.80370e-001 -8.87950e-002 -2.73610e-001 -6.32470e-002
     4.75450e-002   9.41300e-002   8.43060e-001   2.05270e-002   4.11840e-001   2.91390e-002
     2.38230e-005   1.08520e+000 -3.58300e-004   4.86690e-001   1.48500e-005   6.29670e-003
     9.52930e-006 -4.43990e-002   2.59200e-004 -1.41650e-001   1.04570e-004   1.91280e-001
     3.27550e-001   6.33380e-002 -8.15050e+000 -1.81260e-003   2.33770e-001   4.56090e-003
    ]'; D.A(4,:,1) = A(:)';

    % v = 80.0 KTAS
    %
    A = [
    -5.70700e-003 -8.59470e-004   2.30150e-002 -7.20310e-004 -8.07210e-003   2.93460e-004
    -7.31440e-004 -8.77940e-002   4.89230e-003 -1.01780e-002 -7.76930e-004   1.34520e-003
     4.27800e-002   2.40690e-003 -6.36790e-001   1.81170e-003   1.14460e-002 -5.56030e-004
     2.05520e-002 -2.05910e+000 -5.30210e-002 -1.03580e+000   2.64380e-002 -1.17890e-002
     2.63110e+000 -4.12240e-002 -4.07800e-001 -5.84190e-002 -1.65180e+000 -2.79330e-002
```

```
  -6.46630e-002 -2.44250e-001 -1.83310e-001 -8.63580e-002 -2.75520e-001 -6.21810e-002
   4.99400e-002  6.90110e-002  7.23190e-001  1.81860e-002  4.30170e-001  2.50860e-002
   4.24050e-005  1.08640e+000 -5.71760e-004  4.86460e-001  1.98000e-005  7.14560e-003
   1.14350e-005 -3.10170e-002  2.28700e-004 -1.37820e-001  1.31180e-004  1.91540e-001
   4.18550e-001  4.72800e-002 -9.34120e+000 -3.23580e-003  2.26040e-001  5.02230e-003
]'; D.A(5,:,1) = A(:)';

% v = 100.0 KTAS
%
A = [
 -1.26360e-002 -7.51370e-004  7.79880e-002 -6.59260e-004 -6.81070e-003  8.58610e-005
 -1.35680e-003 -1.05140e-001  6.60610e-003 -1.12800e-002 -3.57580e-004  1.77010e-003
  4.98200e-002  8.41670e-004 -6.76910e-001  1.32360e-003  1.16510e-002 -7.02930e-004
  2.15280e-002 -2.00890e+000 -4.85800e-002 -1.01300e+000  3.20850e-002 -1.78010e-002
  2.68250e+000  2.56190e-002 -5.28360e-001 -2.10030e-002 -1.70960e+000 -6.07910e-002
 -6.49300e-002 -2.40140e-001 -1.80540e-001 -8.29250e-002 -2.83950e-001 -6.06080e-002
  5.00190e-002  5.66120e-002  6.17770e-001  9.06130e-003  4.47050e-001  3.78660e-002
  6.24170e-005  1.08910e+000 -7.85210e-004  4.86820e-001  1.36120e-005  7.83530e-003
  1.04820e-005 -2.02930e-002  3.12560e-004 -1.34970e-001  1.52830e-004  1.92080e-001
  4.89300e-001  5.72410e-002 -1.03410e+001 -9.66370e-003  1.99790e-001  8.24070e-003
]'; D.A(6,:,1) = A(:)';

% v = 120.0 KTAS
%
A = [
 -2.77000e-002 -1.34170e-004  6.30760e-002 -4.79240e-004 -4.14310e-003  8.77130e-005
 -1.64920e-003 -1.23550e-001  8.15140e-003 -1.24840e-002  9.20080e-005  2.10200e-003
  5.22720e-002  5.28050e-004 -7.00810e-001  1.12150e-003  1.20600e-002 -7.09630e-004
  2.36600e-002 -1.86590e+000 -3.99660e-002 -9.61180e-001  3.89050e-002 -2.55800e-002
  2.74400e+000  1.25820e-001 -4.73260e-001  2.85120e-003 -1.70350e+000 -6.41210e-002
 -7.00630e-002 -2.03000e-001 -2.14120e-001 -6.99070e-002 -2.98380e-001 -6.68580e-002
  5.27850e-002  3.37610e-002  5.10630e-001  4.49670e-003  4.51130e-001  4.12170e-002
 -2.66820e-005  1.09580e+000 -8.69070e-004  4.88370e-001  8.04370e-006  8.50380e-003
 -7.33760e-005 -1.02440e-002  1.67720e-004 -1.32770e-001  1.72630e-004  1.93300e-001
  5.15320e-001  6.42760e-002 -1.09880e+001 -1.27980e-002  1.82350e-001  1.35210e-002
]'; D.A(7,:,1) = A(:)';

% v = 130.0 KTAS
%
A = [
 -3.78490e-002  2.51630e-004  1.32080e-002 -4.70110e-004 -2.21120e-003 -1.31000e-004
 -1.78130e-003 -1.35140e-001  8.17960e-003 -1.31600e-002  2.78040e-004  2.27430e-003
  4.26380e-002  2.86170e-003 -7.05780e-001  1.31020e-003  1.24230e-002 -6.89930e-004
  2.47760e-002 -1.77710e+000 -3.57920e-002 -9.30250e-001  4.19650e-002 -2.93120e-002
  2.76380e+000  1.67400e-001 -3.02350e-001  1.48530e-002 -1.67720e+000 -6.89040e-002
 -7.88740e-002 -1.85370e-001 -2.56380e-001 -7.06540e-002 -3.08690e-001 -5.64850e-002
  6.57840e-002  2.71970e-002  4.62770e-001  2.11230e-003  4.46010e-001  4.39730e-002
  2.38230e-005  1.10660e+000 -3.58300e-004  4.91790e-001  6.80620e-006  8.25240e-003
  1.76290e-005 -1.51530e-002  5.33640e-005 -1.35500e-001  7.92000e-005  1.95170e-001
  3.55270e-001  5.92710e-002 -1.11430e+001 -1.47050e-002  1.91100e-001  1.50040e-002
]'; D.A(8,:,1) = A(:)';


% SAS On
%
% v = 0.1 KTAS
%
A = [
```

```
  -2.00190e-002 -2.79300e-004  3.13430e-002 -5.33410e-004  1.10900e-002  7.34570e-004
  -4.58720e-004 -1.07040e-001  3.99430e-003 -1.07860e-002  8.69340e-006  6.02580e-004
   2.95890e-002  2.20110e-003 -2.93800e-001  3.92040e-004  6.48540e-004  4.01240e-005
   4.26580e-002 -4.80530e+000 -1.25310e-001 -2.16340e+000  2.95170e-002 -2.27710e-002
   2.76530e+000 -8.48820e-003 -1.16850e-001  8.65030e-002 -1.09920e+000 -1.33820e-001
  -1.59080e-001 -3.54870e-001 -5.24300e-002  5.98430e-002 -2.68650e-001 -3.23810e-001
   5.69980e-002 -4.73250e-004  4.98950e-002 -3.46380e-002  3.28170e-001  5.40740e-002
  -4.76460e-007  1.09170e+000  0.00000e+000  4.86300e-001  6.18750e-007  9.74810e-003
   0.00000e+000  9.87340e-003 -7.62340e-006 -1.26340e-001  6.18750e-007  1.92690e-001
   9.82140e-001  6.57510e-002 -8.47890e+000 -1.70130e-002 -1.43490e-003 -5.47820e-004
]'; D.A(1,:,2) = A(:)';

% v = 20.0 KTAS
%
A = [
 -1.28450e-002  2.05360e-003 -4.05190e-002  3.68320e-004  1.55760e-002  9.31240e-004
  1.43680e-004 -4.69260e-002  4.44410e-003 -1.19320e-002 -8.70520e-004  4.54010e-003
  2.67660e-002  4.35350e-003 -2.82440e-001  8.35320e-004  1.66470e-002  7.11290e-004
  2.73040e-002 -3.47460e+000 -1.00800e-001 -1.76990e+000  1.76080e-002 -1.10830e-002
  2.90000e+000 -1.55300e-001 -2.77560e+000  2.38450e-002 -1.63400e+000 -1.51840e-001
 -1.11040e-001 -1.93430e-001  1.74270e-001  9.46100e-002 -2.47990e-001 -3.10110e-001
  4.22050e-002  6.31900e-002  2.51470e-001 -1.04580e-002  3.35490e-001  5.25420e-002
 -1.95350e-005  1.08670e+000  2.82070e-004  4.85580e-001  5.07370e-005  8.61630e-003
 -8.67170e-005 -7.72250e-003  1.15880e-003 -1.30970e-001  1.16320e-004  1.91730e-001
  7.23850e-001  5.34030e-002 -8.45410e+000 -2.18080e-002 -8.30980e-003  2.06790e-003
]'; D.A(2,:,2) = A(:)';

% v = 40.0 KTAS
%
A = [
 -1.42800e-002  2.09760e-004 -1.04060e-001 -1.66880e-004  3.02760e-003  4.71550e-004
  7.12670e-004 -6.16240e-002  1.55750e-003 -1.53840e-002 -1.52910e-003  8.83450e-003
  2.85590e-002  7.19340e-003 -3.49160e-001  2.75790e-003  2.61800e-002  5.38230e-005
  2.59480e-002 -3.69780e+000 -9.25870e-002 -1.83520e+000  1.27460e-002 -8.27830e-003
  2.80990e+000 -2.62190e-001 -3.29140e+000 -7.03380e-002 -1.76760e+000 -8.23200e-002
 -9.15410e-002 -2.41250e-001  3.20760e-002 -8.39040e-002 -2.56190e-001 -6.83270e-002
  3.53760e-002  1.07330e-001  6.49480e-001  1.62660e-002  3.74470e-001  3.69740e-002
  3.38290e-005  1.08450e+000 -4.11670e-004  4.85580e-001  1.67060e-005  7.62280e-003
  7.62340e-006 -2.32630e-002  1.90590e-004 -1.35310e-001  1.01470e-004  1.91260e-001
  4.91340e-001  6.53570e-002 -7.96770e+000 -9.56410e-003  1.23540e-001  5.36710e-003
]'; D.A(3,:,2) = A(:)';

% v = 60.0 KTAS
%
A = [
 -8.27460e-003 -4.85040e-005 -6.34290e-002 -4.90270e-004 -1.49840e-003  6.84190e-004
  4.55900e-004 -7.65220e-002  2.40440e-003 -1.89950e-002 -1.27800e-003  1.33160e-002
  3.43190e-002  4.43620e-003 -5.62920e-001  2.06160e-003  1.48370e-002 -2.86400e-004
  2.11980e-002 -3.94060e+000 -6.09110e-002 -1.90630e+000  2.00350e-002 -5.59910e-003
  2.63080e+000 -1.33990e-001 -6.40410e-001 -6.64230e-002 -1.58130e+000 -5.01410e-002
 -6.99690e-002 -2.48740e-001 -1.80520e-001 -8.87900e-002 -2.73610e-001 -6.32470e-002
  4.75450e-002  9.41200e-002  8.43140e-001  2.05240e-002  4.11830e-001  2.91370e-002
  1.90590e-005  1.08520e+000 -3.88800e-004  4.86690e-001  4.33130e-006  6.29400e-003
  1.28650e-005 -4.44340e-002  1.82960e-004 -1.41660e-001  1.03330e-004  1.91280e-001
  3.27530e-001  6.33311e-002 -8.15030e+000 -1.81280e-003  2.33750e-001  4.55900e-003
]'; D.A(4,:,2) = A(:)';

% v = 80.0 KTAS
```

```
%
A = [
 -5.01240e-003  1.05650e-004  3.32200e-002 -4.69290e-004 -2.04460e-003  6.48800e-004
 -7.36350e-004 -8.98880e-002  4.92400e-003 -1.68720e-002 -7.82160e-004  1.03840e-002
  4.28110e-002  2.45010e-003 -6.36340e-001  1.82300e-003  1.17170e-002 -5.37880e-004
  2.05250e-002 -4.02230e+000 -5.29830e-002 -1.92140e+000  2.64020e-002 -1.43840e-002
  2.63120e+000 -4.12660e-002 -4.07570e-001 -5.84350e-002 -1.65180e+000 -2.79310e-002
 -6.46790e-002 -2.44270e-001 -1.83170e-001 -8.63610e-002 -2.75610e-001 -6.21850e-002
  4.99380e-002  6.90080e-002  7.23020e-001  1.81850e-002  4.30170e-001  2.50850e-002
  4.19290e-005  1.08640e+000 -5.94630e-004  4.86460e-001  8.04370e-006  7.14940e-003
  1.71530e-005 -3.09520e-002  1.82960e-004 -1.37800e-001  1.31790e-004  1.91540e-001
  4.18540e-001  4.72930e-002 -9.34120e+000 -3.23290e-003  2.26060e-001  5.02440e-003
]'; D.A(5,:,2) = A(:)';

% v = 100.0 KTAS
%
A = [
 -1.21400e-002 -2.12260e-004  8.45320e-002 -5.70060e-004 -2.20040e-003  4.79490e-004
 -1.35350e-003 -1.06330e-001  6.61450e-003 -1.68210e-002 -3.52720e-004  9.49190e-003
  4.98460e-002  8.65710e-004 -6.76670e-001  1.32940e-003  1.18410e-012 -6.89160e-004
  2.15560e-002 -3.97640e+000 -4.71510e-002 -1.89920e+000  3.21750e-002 -2.15830e-002
  2.68240e+000  2.56070e-002 -5.22640e-001 -2.10470e-002 -1.70950e+000 -6.07840e-002
 -6.49100e-002 -2.40130e-001 -1.80540e-001 -8.29660e-002 -2.84000e-001 -6.06040e-002
  5.00630e-002  5.66060e-002  6.18090e-001  9.06090e-003  4.47080e-001  3.78660e-002
  5.47930e-005  1.08910e+000 -7.16600e-004  4.86810e-001  1.67060e-005  7.83420e-003
  1.66760e-005 -2.03130e-002  2.97310e-004 -1.34970e-001  1.77580e-004  1.92080e-001
  4.89350e-001  5.72900e-002 -1.03410e+001 -9.64680e-003  1.99830e-001  8.24110e-003
]'; D.A(6,:,2) = A(:)';

% v = 120.0 KTAS
%
A = [
 -2.72310e-002  1.60600e-004  6.76800e-002 -4.40090e-004 -1.53330e-004  4.51540e-004
 -1.64710e-003 -1.24180e-001  7.99580e-003 -1.74270e-002  1.00270e-004  9.18990e-003
  5.22970e-002  5.26710e-004 -7.00690e-001  1.12160e-003  1.21910e-002 -7.00720e-004
  2.33190e-002 -3.84480e+000 -3.88800e-002 -1.84990e+000  3.86730e-002 -3.06020e-002
  2.74360e+000  1.11460e-001 -4.81120e-001  2.34480e-003 -1.70360e+000 -6.39660e-002
 -6.97970e-002 -2.02890e-001 -2.21880e-001 -6.98590e-002 -2.98370e-001 -6.68540e-002
  5.26670e-002  3.35910e-002  5.13600e-001  4.45150e-003  4.51180e-001  4.11780e-002
  6.76580e-005  1.09570e+000 -8.30950e-004  4.88340e-001  9.28120e-006  8.50630e-003
  2.14410e-005 -1.01920e-002  1.52470e-004 -1.32750e-001  1.75720e-004  1.93290e-001
  5.15400e-001  6.40920e-002 -1.09850e+001 -1.28180e-002  1.82370e-001  1.34750e-002
]'; D.A(7,:,2) = A(:)';

% v = 130.0 KTAS
%
A = [
 -3.72690e-002  4.92160e-004  1.74470e-002 -4.51350e-004  1.73700e-003  2.56790e-004
 -1.78010e-003 -1.35900e-001  8.34420e-003 -1.80350e-002  2.81930e-004  9.20090e-003
  4.26400e-002  2.85720e-003 -7.05740e-001  1.30860e-003  1.24690e-002 -6.85800e-004
  2.47090e-002 -3.77600e+000 -3.51820e-002 -1.82540e+000  4.20970e-002 -3.36860e-002
  2.76380e+000  1.67250e-001 -3.02540e-001  1.47950e-002 -1.67700e+000 -6.88860e-002
 -7.88690e-002 -1.85400e-001 -2.56340e-001 -7.06680e-002 -3.08690e-001 -5.64830e-002
  6.57720e-002  2.72330e-002  4.62820e-001  2.12550e-003  4.46080e-001  4.39700e-002
  3.85940e-005  1.10660e+000 -5.26020e-004  4.91790e-001  1.29940e-005  8.25660e-003
  1.76290e-005 -1.51090e-002  2.28700e-005 -1.35490e-001  8.78620e-005  1.95170e-001
  3.55260e-001  5.91680e-002 -1.11430e+001 -1.47390e-002  1.91010e-001  1.50090e-002
]'; D.A(8,:,2) = A(:)';
```

```
D.m = mass; % Mass (slugs)

D.J = inertia; % Inertia matrix (slugs.ft^2)


% Construct the geometric struct

D.S = struct('Patches',[],'Lines',[],'Links',[]);

D.S.Patches.Data = [
  27.57681    1.60769    4.56059
  23.11464    4.75745    6.95572
  23.11464    4.75745   -2.49356
 -25.42775    4.75745   -2.49356
 -13.96066    6.69324    6.89010
 -13.96066   -6.69324    6.89010
 -25.42775   -4.75745   -2.49356
  23.11464   -4.75745   -2.49356
  23.11464   -4.75745    6.95572
  27.57681   -1.60769    4.56059
  23.11464    1.27959   -2.46075
  23.11464    1.27959   -4.79026
  15.73240    1.27959   -4.42935
  15.73240    1.27959   -2.46075
  15.73240   -1.27959   -2.46075
  15.73240   -1.27959   -4.42935
  23.11464   -1.27959   -4.79026
  23.11464   -1.27959   -2.46075
  -8.21890    1.27959   -2.46075
 -10.41718    1.27959   -8.30093
 -25.08325    1.27959   -9.58052
 -25.42775    1.27959   -2.46075
 -25.42775   -1.27959   -2.46075
 -25.08325   -1.27959   -9.58052
 -10.41718   -1.27959   -8.30093
  -8.21890   -1.27959   -2.46075
];

D.S.Patches.CoordIndex = [
   0   1   2   2  -1 ...
   1   2   3   4  -1 ...
   3   4   5   6  -1 ...
   5   6   7   8  -1 ...
   7   8   9   9  -1 ...
   1   4   5   8  -1 ...
   0   1   8   9  -1 ...
   0   2   7   9  -1 ...
   2   3   6   7  -1 ...
  10  11  12  13  -1 ...
  12  13  14  15  -1 ...
  14  15  16  17  -1 ...
  10  11  16  17  -1 ...
  11  12  15  16  -1 ...
  18  19  20  21  -1 ...
  20  21  22  23  -1 ...
  22  23  24  25  -1 ...
```

```
    18  19  24  25  -1 ...
    19  20  23  24  -1
];


D.S.Lines.Data = [
   51.47889    0.00000   -7.64473
   47.46121   14.99417   -7.64473
   36.48472   25.97066   -7.64473
   21.49055   29.98834   -7.64473
    6.49638   25.97066   -7.64473
   -4.48011   14.99417   -7.64473
   -8.49779    0.00000   -7.64473
   -4.48011  -14.99417   -7.64473
    6.49638  -25.97066   -7.64473
   21.49055  -29.98834   -7.64473
   36.48472  -25.97066   -7.64473
   47.46121  -14.99417   -7.64473
   51.47889   -0.00000   -7.64473
        NaN        NaN        NaN
   10.30234    0.00000  -13.22243
    6.28466   14.99417  -13.22243
   -4.69183   25.97066  -13.22243
  -19.68600   29.98834  -13.22243
  -34.68017   25.97066  -13.22243
  -45.65666   14.99417  -13.22243
  -49.67434    0.00000  -13.22243
  -45.65666  -14.99417  -13.22243
  -34.68017  -25.97066  -13.22243
  -19.68600  -29.98834  -13.22243
   -4.69183  -25.97066  -13.22243
    6.28466  -14.99417  -13.22243
   10.30234   -0.00000  -13.22243
];


D.S.Links.Data = [
    5.91000    0.00000    6.89000
    0.00000    0.00000    6.89000
   -7.42000    0.00000    6.89000
];

if ~isempty(links), D.S.Links.Data = links; end
```

HSL_BOXDAT.M

```
function D = hsl_boxdat(mass,inertia,links,config,bsize)

% HSL_BOXDAT : Box Container aerodynamic, mass, inertial and geometric data
%
%             DAT = HSL_BOXDAT((mass)(,inertia)(,links)(,config)(,bsize))
%
%             mass    : Load mass (slugs)
%             inertia : Inertia matrix (slug.ft^2)
%             links   : Links data matrix (see HSL_INIT)
%             config  : Sling configuration string ['single'|'multiple']
%             bsize   : Box size [x,y,z] (ft)
%
```

```
%                  DAT     : Data structure (see HSL_INIT)

% R.A. Stuckey  01/06/99  (c) 1999, Defence Science and Technology Organisation
% -----------------------------------------------------------------------------

if nargin<5, bsize   = []; end
if nargin<4, config  = []; end
if nargin<3, links   = []; end
if nargin<2, inertia = []; end
if nargin<1, mass    = []; end

% Set some defaults

if isempty(mass),    mass = 1000/32.174; end
if isempty(inertia), inertia = diag([ 0.33 1.20 1.20 ]*mass*32.174); end
if isempty(bsize),   bsize  = [ 6.0 6.0 6.0 ];  end
if isempty(config),  config = 'multiple'; end

D = struct('Name',[],'V',[],'A',[],'m',[],'J',[],'S',[]);

D.Name = 'BOX';

D.V = [ 0.0 ]; % Trim airspeed (KTAS)

% Construct the aerodynamic coefficient matrix

D.A = zeros(1,10*6,1);

% v = 0.0 KTAS
%
A = [
  0.00000e+000  0.00000e+000  0.00000e+000  0.00000e+000  0.00000e+000  0.00000e+000
  0.00000e+000  0.00000e+000  0.00000e+000  0.00000e+000  0.00000e+000  0.00000e+000
  0.00000e+000  0.00000e+000  0.00000e+000  0.00000e+000  0.00000e+000  0.00000e+000
  0.00000e+000  0.00000e+000  0.00000e+000  0.00000e+000  0.00000e+000  0.00000e+000
  0.00000e+000  0.00000e+000  0.00000e+000  0.00000e+000  0.00000e+000  0.00000e+000
  0.00000e+000  0.00000e+000  0.00000e+000  0.00000e+000  0.00000e+000  0.00000e+000
  0.00000e+000  0.00000e+000  0.00000e+000  0.00000e+000  0.00000e+000  0.00000e+000
  0.00000e+000  0.00000e+000  0.00000e+000  0.00000e+000  0.00000e+000  0.00000e+000
  0.00000e+000  0.00000e+000  0.00000e+000  0.00000e+000  0.00000e+000  0.00000e+000
  0.00000e+000  0.00000e+000  0.00000e+000  0.00000e+000  0.00000e+000  0.00000e+000
]'; D.A(1,:,1) = A(:)';

D.m = mass; % Mass (slugs)

D.J = inertia; % Inertia matrix (slugs.ft^2)

% Construct the geometric struct

D.S = struct('Patches',[],'Lines',[],'Links',[]);

D.S.Patches.Data = [
    1   1   1
    1   1  -1
   -1   1  -1
   -1   1   1
   -1  -1   1
   -1  -1  -1
```

```
   1  -1  -1
   1  -1   1
]*diag(bsize/2);

D.S.Patches.CoordIndex = [
   0   1   2   3  -1 ...
   2   3   4   5  -1 ...
   4   5   6   7  -1 ...
   1   2   5   6  -1 ...
   0   1   6   7  -1 ...
   0   3   4   7  -1
];

if strcmpi(config,'single')

   D.S.Lines.Data = [
       1   1  -1
       0   0  -1
     NaN NaN NaN
       1  -1  -1
       0   0  -1
     NaN NaN NaN
      -1   1  -1
       0   0  -1
     NaN NaN NaN
      -1  -1  -1
       0   0  -1
     NaN NaN NaN
   ]*diag(bsize/2);

   D.S.Links.Data = [
       0   0  -1
   ]*diag(bsize.*[ 0.0 0.0 1.0 ]);

   if ~isempty(links)
      if (length(links) == 1)
         D.S.Links.Data(3) = links;
      else
         D.S.Links.Data = links;
      end
   end

   D.S.Lines.Data([2,5,8,11],:) = ones(4,1)*D.S.Links.Data;

elseif strcmpi(config,'multiple')

   D.S.Lines.Data = [];
   D.S.Links.Data = [
       1   1  -1
      -1   1  -1
      -1  -1  -1
       1  -1  -1
   ]*diag(bsize.*[ 0.5 0.5 0.5 ]);

   if ~isempty(links), D.S.Links.Data = links; end
end
```

HSL_LOAD.M

```
function r = hsl_load(r,acj)

% HSL_LOAD : Calculate load positions from the helicopter positions, the
%            helicopter and load attitudes and the cable lengths & orientation
%
%            r = HSL_LOAD(r(,acj))
%
%            r   : Configuration position vector
%                = [ R1*_N ;   R2*_N ; ... ;   Rn*_N
%                       a1 ;      a2 ; ... ;      an ]
%            acj : Cable-angle matrix : Single-cable case only
%                = [ [ 0 0 0 ]' ac2 ... acn ]
%
%            The sub-vectors are defined:
%                                . . .
%            R1*_N : helicopter [x,y,z] position vector in inertial axes
%            Rj*_N : load [x,y,z] position vector in inertial axes
%            a1    : helicopter [phi,theta,psi] Euler angular position vector
%            aj    : load [phi,theta,psi] Euler angular position vector
%
%            acj   : cable/cg-line [phi,theta,psi] angles in cable-axes
%
%            See HSL_INIT for more information

% R.A. Stuckey  01/10/97  (c) 1997, Defence Science and Technology Organisation
% ----------------------------------------------------------------------------

global HDAT_ LDAT_ CDAT_

n = length(LDAT_); n = n+(~n);

if nargin<2, acj = zeros(n,3); end

% Create some transformation matrices

T_jN = zeros(3,3,n); T_cjN = NaN*ones(3,3,n);

T_jN(:,:,1) = euler(r(n*3+[1:3]));

% Determine sling configuration

mj = zeros(1,n);
MultipleCables = NaN; SingleCable = NaN;
for j = 2:n
   mj(j) = length(CDAT_(j).l0);

   MultipleCables(j) = (mj(j)>2) & (~any(diff(sort(CDAT_(j).i(1,:)))));
   SingleCable(j) = (mj(j)==1);
end

% Calculate the load positions

for j = 2:n

   jj = (j-1)*3+[1:3];
```

```
    T_jN(:,:,j) = euler(r(n*3+jj)); % Load-axes transformation


    toplinks = HDAT_.S.Links.Data(CDAT_(j).i(1,:),:);
    botlinks = LDAT_(j).S.Links.Data(CDAT_(j).i(2,:),:);


    if MultipleCables(j)


        if any(diff(CDAT_(j).l))
            error(' Cable lengths must be equal !')
        end

% Calculate load length (x) and width (y)

        Ri1i4_j = diff(botlinks([4,1],:))'; b = sqrt(sum(Ri1i4_j.^2));
        Ri1i2_j = diff(botlinks([2,1],:))'; c = sqrt(sum(Ri1i2_j.^2));

% Calculate distance from load cg to helicopter attachment point

        zl = sqrt(CDAT_(j).l(1)^2-(b/2)^2-(c/2)^2)-botlinks(1,3);

% Update the (load) position vector

        r(jj) = r(1:3) ...
                +T_jN(:,:,1)'*toplinks(1,:)' ...
                +T_jN(:,:,j)'*[ 0 0 zl ]';

    elseif SingleCable(j)

        T_cjN(:,:,j) = euler(acj(:,j)); % Cable-axes transformation

% Update the (load) position vector

        r(jj) = r(1:3) ...
                +T_jN(:,:,1)'*toplinks' ...
                +T_cjN(:,:,j)'*[ 0 0 CDAT_(j).l ]' ...
                -T_jN(:,:,j)'*botlinks';
    end
end
```

HSLSIM.M

```
% HSLSIM : Helicopter Slung-Load dynamic Simulation
%
%          HSLSIM
%
%          Inputs:
%
%          opt_  : GLOBAL options cell array [4x1]
%          HDAT_ : GLOBAL helicopter struct
%          LDAT_ : GLOBAL loads struct array [1xn]
%          CDAT_ : GLOBAL loads struct array [1xn]
%          n     : Number of bodies
%          t     : Time vector [Nx1]
%          TD    : Time & control input matrix [Nx5]
%          D     : System mass/inertia matrix [n*6xn*6]
%          x0    : Trim state vector [n*6x1]
```

```
%           x     : Initial state vector [n*6x1]
%
%           Outputs:
%
%           U     : Generalised velocity coordinate matrix [Nxn*6]
%           R     : Configuration position coordinate matrix using Euler angles [Nxn*6]
%           R_q   : Configuration position coordinate matrix using quaternions [Nxn*7]
%           X     : Full state variable matrix using Euler angles [Nxn*12]
%           X_q   : Full state variable matrix using quaternions [Nxn*13]
%
%           See HSL_INIT for more information

% R.A. Stuckey  01/10/97  (c) 1997, Defence Science and Technology Organisation
% -----------------------------------------------------------------------------

global HDAT_ LDAT_ CDAT_ opt_

% Check input variables and set defaults

if length(opt_)<4
   {'combined','euler',0,1};
   for i = length(opt_)+1:4
      opt_{i} = ans{i};
      warning([' Using opt_{',int2str(i),'} = ',opt_{i}])
   end
end

if (~strncmpi(opt_{1},'longitudinal',length(opt_{1}))) ...
 & (~strncmpi(opt_{1},'lateral',length(opt_{1}))) ...
 & (~strncmpi(opt_{1},'combined',length(opt_{1})))
   error(' Option, opt_{1} = ',opt_{1},' not recognised !')
end

opt_2 = strncmpi(opt_{2},'quaternion',length(opt_{2})); o2 = opt_2+3;
if (~opt_2)&(~strncmpi(opt_{2},'euler',length(opt_{2})))
   error(' Option, opt_{2} = ',opt_{2},' not recognised !')
end

if ~any(opt_{3}==[0,1])
   error(' Option, opt_{3} = ',int2str(opt_{3}),' not recognised !')
end
if opt_{3}
   for j = 2:n
      if isempty(CDAT_(j).K)
         error(' Empty stiffness/damping matrix, CDAT_(',int2str(j),').K !')
      end
   end
end

if ~any(opt_{4}==[0,1])
   error(' Option, opt{4} = ',int2str(opt_{4}),' not recognised !')
end
if (~opt_{4})&(~exist('control','dir'))
   error(' Linear simulation requires CONTROL SYSTEM TOOLBOX !')
end

% Determine sling configuration
```

```
mj = zeros(1,n);
MultipleCables = NaN; SingleCable = NaN;
for j = 2:n
    mj(j) = length(CDAT_(j).10);

    MultipleCables(j) = (mj(j)>2) & (~any(diff(sort(CDAT_(j).i(1,:)))));
    SingleCable(j) = (mj(j)==1);
end

% Construct inverse mass/inertia matrix

finD = isfinite(diag(D)); finDn = find(finD);
diag(inf*ones(1,n*6)); ans(finDn,finDn) = D(finDn,finDn); D = ans;
zeros(n*6); ans(finDn,finDn) = inv(D(finDn,finDn)); Di = ans;

% Determine trim configuration velocities

[xdot0,va0] = hsl_fun(0,zeros(n*12,1),[],D,Di,x0,zeros(n*6,1),zeros(1,5));

% Set initial, perturbed state from trim

if ~opt_2
    dx = x-x0;
else
    x0_q = [x0(1:n*9);zeros(n*4,1)]; x_q = [x(1:n*9);zeros(n*4,1)];
    for j = 1:n
        x0_q(n*9+(j-1)*4+[1:4]) = e2q1(x0(n*9+(j-1)*3+[1:3]));
        x_q(n*9+(j-1)*4+[1:4]) = e2q1(x(n*9+(j-1)*3+[1:3]));
    end
    dx_q = x_q-x0_q;
end

% Run the simulation

if opt_{4}==1 % Nonlinear simulation:
                % Uses 4/5th order R-K integration routine with fixed step-size

    options = odeset;

    if ~opt_2  % Euler representation
        [t,dX] = ode45f('hsl_fun',t,dx,options, D,Di,x0,va0,TD);

    else       % Quaternion representation
        [t,dX_q] = ode45f('hsl_fun',t,dx_q,options, D,Di,x0_q,va0,TD);
    end
else           % Linear simulation:
                % Uses linear time-invariant time response kernel

    if ~opt_2  % Euler representation
        del = 1e-3*ones(n*12,1); %%% DELTA FOR JACOBIAN COMPUTATION

        dx0 = zeros(n*12,1);

% Compute the state and control jacobian matrices

        fac = []; vec = []; del = 1e-3*ones(n*12,1);
        DFDY = numjac('hsl_fun',0,dx0,fty,del,fac,vec,[],[],[], D,Di,x0,va0,zeros(1,5));
```

```
        del = 1e-3*ones(4,1);     %%% DELTA
        ydel = diag(del); fdel = zeros(n*12,4);
        for j = 1:4
            fdel(:,j) = hsl_fun(0,dx0,[], D,Di,x0,va0,[0,ydel(:,j)']);
        end
        DFDD = (fdel-fty(:,ones(1,4)))*diag(1 ./del);

% Convert linear system from continuous to discrete

        sys = ss(DFDY,DFDD,eye(n*12),zeros(n*12,4));
        sysd = c2d(sys,t(2)-t(1),'foh');

% Implement any initial velocities and perform the simulation

        r0dot = [v0(1:n*3);zeros(n*3,1)];
        for j = 1:n
            Wij_j = eratesi(x0(n*9+(j-1)*3+[1:3]));
            r0dot(n*3+(j-1)*3+[1:3]) = Wij_j*v0(n*3+(j-1)*3+[1:3]);
        end

        dX = lsim(sysd,TD(:,2:5),t,dx)+t*[zeros(1,n*6),r0dot'];

    else       % Quaternion representation
        del = 1e-3*ones(n*13,1); %%% DELTA FOR JACOBIAN COMPUTATION

        dx0_q = zeros(n*13,1);

% Compute the state and control jacobian matrices

        fac = []; vec = []; del = 1e-3*ones(n*12,1);
        DFDY = numjac('hsl_fun',0,dx0_q,fty,del,fac,vec,[],[],[], D,Di,x0_q,va0,zeros(1,5));

        del = 1e-3*ones(4,1);     %%% DELTA
        ydel = diag(del); fdel = zeros(n*13,4);
        for j = 1:4
            fdel(:,j) = hsl_fun(0,dx0,[], D,Di,x0,va0,[0,ydel(:,j)']);
        end
        DFDD = (fdel-fty(:,ones(1,4)))*diag(1 ./del);

% Convert linear system from continuous to discrete

        sys = ss(DFDY,DFDD,eye(n*13),zeros(n*13,4));
        sysd = c2d(sys,t(2)-t(1),'foh');

% Implement any initial velocities and perform the simulation

        r0dot_q = [v0(1:n*3);zeros(n*4,1)];
        for j = 1:n
            Wij_j = qratesi(x0_q(n*9+(j-1)*4+[1:4]));
            r0dot_q(n*3+(j-1)*4+[1:4]) = Wij_j*v0(n*3+(j-1)*3+[1:3]);
        end

        dX_q = lsim(sysd,TD(:,2:5),t,dx_q)+t*[zeros(1,n*6),r0dot_q'];
    end
end

% Create the full state variable matrices
```

```
if ~opt_2      % Euler representation

% Detect and remove erroneous (divergent) observations from the simulation

   isdiv = (sign(abs(imag(dX)))|isinf(dX)|isnan(dX));

   if any(any(isdiv))
      warning('Divergent solution !')
      N = min(find(sum(isdiv,2)))-1; dX = dX(1:N,:);
   else
      N = size(dX,1);
   end
   t = t(1:N); TD = TD(1:N,:);

% Add initial state to perturbed state and calculate quaternions

   X = dX+ones(N,1)*x0'; R = X(:,n*6+[1:n*6]);

   U = X(:,1:n*6); R_q = [R(:,1:n*3),zeros(N,n*3)];
   for j = 1:n
      R_q(:,n*3+(j-1)*4+[1:4]) = e2q(R(:,n*3+(j-1)*3+[1:3]));
   end
   X_q = [U,R_q];
else           % Quaternion representation

% Detect and remove erroneous (divergent) observations from the simulation

   isdiv = (sign(abs(imag(dX_q)))|isinf(dX_q)|isnan(dX_q));

   if any(any(isdiv))
      warning('Divergent solution !')
      N = min(find(sum(isdiv,2)))-1; dX_q = dX_q(1:N,:);
   else
      N = size(dX_q,1);
   end
   t = t(1:N); TD = TD(1:N,:);

% Add initial state to perturbed state and calculate Euler angles

   X_q = dX_q+ones(N,1)*x0_q'; R_q = X_q(:,n*6+[1:n*7]);

   U = X_q(:,1:n*6); R = [R_q(:,1:n*3),zeros(N,n*4)];
   for j = 1:n
      R(:,n*3+(j-1)*3+[1:3]) = q2e(R_q(:,n*3+(j-1)*4+[1:4]));
   end
   X = [U,R];
end

% Compute body-axes velocities, cable angles and internal cable forces

Va = zeros(N,n*6); Vadot = zeros(N,n*6); TDD = zeros(N,5);
if n>1
   Acj = zeros(N,(n-1)*3); FC = zeros(N,n-1);
end

for i = 1:N % Evaluation loop (no integration)

% Call the function with all output arguments
```

```
    if ~opt_2  % Euler representation
       [xdot,va,vadot,acj,fc,d] = hsl_fun(t(i),dX(i,:)',[],D,Di,x0,va0,TD);

    else       % Quaternion representation
       [xdot_q,va,vadot,acj,fc,d] = hsl_fun(t(i),dX_q(i,:)',[],D,Di,x0_q,va0,TD);
    end

% Insert the variables into their respective observation matrices

    Va(i,:) = va'; Vadot(i,:) = vadot';
    if n>1
       squeeze(acj(:,1,2:n)); Acj(i,:) = ans(:)';
       FC(i,:) = (fc./diag(D([2:n]*3,[2:n]*3))/32.174)';
    end
    TDD(i,:) = [t(i),d'];
end
```

ODE45F.M

```
function [T,Y,Yd] = ode45f(odefile,T,y0,options,varargin)

% ODE45F : Solve differential equations - higher order method
%
%          [T,Y,Yd] = ODE45F('F',T,y0,options(,varargin))
%
%          F  : String containing the name of the ODE function
%
%          where  yd = F(t,y)
%
%          T  : Time vector [Nx1]
%          y0 : Initial conditions [nx1]
%
%          Y  : Solution matrix [Nxn]
%          Yd : Differential matrix [Nxn]
%
%          See ODE45, ODE

% Modified from ODE45.M:
%
% C.B. Moler, 3-25-87, 8-26-91, 9-08-92.
% Copyright (c) 1984-94 by The MathWorks, Inc.

% R.A. Stuckey  10/12/97  (c) 1997, Defence Science and Technology Organisation
% ----------------------------------------------------------------------------

% Initialise the integration parameters and matrices

alf=[ 1/4  3/8  12/13  1  1/2 ]';
bet=[ [  1        0       0       0       0       0     ]/4
      [  3        9       0       0       0       0     ]/32
      [  1932   -7200    7296     0       0       0     ]/2197
      [  8341  -32832   29440   -845      0       0     ]/4104
      [ -6080   41040  -28352   9295    -5643     0     ]/20520   ];
gam=[ [  902880   0     3953664  3855735 -1371249  277020 ]/7618050
      [ -2090     0      22528    21970   -15048   -27360 ]/752400  ];
```

```
T = T(:);

N = size(T,1); ny = size(y0,1); Nb = size(bet);

H = diff(T); f = zeros(ny,Nb(2)); Y = zeros(N,ny); Yd = Y;

Y(1,:) = y0';

% Set the output function

if isempty(options)
   outfun = '';
else
   outfun = odeget(options,'OutputFcn');
end

if ~isempty(outfun)
   feval(outfun,T([1,N]),y0,'init');
end

for n = 1:N-1 % The main loop ...

% Compute the slopes

   f(:,1) = feval(odefile,T(n),Y(n,:)',[],varargin{:});

   Yd(n,:) = f(:,1)';

   for j = 1:Nb(1)
      f(:,j+1) = feval(odefile,T(n)+H(n)*alf(j),Y(n,:)'+H(n)*f*bet(j,:)',[],varargin{:});
   end

% Estimate the error
%
%   delta = norm(H(n)*f*gam(2,:)','inf');

% Update the solution

   Y(n+1,:) = Y(n,:)+H(n)*gam(1,:)*f';

% Check the status of the output function

   if ~isempty(outfun)
      status = feval(outfun,T(n+1),Y(n+1,:));
      if status, break, end
   end
end

% Evaluate the last time point and truncate output matrices if necessary

Yd(n+1,:) = feval(odefile,T(n+1),Y(n+1,:)',[],varargin{:})';

N = n+1; T = T(1:N); Y = Y(1:N,:); Yd = Yd(1:N,:);

% Set the output status

if ~isempty(outfun)
```

```
    feval(outfun,[],[],'done');
end
```

HSL_FUN.M

```
function [xdot,va,vadot,acj,Fc,d] = hsl_fun(t,dx,FLAG,D,Di,x0,va0,TD)

% HSL_FUN : ODE function for helicopter slung-load system
%
%           [xdot,va,vadot,acj,Fc,d] = HSL_FUN(t,dx,FLAG,D,Di,x0,va0,TD)
%
%           t     : Current time variable
%           dx    : Current perturbed state vector [n*6x1]
%           FLAG  : String with the type of information to return *NOT USED*
%           D     : System mass/inertia matrix [n*6xn*6]
%           Di    : Inverse system mass/inertia matrix [n*6xn*6]
%           x0    : Trim state vector [n*6x1]
%           va0   : Trim body-axes velocity vector [n*6x1]
%           TD    : Time & control input matrix [Nx5]
%
%           xdot  : Current state rate vector [n*6x1]
%           va    : Current body-axes velocity vector [n*6x1]
%           vadot : Current body-axes acceleration vector [n*6x1]
%           acj   : Cable angle matrix [3x4xn]
%           Fc    : Internal cable force vector [n-1x1]
%           d     : Current control input vector [4x1]
%
%           See HSLSIM for details

% R.A. Stuckey  01/10/97  (c) 1997, Defence Science and Technology Organisation
% ----------------------------------------------------------------------------

global HDAT_ LDAT_ CDAT_ opt_ tdd_ vadot_ rdot_

n = length(LDAT_); n = n+(~n); nx = length(x0);
opt_2 = (nx==n*13); o2 = opt_2+3;

% Early exit if dx is in err

if  (~isreal(dx)|any(isinf(dx)|isnan(dx)))
   xdot = dx; return
end

% Define some strings for FEVAL function evaluation, below

if opt_2
   anglestr = 'quaternion'; ratesstr = 'qratesi';
else
   anglestr = 'euler'; ratesstr = 'eratesi';
end

% Determine axes to be used in solution (the sub-space)

if strncmpi(opt_{1},'longitudinal',length(opt_{1}))
% For n=2, ans = [1,3,8,4,6,11]; nsys = [ans,ans+12];
```

```
    [1,3,n*3+2,n*6+[1,3]]'*ones(1,n)+ones(5,1)*[0:n-1]*3; nsys = ans(:)';
    if opt_2
        [n*9+[1,3]]'*ones(1,n)+ones(2,1)*[0:n-1]*4;
    else
        [n*9+[2]]'*ones(1,n)+ones(1,1)*[0:n-1]*3;
    end
    nsys = [nsys,ans(:)'];

elseif strncmpi(opt_{1},'lateral',length(opt_{1}))
% For n=2, ans = [2,7,9,5,6,10,12]; nsys = [ans,ans+12];

    [2,n*3+[1,3],n*6+[2,3]]'*ones(1,n)+ones(5,1)*[0:n-1]*3; nsys = ans(:)';
    if opt_2
        [n*9+[1:4]]'*ones(1,n)+ones(4,1)*[0:n-1]*4;
    else
        [n*9+[1,3]]'*ones(1,n)+ones(2,1)*[0:n-1]*3;
    end
    nsys = [nsys,ans(:)'];

else
% For n=2, ans = [1:3,7:9,4:6,10:12]; nsys = [ans,ans+12];

    [1:3,n*3+[1:3],n*6+[1:3]]'*ones(1,n)+ones(9,1)*[0:n-1]*3; nsys = ans(:)';
    if opt_2
        [n*9+[1:4]]'*ones(1,n)+ones(4,1)*[0:n-1]*4;
    else
        [n*9+[1:3]]'*ones(1,n)+ones(3,1)*[0:n-1]*3;
    end
    nsys = [nsys,ans(:)'];
end

x = x0+dx; % Current state = trim + perturbation

% Set all other variables, outside the solution space, to zero

zeros(nx,1); ans(nsys) = x(nsys); x = ans;
u0 = x0(1:n*6); r0 = x0(n*6+[1:n*(o2+3)]);
u = x(1:n*6); r = x(n*6+[1:n*(o2+3)]);

% Create some transformation matrices

T_jN = zeros(3,3,n); T_cjN = NaN*ones(3,3,4,n);

T_jN(:,:,1) = feval(anglestr,r(n*3+[1:o2]));

% Determine sling configuration

mj = zeros(1,n);
MultipleCables = NaN; SingleCable = NaN;
for j = 2:n
    mj(j) = length(CDAT_(j).l0);

    MultipleCables(j) = (mj(j)>2) & (~any(diff(sort(CDAT_(j).i(1,:)))));
    SingleCable(j) = (mj(j)==1);
end

kcj_N = NaN*ones(3,4,n); acj = NaN*ones(3,4,n); wcj_cj = NaN*ones(3,4,n);
```

```
    R1sjs_N = NaN*ones(3,n);

    % Calculate the cable properties for each load

    for j = 2:n

        T_jN(:,:,j) = feval(anglestr,r(n*3+(j-1)*o2+[1:o2])); % Load-axes
        R1sjs_N(:,j) = -r(1:3)+r((j-1)*3+[1:3]);

        toplinks = HDAT_.S.Links.Data(CDAT_(j).i(1,:),:);
        botlinks = LDAT_(j).S.Links.Data(CDAT_(j).i(2,:),:);

        if MultipleCables(j)
            Rajjs_N = R1sjs_N(:,j)*ones(1,mj(j))-T_jN(:,:,1)'*toplinks';
            CDAT_(j).Raji_N = Rajjs_N+T_jN(:,:,j)'*botlinks';  % Attachment-attachment
            CDAT_(j).l = sqrt(sum((CDAT_(j).Raji_N).^2,1));       % Cable length
            CDAT_(j).ldot = u((j-2)*3+3+[1:3])'*(T_jN(:,:,j)*CDAT_(j).Raji_N)./(CDAT_(j).l);
        elseif SingleCable(j)
            Rajjs_N = R1sjs_N(:,j)-T_jN(:,:,1)'*toplinks';
            CDAT_(j).Raji_N = Rajjs_N+T_jN(:,:,j)'*botlinks';  % Attachment-attachment
            CDAT_(j).l = sqrt(sum((CDAT_(j).Raji_N).^2,1));     % Cable length
            CDAT_(j).ldot = u((j-2)*3+3+[3]);
        end

        for i = 1:mj(j)
            kcj_N(:,i,j) = CDAT_(j).Raji_N(:,i)/CDAT_(j).l(i); % Cable unit-vectors
            acj(:,i,j) = k2a(kcj_N(:,i,j));                       % Cable angles
            T_cjN(:,:,i,j) = euler(acj(:,i,j));                  % Transformations
        end
    end

    % Construct the configuration matrices

    [A,Ai,Adot,H] = hsl_config(u,T_jN,T_cjN,R1sjs_N,acj);

    % Correct the system mass/inertia matrix for implementation into the equations

    finD = isfinite(diag(D)); finDn = find(finD);
    D2 = zeros(n*6,n*6); D2(finDn,finDn) = D(finDn,finDn);
    for j = 1:n
        jj = (j-1)*3+[1:3];
        D2(jj,jj) = [  1 -1 -1 ; -1  1 -1 ; -1 -1  1 ].*D2(jj,jj);
    end

    % Compute the gravitational force

    g = 32.174; g_N = [ 0 0 g ]'*[ones(1,n),zeros(1,n)];

    fg = zeros(n*6,1);
    for j = 1:n
        jj = (j-1)*3+[1:3]; fg(jj) = D2(jj(3),jj(3))*[ 0 0 g ]';
    end

    % Calculate the body-axes velocities and current control inputs

    v = A*u; va = v;

    for j = 1:n
```

```
      jj = (j-1)*3+[1:3]; va(jj) = T_jN(:,:,j)*v(jj);
end

if all(size(TD)==[1,5])
   d = TD(2:5)';
else
   tdi = (TD(:,1)==t);
   if any(tdi)
      d = TD(find(tdi),2:5)';
   else
      d = interp1q(TD(:,1),TD(:,2:5),t)';
   end
end

% Compute the aerodynamic force and convert back to inertial axes

[AA,BA] = hsl_faero(va);
fa = AA*(va-va0) + BA*d; fa = diag(D2).*fa;

for j = 1:n
   jj = (j-1)*3+[1:3]; fa(jj) = T_jN(:,:,j)'*fa(jj);
end

% Calculate the total static weight and moments on the helicopter

d1 = D2(1,1); m1 = 0;

for j = 2:n
   jj = (j-1)*3+[1:3];
   d1 = d1+D2(jj(1),jj(1)); m1 = m1+D2(jj(1),jj(1))*(r0(1)-r0(jj(1)));
end

% Compute the thrust force (approximation) and convert back to inertial axes

ft = zeros(n*6,1);

if 0 % thrust (resultant) is vertical

   ft(3) = -d1*32.174;
   ft(n*3+2) = -m1*32.174;

else % thrust is normal to body

   ft(3) = -d1*32.174;
   ft(n*3+2) = -m1*32.174;

   for j = 1:n
      jj = (j-1)*3+[1:3]; ft(jj) = T_jN(:,:,j)'*ft(jj);
   end
end

% Compute the Coriolis forces and then the combined forces

X = zeros(n*6,1);
for j = 1:n
   jj = (n+j-1)*3+[1:3];
   X(jj) = skew3(u(jj))*D2(jj,jj)*u(jj);
end
```

```
    fx = -X-D2*Adot*u; fo = fa+fg+ft+fx;

    % Determine a solution for the cable forces

    fc = zeros(n*6,1); sf = fc;

    H = H(finDn,:); Di = Di(finDn,finDn); % The sub-space defined above

    if opt_{3} % Elastic solution
       FC = zeros(n*12,1); hi = zeros(1,n*12);

       for j = 2:n
          jj = (j-1)*3+[1:3];

          if MultipleCables(j)
             fC = (CDAT_(j).K(1,:)).*(1-(CDAT_(j).l0)./(CDAT_(j).l)) ...
                    +(CDAT_(j).K(2,:)).*(CDAT_(j).ldot)./(CDAT_(j).l);
             FC(jj) = sum(ones(3,1)*max(0,fC).*(CDAT_(j).Raji_N),2); hi(jj) = 1;
          elseif SingleCable(j)
             fC = (CDAT_(j).K(1)).*(1-(CDAT_(j).l0)./(CDAT_(j).l)) ...
                    +(CDAT_(j).K(2)).*(CDAT_(j).ldot)./(CDAT_(j).l);
             FC(jj(1)) = max(0,fC).*(CDAT_(j).l); hi(jj(1)) = 1;
          end
       end

       FC = FC(find(hi));
    else       % Inelastic solution

       FC = -(H'*Di*H)\(H'*Di*fo(finDn));
    end

    fc(finDn) = H*FC; % The cable forces

    Fc = zeros(n-1,1);
    for j = 2:n
       jj = (j-1)*3+[1:3];
       Fc(j-1) = sqrt(fc(jj)'*fc(jj)); % The total cable force for each load
    end

    % Compute the specific force

    sf(finDn) = Di*(fo(finDn)+fc(finDn));

    % Calculate the accelerations and rates required by the integration

    udot = Ai*sf; rdot = zeros(n*(o2+3),1); rdot(1:n*3) = v(1:n*3);

    for j = 1:n
       Wij_j = feval(ratesstr,r(n*3+(j-1)*o2+[1:o2]));

       rdot(n*3+(j-1)*o2+[1:o2]) = Wij_j*v(n*3+(j-1)*3+[1:3]);
    end

    % Update the body-axes accelerations for the next iteration

    vdot = Adot*u+A*udot; vadot = vdot;
```

```
for j = 1:n
   jj = (j-1)*3+[1:3]; vadot(jj) = T_jN(:,:,j)*vdot(jj);
end

% Combine the velocities and positions into the state rate vector

xdot = [udot;rdot];

% Augment the state rate with the null axes (non-solution space)

zeros(nx,1); ans(nsys) = xdot(nsys); xdot = ans;
```

HSL_FAERO.M

```
function [A,B] = hsl_faero(va)

% HSL_FAERO : Function to compute aerodynamic state-space matrices
%
%              [A,B] = HSL_FAERO(va)
%
%              va : Body-axes velocity vector [n*6x1]
%
%              A  : State matrix [n*6xn*6]
%              B  : Control matrix [n*6x4]
%
%              See HSL_FUN for more information

% R.A. Stuckey  01/10/97  (c) 1997, Defence Science and Technology Organisation
% -----------------------------------------------------------------------------

global HDAT_ LDAT_ opt_

n = length(va)/6;

% Determine aerodynamic derivatives to be used in solution

if strncmpi(opt_{1},'longitudinal',length(opt_{1}))
   [ 1 0 1 0 1 0 ]'*[ 1 0 1 0 1 0 1 0 0 1 ]; I = ans(:)';
elseif strncmpi(opt_{1},'lateral',length(opt_{1}))
   [ 0 1 0 1 0 1 ]'*[ 0 1 0 1 0 1 0 1 1 1 ]; I = ans(:)';
else
   I = ones(1,60);
end

% Aerodynamic coefficient matrices for the helicopter

Vj = sqrt(va(1:3)'*va(1:3))*0.5925; nv = length(HDAT_.V); % Velocity (knots)
if Vj<HDAT_.V(1)
   Vj = HDAT_.V(1);
elseif Vj>HDAT_.V(nv)
   Vj = HDAT_.V(nv);
end
if nv>1

% Interpolate between state/control matrices based on velocity
```

```
    if 1 %%% SAS off
        Aj = interp1q(HDAT_.V,HDAT_.A(:,:,1),Vj).*I;
    else %%% SAS on
        Aj = interp1q(HDAT_.V,HDAT_.A(:,:,2),Vj).*I;
    end
else
    Aj = HDAT_.A.*I;
end

% Integrate derivatives into the system state-space matrices

a = zeros(6,6); A = zeros(n*6,n*6);
b = zeros(6,4); B = zeros(n*6,4);

jj = [1:3,n*3+[1:3]];

a(:) = Aj(1:36); A(jj,jj) = a;
b(:) = Aj(37:60); B(jj,:) = b;

% Aerodynamic coefficient matrices for each load

for j = 2:n
    jj = (j-1)*3+[1:3];

    Vj = sqrt(va(jj)'*va(jj))*0.5925; nv = length(LDAT_(j).V);
    if Vj<LDAT_(j).V(1)
        Vj = LDAT_(j).V(1);
    elseif Vj>LDAT_(j).V(nv)
        Vj = LDAT_(j).V(nv);
    end

% Interpolate between state/control matrices based on velocity

    if nv>1
        Aj = interp1q(LDAT_(j).V,LDAT_(j).A,Vj).*I;
    else
        Aj = LDAT_(j).A.*I;
    end

% Integrate derivatives into the system state-space matrices

    jj = [(j-1)*3+[1:3],n*3+(j-1)*3+[1:3]];

    a(:) = Aj(1:36); A(jj,jj) = a;
    b(:) = Aj(37:60); B(jj,:) = b;
end

if 0 %%% CONTROL INPUTS ARE IN 0.1IN UNITS
    B = B*0.1;
end
```

HSL_CONFIG.M

```
function [A,Ai,Adot,H] = hsl_config(u,T_jN,T_cjN,R1sjs_N,acj)

% HSL_CONFIG : Calculate the configuration matrix and its inverse
```

```
%
%               [A,Ai,Adot,H] = HSL_CONFIG(u,T_jN,T_cjN,R1sjs_N,acj)
%
%               u       : Generalised velocity vector [n*6x1]
%               T_jN    : Load-axes transformation matrix [3x3xn]
%               T_cjN   : Cable-axes transformation matrix [3x3xn]
%               R1sjs_N : Position vector from helicopter to load cg [3xn]
%               acj     : Cable angle matrix [3x4xn]
%
%               A       : Configuration matrix [n*6xn*6]
%               Ai      : Inverse configuration matrix [n*6xn*6]
%               Adot    : Configuration rate matrix [n*6xn*6]
%               H       : Basis matrix [n*6xnh]
%
%               See HSL_FUN for more information

% Also see reference [1] for details of the configuration matrices.
%
% 1. Stuckey, R.A
%    "Mathematical Modelling of Helicopter Systems"
%    DSTO-TR-000, Defence Science and Technology Organisation, Sep, 1999

% R.A. Stuckey  28/07/98  (c) 1998, Defence Science and Technology Organisation
% ----------------------------------------------------------------------------

global HDAT_ LDAT_ CDAT_ opt_

n = length(LDAT_); n = n+(~n);

% Determine sling configuration

mj = zeros(1,n);
MultipleCables = NaN; SingleCable = NaN;
for j = 2:n
   mj(j) = length(CDAT_(j).l0);

   MultipleCables(j) = (mj(j)>2) & (~any(diff(sort(CDAT_(j).i(1,:)))));
   SingleCable(j) = (mj(j)==1);
end

% Construct the configuration matrices

A = eye(n*6,n*6); Ai = A; Adot = zeros(n*6,n*6); H = zeros(n*6,n*12);

for j = 2:n
   jj = (j-1)*3+[1:3];

   toplinks = HDAT_.S.Links.Data(CDAT_(j).i(1,:),:);
   botlinks = LDAT_(j).S.Links.Data(CDAT_(j).i(2,:),:);

   if MultipleCables(j)
      Rjsaj_j = T_jN(:,:,j)*(-R1sjs_N(:,j)+T_jN(:,:,1)'*toplinks(1,:)');

      A(jj,1:3) = eye(3);
      A(jj,jj) = T_jN(:,:,j)';
      A(jj,n*3+[1:3]) = -T_jN(:,:,1)'*skew3(toplinks(1,:));   % A_j,n+1
      A(jj,n*3+jj) = T_jN(:,:,j)'*skew3(Rjsaj_j);             % A_j,n+j
```

```
    if nargout>1
        Ai(jj,1:3) = -T_jN(:,:,j);
        Ai(jj,jj) = T_jN(:,:,j);
        Ai(jj,n*3+[1:3]) = -T_jN(:,:,j)*A(jj,n*3+[1:3]);      % B_j,n+1
        Ai(jj,n*3+jj) = -T_jN(:,:,j)*A(jj,n*3+jj);            % B_j,n+j
    end
    if nargout>2
        Adot(jj,jj) = T_jN(:,:,j)'*skew3(u(n*3+jj));
        Adot(jj,n*3+[1:3]) = ...
         -T_jN(:,:,1)'*skew3(u(n*3+[1:3]))*skew3(toplinks(1,:));         % Adot_j,n+1
        Adot(jj,n*3+jj) = ...
           T_jN(:,:,j)'*( skew3(u(n*3+jj))*skew3(Rjsaj_j)-skew3(u(jj)) ); % Adot_j,n+j
    end
    if nargout>3
        H(1:3,jj) = eye(3);
        H(jj,jj) = -eye(3);
        H(n*3+[1:3],jj) =  skew3(toplinks(1,:))*T_jN(:,:,1); % Z1j_1
        H(n*3+jj,jj)    = -skew3(Rjsaj_j)*T_jN(:,:,j);       % Zjj_j
    end
elseif SingleCable(j)
    A(jj,1:3) = eye(3);
    A(jj,jj) = T_cjN(:,:,1,j)';
    A(jj,n*3+[1:3]) = -T_jN(:,:,1)'*skew3(toplinks);         % A_j,n+1
    A(jj,n*3+jj) = T_jN(:,:,j)'*skew3(botlinks);             % A_j,n+j

    if nargout>1
        Ai(jj,1:3) = -T_cjN(:,:,1,j);
        Ai(jj,jj) = T_cjN(:,:,1,j);
        Ai(jj,n*3+[1:3]) = -T_cjN(:,:,1,j)*A(jj,n*3+[1:3]);  % B_j,n+1
        Ai(jj,n*3+jj) = -T_cjN(:,:,1,j)*A(jj,n*3+jj);        % B_j,n+j
    end
    if nargout>2
        acjdot = hsl_config_ac(acj(1,1,j),CDAT_(j).l,u(jj));
        Wcj_cj = erates(acj(:,1,j)); wcj_cj = Wcj_cj*acjdot;

        Adot(jj,jj) = T_cjN(:,:,1,j)'*skew3(wcj_cj);
        Adot(jj,n*3+[1:3]) = ...
         -T_jN(:,:,1)'*skew3(u(n*3+[1:3]))*skew3(toplinks);  % Adot_j,n+1
        Adot(jj,n*3+jj) = ...
           T_jN(:,:,j)'*( skew3(u(n*3+jj))*skew3(botlinks) ); % Adot_j,n+j
    end
    if nargout>3
        H(1:3,jj)        =  eye(3);
        H(jj,jj)         = -eye(3);
        H(n*3+[1:3],jj) =  skew3(toplinks)*T_jN(:,:,1);      % Z1j_1
        H(n*3+jj,jj)    = -skew3(botlinks)*T_jN(:,:,j);      % Zjj_j
    end
end

if 0 %%% CHECK EXPLICIT INVERSE
    fprintf('\n CHECKING INVERSE ...')
    inverr = max(max(abs(inv(A)-Ai)));
    if (inverr>1e-6)
        error(sprintf(' Inverse not accurate: ERR = %g',inverr))
    end
end
end
```

```
% Construct the basis matrix

hi = zeros(1,n*12);

kcj_N = zeros(3,n); kc1_N = kcj_N; kc2_N = kcj_N;

for j = 2:n
   jj = (j-1)*3+[1:3];

   if MultipleCables(j)  % Use entire force-space

      hi(jj) = 1;
   elseif SingleCable(j) % Use only cable z-axis

      kcj_N(:,j) = T_cjN(3,:,1,j)';
      H(:,jj(1)) = H(:,jj)*kcj_N(:,j); hi(jj(1)) = 1;
   end
end

H = H(:,find(hi));


% -------------------------------------------------------------------------------

function acdot = hsl_config_ac(ac,l,vc)

% hsl_config_ac : Calculate cable angular rates
%
%               acdot = HSL_CONFIG_AC(ac,l,vc)
%
%               ac   : Cable angle vector [1xn]
%               l    : Cable length vector [1xn]
%               vc   : Cable velocity vector [1xn]
%
%               acdot : Cable angle-rate matrix [3xn]
%
%               See HSL_CONFIG

m = length(l);

acdot = [ vc(1)./l./cos(ac(1,:)) ; -vc(2)./l ; zeros(1,m) ];
```

EULER.M

```
function T = euler(e)

% EULER : Euler-angle transformation matrix
%
%         T = EULER(e)
%
%         e : vector of Euler angles [1x3]
%           = [ phi theta psi ]
%
%         T : transformation matrix [3x3]
%
%         where the transformation from inertial (N) to body (b) axes follows:
```

```
%
%          F_b = T_bN * F_N ; T_bN = euler(e)
%
%          See HSL_FUN

% R.A. Stuckey  01/10/97  (c) 1997, Defence Science and Technology Organisation
% ----------------------------------------------------------------------------

ce = cos(e); se = sin(e);

T = [ ce(2)*ce(3)                    ce(2)*se(3)                   -se(2)
      se(1)*se(2)*ce(3)-se(3)*ce(1)  se(3)*se(2)*se(1)+ce(3)*ce(1)  se(1)*ce(2)
      ce(3)*ce(1)*se(2)+se(3)*se(1)  se(3)*ce(1)*se(2)-ce(3)*se(1)  ce(1)*ce(2) ];
```

E2Q.M

```
function Q = e2q(E)

% E2Q : Convert angular positions from Euler to quaternion representation
%
%        Q = E2Q(E)
%
%        E : Euler matrix [mx3]|[3xn]
%          = [ Phi Theta Psi ]
%
%        Q : quaternion matrix [mx4]|[4xn]
%          = [ E0 E1 E2 E3 ]
%
%        See also Q2E

% R.A. Stuckey  07/05/98  (c) 1998, Defence Science and Technology Organisation
% ----------------------------------------------------------------------------

Ne = size(E); trans = (Ne(2)~=3);

if trans, E = E'; Ne = Ne([2,1]); end

SE = sin(E/2); CE = cos(E/2); Q = zeros(Ne(1),4);

Q(:,1) =  SE(:,1).*SE(:,2).*SE(:,3) + CE(:,1).*CE(:,2).*CE(:,3);
Q(:,2) = -CE(:,1).*SE(:,2).*SE(:,3) + SE(:,1).*CE(:,2).*CE(:,3);
Q(:,3) =  SE(:,1).*CE(:,2).*SE(:,3) + CE(:,1).*SE(:,2).*CE(:,3);
Q(:,4) =  CE(:,1).*CE(:,2).*SE(:,3) - SE(:,1).*SE(:,2).*CE(:,3);

if trans, Q = Q'; end
```

ERATES.M

```
function W = erates(e)

% ERATES : Euler transform matrix for angular velocities
%
%          W = ERATES(e)
```

```
%
%          e : vector of Euler angles [1x3]
%           = [ phi theta psi ]
%
%          W : transformation matrix [3x3]
%
%          where
%                        .    .    .
%          [ p q r ]' = W * [ phi theta psi ]'
%
%          See also ERATESI

% R.A. Stuckey  07/05/98  (c) 1998, Defence Science and Technology Organisation
% ----------------------------------------------------------------------------

ce = cos(e); se = sin(e);

W = [ 1  0     -se(2)
      0  ce(1)  se(1)*ce(2)
      0 -se(1)  ce(1)*ce(2) ];
```

ERATESI.M

```
function Wi = eratesi(e)

% ERATESI : Inverse Euler transform matrix for angular velocities
%
%          Wi = ERATESI(e)
%
%          e  : vector of Euler angles [1x3]
%             = [ phi theta psi ]
%
%          Wi : inverse transformation matrix [3x3]
%
%          where
%               .    .    .
%          [ phi theta psi ]' = Wi * [ p q r ]'
%
%          See also ERATES

% R.A. Stuckey  07/05/98  (c) 1998, Defence Science and Technology Organisation
% ----------------------------------------------------------------------------

ce = cos(e); se = sin(e); te = tan(e);

Wi = [ 1  se(1)*te(2)  ce(1)*te(2)
       0  ce(1)        -se(1)
       0  se(1)/ce(2)  ce(1)/ce(2) ];
```

K2A.M

```
function acj = k2a(kcj)
```

```
% K2A : Convert k-unit vectors to cable-oriented Euler angles
%
%          a = K2A(k)
%
%          k : unit vectors [nx3]
%
%          a : Euler angle vector [nx3]
%
%          See HSL_FUN

% R.A. Stuckey  20/04/99  (c) 1999, Defence Science and Technology Organisation
% ----------------------------------------------------------------------------

nk = size(kcj);

if ~any(nk==3), error(' size(kcj,2)~=3!'), end

if nk(2)~=3, kcj = kcj'; end

acj = 0*kcj;

acj(:,1) = asin(-kcj(:,2));
acj(:,2) = asin( kcj(:,1)./cos(acj(:,1)) );
acj(:,3) = 0;

if nk(2)~=3, acj = acj'; end
```

SKEW3.M

```
function S = skew3(v)

% SKEW3 : The general skew-symmetric matrix, S(x,y,z)
%
%          S = skew3(v)
%
%          v : Generic [x,y,z] vector
%
%          S : Skew matrix [3x3]
%
%          See HSL_CONFIG, HSL_FUN

% R.A. Stuckey  20/04/99  (c) 1999, Defence Science and Technology Organisation
% ----------------------------------------------------------------------------

S = [  0    -v(3)  v(2)
       v(3)  0    -v(1)
      -v(2)  v(1)  0    ];
```

HSLPLOT.M

```
% HSLPLOT : Plot output from HSLSIM
%
%          HSLPLOT
```

```
%
%              Inputs:
%
%              opt_  : GLOBAL options cell array [4x1]
%
%              Va    : Body-axes velocity matrix [Nxn*6]
%              Vadot : Body-axes acceleration matrix [Nxn*6]
%              FC    : Cable force matrix [Nx(n-1)]
%              R     : Configuration position coordinate matrix [Nxn*6]
%              Acj   : Cable angle matrix [Nx(n-1)*3]
%              TDD   : Updated time & control input matrix [Nx5]
%
%              See HSL_INIT, HSLSIM

% R.A. Stuckey  01/10/97  (c) 1997, Defence Science and Technology Organisation
% ----------------------------------------------------------------------------

yv = {'Rotation',0,'HorizontalAlignment','right'};

% Determine axes to be plot

if strncmpi(opt_{1},'longitudinal',length(opt_{1}))

   Plots = { 'u' 't' ; 'w' 'tc' ; 'q' 'db' ; 'fc' 'dc' };
   if ~any(any(TDD(xn,[2,5])))
   Plots = { 'u' 't' ; 'w' 'tc' ; 'q' 'ud' ; 'fc' 'wd' };
   end

elseif strncmpi(opt_{1},'lateral',length(opt_{1}))

   Plots = { 'v' 'h' ; 'w' 't' ; 'r' 's' ; 'fc' 'da' ; '' 'dr' ; '' 'dc' };
   if ~any(any(TDD(xn,[3:5])))
   Plots = { 'v' 'h' ; 'w' 't' ; 'r' 's' ; 'fc' 'vd' ; '' 'wd' };
   end
   Plots = { 'v' 'h' ; 'w' 't' ; 'r' 's' ; 'fc' 'vd' };

elseif strncmpi(opt_{1},'combined',length(opt_{1}))

   Plots = { 'u' 'p' ; 'v' 'q' ; 'w' 'r' ; 'h' 'da' ; 'hc' 'db' ; 't' 'dr' ; 'tc' 'dc' };
   if ~any(any(TDD(xn,[2:5])))
   Plots = { 'u' 'h' ; 'v' 'hc' ; 'w' 't' ; 'p' 'tc' ; 'q' 'ud' ; 'r' 'vd' ; 'fc' 'wd' };
   end
end

sp = {size(Plots,1),size(Plots,2)};

Plots(sp{1}+1,:) = { '' '' }; sp{1} = sp{1}+1;

if (sp{1}>8), warning(' Too many subplots ! Figure size will be reduced.'), end

ha = zeros(sp{:}); hL = zeros(n,sp{1}*sp{2});

pos = get(0,'DefaultFigurePosition');
pos(2) = pos(2)-pos(4)*(sp{1}-4)/4; pos(4) = pos(4)*sp{1}/4; pos(3) = pos(3);
h = figure('Position',pos);

set(h,'DefaultAxesPosition',[0.26 0.19 0.70 0.73])
```

```
    for i = 1:sp{1}
       for j = 1:sp{2}
          if ~isempty(Plots{i,j})
             k = (i-1)*sp{2}+j;
             ha(i,j) = subplot(sp{:},k);

             if (i<sp{1})&(~isempty(Plots{i+1,j}))
                set(ha(i,j),'XTickLabel',[]);
             else
                xlabel('t, sec')
             end
          end
       end

% Plot each set of variables

       nn = [0:n-1];
       switch Plots{i,j}
          case 'u'
             hL(:,k) = plot(t(xn),Va(xn,nn*3+1),'-k'); ylabel({'u','ft/s'},yv{:})
          case 'v'
             hL(:,k) = plot(t(xn),Va(xn,nn*3+2),'-k'); ylabel({'v','ft/s'},yv{:})
          case 'w'
             hL(:,k) = plot(t(xn),Va(xn,nn*3+3),'-k'); ylabel({'w','ft/s'},yv{:})
          case 'p'
             hL(:,k) = plot(t(xn),Va(xn,n*3+nn*3+1)*180/pi,'-k'); ylabel({'p','deg/s'},yv{:})
          case 'q'
             hL(:,k) = plot(t(xn),Va(xn,n*3+nn*3+2)*180/pi,'-k'); ylabel({'q','deg/s'},yv{:})
          case 'r'
             hL(:,k) = plot(t(xn),Va(xn,n*3+nn*3+3)*180/pi,'-k'); ylabel({'r','deg/s'},yv{:})
          case 'fc'
             hL(2:n,k) = plot(t(xn),FC(xn,:),'-k'); ylabel({'fc','/g'},yv{:})
          case 'h'
             hL(:,k) = plot(t(xn),R(xn,n*3+nn*3+1)*180/pi,'-k'); ylabel({'\phi','deg'},yv{:})
          case 't'
             hL(:,k) = plot(t(xn),R(xn,n*3+nn*3+2)*180/pi,'-k'); ylabel({'\theta','deg'},yv{:})
          case 's'
             hL(:,k) = plot(t(xn),R(xn,n*3+nn*3+3)*180/pi,'-k'); ylabel({'\psi','deg'},yv{:})
          case 'hc'
             hL(2:n,k) = plot(t(xn),Acj(xn,[0:n-2]*3+1)*180/pi,'-k');
             ylabel({'\phi_c','deg'},yv{:})
          case 'tc'
             hL(2:n,k) = plot(t(xn),Acj(xn,[0:n-2]*3+2)*180/pi,'-k');
             ylabel({'\theta_c','deg'},yv{:})
          case 'sc'
             hL(2:n,k) = plot(t(xn),Acj(xn,[0:n-2]*3+3)*180/pi,'-k');
             ylabel({'\psi_c','deg'},yv{:})
          case 'db'
             hL(1,k) = plot(t(xn),TDD(xn,2)); ylabel({'\delta_b','in'},yv{:})
          case 'da'
             hL(1,k) = plot(t(xn),TDD(xn,3)); ylabel({'\delta_a','in'},yv{:})
          case 'dr'
             hL(1,k) = plot(t(xn),TDD(xn,4)); ylabel({'\delta_r','in'},yv{:})
          case 'dc'
             hL(1,k) = plot(t(xn),TDD(xn,5)); ylabel({'\delta_c','in'},yv{:})
          case 'ud'
             hL(:,k) = plot(t(xn),Vadot(xn,nn*3+1),'-k');
             ylabel({'\fontsize{6}\bullet','\fontsize{10}u','ft/s^2'},yv{:})
          case 'vd'
```

```
            hL(:,k) = plot(t(xn),Vadot(xn,nn*3+2),'-k');
            ylabel({'\fontsize{6}\bullet','\fontsize{10}v','ft/s^2'},yv{:})
        case 'wd'
            hL(:,k) = plot(t(xn),Vadot(xn,nn*3+3),'-k');
            ylabel({'\fontsize{6}\bullet','\fontsize{10}w','ft/s^2'},yv{:})
        case 'pd'
            hL(:,k) = plot(t(xn),Vadot(xn,n*3+nn*3+1)*180/pi,'-k');
            ylabel({'\fontsize{6}\bullet','\fontsize{10}p','deg/s^2'},yv{:})
        case 'qd'
            hL(:,k) = plot(t(xn),Vadot(xn,n*3+nn*3+2)*180/pi,'-k');
            ylabel({'\fontsize{6}\bullet','\fontsize{10}q','deg/s^2'},yv{:})
        case 'rd'
            hL(:,k) = plot(t(xn),Vadot(xn,n*3+nn*3+3)*180/pi,'-k');
            ylabel({'\fontsize{6}\bullet','\fontsize{10}r','deg/s^2'},yv{:})
        end
    end
end

SP = diag([1:sp{1}])*(ha>0); [ans,ans] = max(SP); [spi,spj] = max(ans);

set(ha(find(ha)),'XLim',[0 round(t(xn(end)))])
set(ha(find(ha)),'XGrid','on','YGrid','on')

% Change line properties for clarity

set(hL(1,find(hL(1,:))),'LineStyle','-','Linewidth',1.0,'Color',[ 0 0 0 ])

if n>1, set(hL(2,find(hL(2,:))),'LineStyle','-','LineWidth',0.5,'Color',0.5*[ 1 1 1 ]), end
if n>2, set(hL(3,find(hL(3,:))),'LineStyle','--','LineWidth',0.5,'Color',0.5*[ 1 1 1 ]), end
if n>3, set(hL(4,find(hL(4,:))),'LineStyle',':','LineWidth',0.5,'Color',0.5*[ 1 1 1 ]), end

% Add a legend

if n==1
    return
elseif n==2
    [hl,ho] = legend(hL(1:2,1),'Helicopter','Slung-load',2);
elseif n==3
    [hl,ho] = legend(hL(1:3,1),'Helicopter','Aft Load','Forward Load',3);
elseif n==4
    [hl,ho] = legend(hL(1:4,1),'Helicopter','AftLoad','MidLoad','FwdLoad',4);
end

% Remove those pesky callbacks (created by LEGEND)

set(hl,'ButtonDownFcn','', ...
        'DeleteFcn','', ...
        'UserData',[])
set(ho,'ButtonDownFcn','')

% Fix up the legend text

ht = findobj(ho,'Type','text');

set(ht,'FontUnits','points');

tp1 = get(ht(1),'Position');
set(ht(1),'Units','pixels')
```

```
a5e = get(ht(1),'Extent');
set(ht(1),'Units','data','Position',tp1)

set(hl,'Units','pixels')
lp = get(hl,'Position');
lp(4) = 1.5*a5e(4);
set(hl,'Position',lp)
set(hl,'Units','normalized')

lp = get(hl,'Position');

a1p = get(ha(1,1),'position'); a2p = get(ha(1,2),'position');
a3p = get(ha(spi-1,spj),'position'); a4p = get(ha(spi,spj),'position');

lp(1) = (a1p(1)+a1p(3)+a2p(1))/2-lp(3)/2;
lp(2) = a4p(2)-2*(a3p(2)-(a4p(2)+a4p(4)))-lp(4);
set(hl,'Position',lp)
```

Mathematical Modelling of Helicopter Slung-Load Systems

R.A. Stuckey

Number of Copies

DEFENCE ORGANISATION

Task Sponsor

CAPT Brad Warren, Headquarters Aviation Support Group, Oakey, QLD 4401   1

S&T Program

Chief Defence Scientist	
FAS Science Policy	
AS Science Corporate Management	1
Director General Science Policy Development	

Counsellor, Defence Science, London   Doc Data Sht

Counsellor, Defence Science, Washington   Doc Data Sht

Scientific Adviser to MRDC, Thailand   Doc Data Sht

Scientific Adviser Joint   1

Navy Scientific Adviser   Doc Data Sht

Scientific Adviser, Army   Doc Data Sht

Air Force Scientific Adviser   1

Director Trials   1

Aeronautical and Maritime Research Laboratory

Director, Aeronautical and Maritime Research Laboratory   1

Chief Air Operations Division   1

Research Leader Crew Environments and Training Technologies   1

Research Leader Flight Mechanics   1

Head Helicopter Operations   1

Head Flight Mechanics   1

R.A. Stuckey   2

A. Arney   1

J. Blackwell   1

R. Reddy   1

T. Truong   1

Electronics and Surveillance Research Laboratory

Director, Electronics and Surveillance Research Laboratory   Doc Data Sht

DSTO Research Library and Archives

Library Fishermans Bend   Doc Data Sht

Library Maribyrnong	Doc Data Sht
Library Salisbury	1
Australian Archives	1
Library, MOD, Pyrmont	Doc Data Sht
US Defense Technical Information Center	2
UK Defence Research Information Centre	2
Canada Defence Scientific Information Service	1
NZ Defence Information Centre	1
National Library of Australia	1

Capability Systems Staff

Director General Maritime Development	Doc Data Sht
Director General Land Development	1
Director General C3I Development	Doc Data Sht
Director General Aerospace Development	Doc Data Sht

Navy

SO(Science), Director of Naval Warfare, Maritime Headquarters Annex, Garden Island	Doc Data Sht

Army

FLTLT Gerry Van Leeuwen, CENGR, AMTDU, RAAF Base Richmond, NSW 2755	1
LTCOL Philip Smith, SO1 Aviation Development Branch, Victoria Barracks, Paddington, NSW 2021	1
ABCA Standardisation Officer, Puckapunyal	4
SO(Science), DJFHQ(L), MILPO, Enoggera, QLD 4057	Doc Data Sht

Intelligence Program

DGSTA, Defence Intelligence Organisation	1
Manager, Information Centre, Defence Intelligence Organisation	1

Corporate Support Program

Officer in Charge, TRS, Defence Regional Library, Canberra	1

INTERNATIONAL COLLABORATIVE PARTNERS

Defence Research & Development Canada, Ottawa, CA

LCOL M Haines	1

National Research Council of Canada, Ottawa, CA

S Zan	1
S Cariguan	1

Defence Science and Technology Laboratory, Farnborough, UK

    T Cansdale   1

Defence Science and Technology Laboratory, Bedford, UK

    B Lumsden   1

Ames Research Center, California, USA

    M Whalley   1

    J Schroeder   1

    L Cicolani   1

Naval Air Systems Command, Patuxent River, USA

    J Clark Jr   1

UNIVERSITIES AND COLLEGES

Australian Defence Force Academy Library	1
Head of Aerospace and Mechanical Engineering, ADFA	1
Deakin University Library, Serials Section (M List)	1
Hargrave Library, Monash University	Doc Data Sht
Librarian, Flinders University	1

OTHER ORGANISATIONS

NASA (Canberra)	1
Info Australia	1

SPARES

DSTO Melbourne Research Library	6

Total number of copies: 57

DEFENCE SCIENCE AND TECHNOLOGY ORGANISATION DOCUMENT CONTROL DATA		1. CAVEAT/PRIVACY MARKING	
2. TITLE Mathematical Modelling of Helicopter Slung-Load Systems		3. SECURITY CLASSIFICATION Document (U) Title (U) Abstract (U)	
4. AUTHOR R.A. Stuckey		5. CORPORATE AUTHOR Aeronautical and Maritime Research Laboratory 506 Lorimer St, Fishermans Bend, Victoria, Australia 3207	
6a. DSTO NUMBER DSTO–TR–1257	6b. AR NUMBER AR–012–114	6c. TYPE OF REPORT Technical Report	7. DOCUMENT DATE December, 2001

8. FILE NUMBER M1/9/970	9. TASK NUMBER ARM 99/102	10. SPONSOR HQASG	11. No OF PAGES 95	12. No OF REFS 36

13. URL OF ELECTRONIC VERSION http://www.dsto.defence.gov.au/corporate/ reports/DSTO–TR–1257.pdf	14. RELEASE AUTHORITY Chief, Air Operations Division

15. SECONDARY RELEASE STATEMENT OF THIS DOCUMENT   *Approved For Public Release*   OVERSEAS ENQUIRIES OUTSIDE STATED LIMITATIONS SHOULD BE REFERRED THROUGH DOCUMENT EXCHANGE, PO BOX 1500, SALISBURY, SOUTH AUSTRALIA 5108
16. DELIBERATE ANNOUNCEMENT   No Limitations
17. CITATION IN OTHER DOCUMENTS   No Limitations
18. DEFTEST DESCRIPTORS   Chinook helicopter; Slung load; Modelling; Simulation

19. ABSTRACT

The primary goal of this work is to use mathematical modelling to assist in defining the operational limits of the Australian Army CH-47D Chinook when carrying mixed density slung loads. This report presents the first phase in the program: the development of a simple helicopter slung-load model for simulation and analysis of the system dynamics.

General system equations of motion are obtained from the Newton-Euler equations in terms of generalized coordinates and velocities. The system is partitioned into coordinates such that the motion due to cable stretching is separated from that due to rigid-body, coupled dynamics. In the formulation used, the constraint forces appear explicitly and a solution to the resultant generalized accelerations can be determined by modelling the cable as a simple spring. An inelastic solution is also possible by nulling the stretching coordinates to obtain a relation for the suspension forces. The system equations are also extended for the multiple load case.

The model is verified by imposing certain constraints in order to approximate a simple pendulum system and then comparing its behaviour with analytical results. Various configurations of the complete helicopter slung-load system, based on the CH-47B Chinook carrying standard military containers, are then examined in an investigation of the open-loop characteristics. In the investigation, several parameters such as the helicopter-load mass ratio, suspension configuration, and number of loads are varied and the resulting system modes examined. A number of simulations are also presented which demonstrate the characteristic behaviour of such systems.